

Jackeline Gallo do Amaral

**ANÁLISE ESTRUTURAL E BIOQUÍMICA DA
HIDROXIAPATITA SUBMETIDA AO TRATAMENTO COM
FLUORETO E POLIFOSFATOS**

Tese apresentada à Faculdade de Odontologia de Araçatuba da Universidade Estadual Paulista “Júlio de Mesquita Filho” – UNESP, como parte dos requisitos para a obtenção do título de Doutor em Ciência Odontológica – Área Saúde Bucal da Criança.

Orientador: Prof. Dr. Alberto Carlos Botazzo Delbem

Coorientador: Prof. Dr. Juliano Pelim Pessan

Araçatuba - SP

2014

Catálogo-na-Publicação

Serviço Técnico de Biblioteca e Documentação – FOA / UNESP

A485a Amaral, Jackeline Gallo do.
Análise estrutural e bioquímica da hidroxiapatita submetida
ao tratamento com fluoreto e polifosfatos / Jackeline Gallo do
Amaral. -Araçatuba, 2014
112 f. : il. ; tab. + 1 CD-ROM

Tese (Doutorado) – Universidade Estadual Paulista,
Faculdade de Odontologia de Araçatuba
Orientador: Prof. Alberto Carlos Botazzo Delbem
Coorientador: Prof. Juliano Pelim Pessan

1. Polifosfatos 2. Fluoretos 3. Durapatita 4. Dissolução
5. Saliva I. Título

Black D27
CDD 617.645

DADOS CURRICULARES

JACKELINE GALLO DO AMARAL

Nascimento	08.05.1987 – São José do Rio Preto – SP
Filiação	Luis Carlos Paulo do Amaral Aida Maria Gallo do Amaral
2005/2008	Curso de Graduação em Odontologia pela Faculdade de Odontologia de Araçatuba – UNESP
2009/2011	Curso de Pós Graduação em Ciência Odontológica – Área Saúde Bucal da Criança, nível de Mestrado, na Faculdade de Odontologia de Araçatuba – UNESP
2012/2012	Estágio de Doutorado no Exterior, na University of Bristol, Reino Unido
2011/2014	Obtenção dos créditos referentes ao curso de Pós Graduação em Ciência Odontológica – Área Saúde Bucal da Criança, nível de Doutorado, na Faculdade de Odontologia de Araçatuba – UNESP
Associações	CROSP - Conselho Regional de Odontologia de São Paulo SBPqO - Sociedade Brasileira de Pesquisa Odontológica IADR – International Association for Dental Research

DEDICATÓRIA

Dedico a realização deste trabalho,

Aos meus pais, *Luis Carlos e Aida*, que nunca mediram esforços para que eu pudesse realizar meus sonhos, sempre me incentivando a persistir na busca dos meus ideais. O constante apoio e incentivo de vocês foram fundamentais para que eu pudesse chegar até aqui. Agradeço por tudo que me ensinaram, pelo exemplo de determinação, simplicidade, honestidade, felicidade e amor. Por todos os momentos em que podemos estar juntos e pelas palavras de conforto que sempre trazem segurança e tranquilidade. Não há palavras que expressem meu amor e admiração por vocês.

Muito obrigada por tudo!

AGRADECIMENTOS ESPECIAIS

AGRADECIMENTOS ESPECIAIS

Agradeço a *Deus* pela minha vida, por sua proteção e por guiar os meus passos rumo às minhas realizações. Devo a Ele todos os meus momentos de alegria e sucesso até aqui conquistados.

Ao meu irmão, *Rodolfo*, pelos incentivos durante a minha vida, sempre presente nos momentos em que precisava. Por me fazer compreender como é bom ter uma família. Agradeço pelos momentos de alegria, pelo apoio e torcida.

À *minha família*, sempre presente em minha vida, pelo apoio e confiança em mim depositados em toda a minha caminhada. Obrigada por fazerem parte da minha vida!

Ao meu namorado, *Gabriel*, obrigada por ter estado ao meu lado durante esta caminhada, sempre me incentivando. Agradeço pela paciência, pelo carinho que sempre demonstrou por mim, por me ouvir e compreender minhas dificuldades. Desejo que nossas vidas sejam cada vez mais abençoadas com muita paz, união e amor. Obrigada por fazer parte da minha vida, e conseqüentemente das minhas conquistas!

Ao meu orientador, *Prof. Dr. Alberto Carlos Botazzo Delbem*, primeiramente pela confiança depositada em mim, pela disponibilidade, paciência e oportunidades ao decorrer destes anos. Agradeço por todo o esforço que dedicou ao desenvolvimento deste trabalho e por ter me proporcionado esses anos de orientação. Exemplo de dedicação, responsabilidade, competência, humildade e determinação com a pesquisa. Agradeço pelas grandes oportunidades e ensinamentos a mim proporcionadas ao longo da nossa convivência. Minha eterna gratidão e admiração.

Ao meu coorientador, *Prof. Juliano Pelim Pessan*, pela paciência, apoio e incentivo para que eu aproveitasse as oportunidades ao longo desta caminhada. Agradeço por todo o esforço que dedicou a esse trabalho e a preocupação para que eu pudesse aprimorar meus conhecimentos científicos. A seriedade, competência e dedicação que tem com a pesquisa e a docência são admiráveis. Agradeço toda ajuda e disponibilidade, eu aprendi muito estando ao seu lado.

À *Profa. Michele Barbour*, minha admiração. Agradeço toda a sabedoria dividida no tempo em que pude aproveitar estando em seu grupo de pesquisa na Universidade de Bristol. Muito obrigada pela oportunidade.

“Um bom professor educa seus alunos para uma profissão, um professor fascinante os educa para a vida”. (Augusto Cury)

À Fundação de Amparo à Pesquisa do Estado de São Paulo (FAPESP) e à Coordenação de Aperfeiçoamento de Pessoal de Nível Superior (CAPES) pelo grande incentivo, que tornaram possível a realização da minha pós-graduação, na forma de Bolsa de Doutorado (FAPESP, Processo 2011/17234-9), Auxílio Pesquisa Regular (FAPESP, Processo 2011/07788-7) para o desenvolvimento deste estudo e Bolsa para o Programa de Estágio de Doutorado no Exterior (CAPES, Processo BEX 9221-12-3).

AGRADECIMENTOS

AGRADECIMENTOS

À Faculdade de Odontologia de Araçatuba – UNESP, na pessoa de sua diretora, Profa. Dra. Ana Maria Pires Soubhia, e seu vice-diretor, Prof. Dr. Wilson Roberto Poi, pela oportunidade de realização do curso de Doutorado e toda minha formação nesta instituição, pelo aprendizado e crescimento pessoal e profissional proporcionado ao longo destes anos.

Ao curso de pós-graduação em Ciência Odontológica da Faculdade de Odontologia Araçatuba – UNESP, na pessoa do seu Coordenador, Prof. Dr. Alberto Carlos Botazzo Delbem. Minha sincera admiração pela competência e dedicação que tem para com o curso de pós-graduação.

Aos professores da Disciplina de Odontopediatria da UNESP-Araçatuba, Dr. Alberto, Dr. Célio, Dra. Cristiane, Dr. Juliano, Dr. Robson, Dra. Rosângela e Dra. Sandra. Obrigada por todos os ensinamentos e pela valiosa contribuição na minha formação acadêmica. Vocês proporcionaram oportunidades muito importantes para minha vida profissional. Não tenho palavras para agradecer todos os ensinamentos. Meus sinceros agradecimentos e admiração.

Ao Prof. Robson por seu exemplo de dedicação ao ensino da Odontopediatria. Obrigada pelos momentos valiosos de aprendizado durante as disciplinas teóricas e durante os atendimentos na Bebê Clínica e Graduação. Cada minuto ao seu lado é suficiente para grandes aprendizados. Tenho muita admiração pela forma como orienta seus alunos.

À Universidade de Bristol e ao Bristol Dental Hospital pela receptividade e grande oportunidade de realizar o doutorado sanduíche.

Ao Prof. João Carlos Silos Moraes do Departamento de Física e Química da Faculdade de Engenharia de Ilha Solteira - UNESP pela colaboração imprescindível para a realização deste projeto, pela paciência e por sempre nos receber tão bem em Ilha Solteira. Muito obrigado por tudo.

Ao Departamento de Física e Química da Faculdade de Engenharia de Ilha Solteira- UNESP, representado por todos os seus Professores e Funcionários, pela oportunidade de realizar parte do meu trabalho e por todo o aprendizado.

Aos alunos de Mestrado, Doutorado, Pós-Doutorado e Iniciação Científica: Ana Laura, Fernanda, Jaqueline, José Antônio, Kevin, Marcela, Márjully, Mariana, Thayse, Valéria, Lais, Giovana, Samia, Daniela Oliveira, Danielle, Maria Daniela, Michele, Nathália, Natália, Paula, Tatiana, Remberto, Carla, Karina, Kelly, Carolina Lodi, Douglas, Vinicius, Kamila, Flávia, Jéssica, Amanda, Adriana e Thiago pela amizade, experiências compartilhadas e pelos momentos divertidos que passamos juntos.

Ao aluno de mestrado José Antonio, pelo grande auxílio para o desenvolvimento deste trabalho.

A Profa. Cleide, pela amizade, pelos ensinamentos e orientação durante o início da minha pós graduação.

À amiga Karina Kondo, agradeço pela amizade sincera, pelo apoio, e pelos momentos de diversão. Senti muita falta da sua companhia aqui quando você terminou a pós-graduação. Torço muito pelo seu sucesso e felicidade.

À amiga Janaína, muito obrigado por ter sido uma grande amiga para mim durante esses anos, pela ajuda, e mesmo com a distância, por estar sempre presente de alguma forma. Desejo muita felicidade e sucesso.

Aos colegas do Laboratório de pesquisa da Universidade de Bristol, Natalie, Ahmed, Olivia e Ed por toda ajuda quando cheguei à Universidade de Bristol e durante a minha estadia na Inglaterra, pela amizade e pelos momentos de diversão. A todos os amigos brasileiros e estrangeiros que fiz durante a minha estadia na Inglaterra, que tornaram a distância do Brasil um pouco menor.

Aos funcionários da biblioteca e da seção de pós-graduação da Faculdade de Odontologia de Araçatuba, pelos serviços prestados sempre com muita competência

e pela disponibilidade em ajudar. Em especial, Valéria, Cristiane e Lilian, pela atenção e ajuda dada para a realização do Estágio PDSE.

À Profa. Dra. Kikue, pela ajuda, paciência e disponibilidade com que sempre me atendeu, desde a graduação até o início deste trabalho. Aprendi muito ao seu lado. Muito obrigada.

À funcionária da Disciplina de Odontopediatria, Maria dos Santos Ferreira Fernandes, por toda ajuda nos procedimentos laboratoriais desde minha graduação, além da amizade e convivência, sou muito grata por tudo. Você faz muita falta no laboratório!

Aos demais professores e funcionários da Faculdade de Odontologia de Araçatuba – UNESP, por todos os ensinamentos ao longo destes anos, pelo exemplo que são e pela convivência sempre agradável.

A todos aqueles que contribuíram para a elaboração e conclusão deste trabalho,

Meus sinceros agradecimentos.

EPÍGRAFE

*“A mente humana que se abre a uma nova idéia jamais voltará
ao seu tamanho original.”*

Albert Einstein

RESUMO GERAL

Amaral, JG. Análise estrutural e bioquímica da hidroxiapatita submetida ao tratamento com fluoreto e polifosfatos. [tese] Araçatuba: Universidade Estadual Paulista; 2014.

RESUMO GERAL

Este estudo avaliou o efeito do trimetafosfato de sódio (TMP) e hexametafosfato de sódio (HMP) associados ou não ao fluoreto (F) na dissolução e estrutura da hidroxiapatita (HA). Para tanto, o estudo foi dividido em três subprojetos. Nos subprojetos 1 e 2, o pó de HA sintética (n=6) foi tratado com soluções contendo entre 0 e 10% de TMP associado a 0, 100, 250, 500 (Subprojeto 1) e a 0, 1100, 4500 e 9000 ppm F (Subprojeto 2), sendo submetido a um ciclo de pH. As concentrações de F alcali- e ácido solúvel, cálcio (Ca) e fósforo (P) foram determinadas na HA, e as de P e F no sobrenadante. As amostras foram analisadas pela espectroscopia no infravermelho (FTIR), difração de Raios-X (DRX) e espectroscopia de energia dispersiva (EDX). No Subprojeto 3, discos de HA foram empregados para avaliar a taxa de dissolução da mesma utilizando o sistema pH-stat. Estes foram tratados com soluções contendo 1100 ppm F, 1 e 8% de HMP ou TMP e 1100 ppm F associado com 1 e 8% de HMP ou TMP, totalizando 9 grupos (n=8). A influência da película salivar também foi avaliada. Discos de HA foram mantidos em saliva humana previamente ao tratamento com água deionizada e 1100 ppm F associado com 1 e 8% de HMP ou TMP, totalizando 5 grupos (n=8). A taxa de dissolução pós-tratamento foi determinada a partir de 3 medidas consecutivas a cada 30 min. Os dados foram submetidos a ANOVA, teste de Student-Newman-Keul's e coeficiente de correlação de Pearson (Subprojetos 1 e 2) e a ANOVA e testes de Fisher e Holm-Sidak (Subprojeto 3) ($\alpha=0,05$). Valores de proporção Ca/P maiores foram observados para as soluções fluoretadas quando comparados à solução sem F e TMP, sendo os mesmos dependentes da proporção F:TMP ($p<0,05$). A deposição do F alcali-solúvel foi diretamente relacionada com as concentrações de TMP nas soluções, enquanto que a de F ácido-solúvel foi inversamente relacionada ($p<0,05$). Além disso, a adsorção de P esteve relacionada à concentração de F e TMP ($p<0,05$). Os dados da DRX indicaram que a cristalinidade da HA é alterada de acordo com a proporção de F:TMP adicionada. Além disso, os difratogramas e espectros obtidos apresentaram padrão similar ao da

HA sintetizada. Todas as soluções avaliadas mostraram uma redução na taxa de dissolução dos discos de HA (30 min) ($p < 0,001$). No entanto, a duração do efeito inibitório foi maior quando 8% de HMP e 1 ou 8% de HMP com F foram testadas ($p < 0,001$). A presença da película salivar promoveu maior proteção para todos os grupos, comparado com outros discos sem película ($p < 0,001$). Em conclusão, quando TMP e F são coadministrados, estes competem pelo mesmo sítio de ligação na HA. Uma proporção de TMP:F ideal pode proporcionar uma melhora dos produtos fluoretados e precipitar uma HA com baixa solubilidade. A redução da dissolução da HA, bem como a duração deste efeito foi influenciada pelo fluoreto, tipo e concentração de sal de fosfato, além da presença da película salivar.

Palavras-chave: Polifosfatos, Fluoretos, Durapatita, Dissolução, Saliva.

GENERAL ABSTRACT

Amaral, JG. Structural and biochemical analysis of hydroxyapatite submitted to the treatment with fluoride and polyphosphates. [thesis]. Araçatuba: Universidade Estadual Paulista; 2014.

GENERAL ABSTRACT

This study evaluated the effect of sodium trimetaphosphate (TMP) and sodium hexametaphosphate (HMP) associated or no with fluoride (F) on the structure and dissolution of hydroxyapatite (HA). For this purpose, the study was divided into three subprojects. In Subprojects 1 and 2, synthetic HA powder (n=6) was treated with solutions containing TMP varying at 0-10% associated with 0, 100, 250, 500 (Subproject 1) and 0, 1100, 4500 and 9000 ppm F (Subproject 2) and submitted to a pH cycle. Afterwards, alkali- and acid soluble F, Ca and P were determined in/on HA, and P and F in the supernatants. Samples were analyzed by infrared spectroscopy (FTIR), X-ray diffraction (XDR) and energy-dispersive X-ray spectroscopy (EDX). In Subproject 3, HA discs were used to assess the dissolution rate of HA using a pH-stat system. HA discs were treated with 1100 ppm F, 1% and 8% of HMP or TMP and 1100 ppm F associated with 1% and 8% of HMP or TMP, totaling 9 groups (n=8). The influence of a salivary pellicle on HA dissolution was also assessed. HA discs were kept in pooled human saliva before treatment with deionised water and 1100 ppm F associated with 1% and 8% of HMP or TMP, totaling 5 groups (n=8). The post-treatment dissolution rate was determined from three consecutive 30-min assays. Data were submitted to ANOVA, Student-Newman-Keuls' test and Pearson's correlation coefficient (Subprojects 1 and 2), and to ANOVA and Fisher and Holm-Sidak methods (Subproject 3) ($\alpha=0.05$). Ca/P ratios values were higher for the fluoride solutions when compared with the no F and TMP groups and dependent of the F:TMP ratio used ($p<0.05$). The overall trend was that alkali-soluble F deposition was directly related to TMP concentrations in the treatment solutions, while acid-soluble incorporation was inversely related to TMP concentrations ($p<0.05$). Additionally, the P adsorption is related to the F and TMP concentration used ($p<0.05$). XDR data indicated that HA powder crystallinity is altered according to the addition of F/TMP. In addition to, diffractograms and spectra obtained showed a similar pattern that for pure HA. All tested solutions promoted reduction in HA dissolution rate ($p<0.001$). However, the duration of the inhibitory effect was greater

when 8% HMP and 1 or 8% HMP associated with F were assessed ($p < 0.001$). The presence of salivary pellicle led to higher protection for all groups when compared to discs without pellicle ($p < 0.001$). In conclusion, when TMP and F are co-administered, TMP and F compete for the same binding sites in the HA. An ideal TMP:F ratio can provide an enhancement of the fluoride products and precipitate a HA with low solubility. In addition to, the reduction of HA discs dissolution rate, as well as the duration of this effect were influenced by fluoride, type and concentration of phosphate salt and the presence of a salivary pellicle.

Key-words: Polyphosphates, Fluoride, Durapatite, Dissolution, Saliva.

LISTAS

LISTA DE FIGURAS

Capítulo 1	Effect of sodium trimetaphosphate and fluoride on hydroxyapatite solubility: an <i>in vitro</i> study.....	37
Figure 1	a: XRD patterns of the synthetic HA and CRYSTMET database. b: HA spectra obtained for synthetic HA (Peaks 1,2: PO ₄ ³⁻ , 3: OH ⁻ , 4: HPO ₄ ²⁻ , 5, 6 and 7, PO ₄ ³⁻ ; 8 and 9: CO ₃ ⁻ ; 10: H ₂ O).....	51
Figure 2	XRD patterns of HA according to the groups evaluated associated with TMP. 0 ppm F (a); 100 ppm F (b); 250 ppm F (c); 500 ppm F (d). The diameter values (nm) of the crystal after pH cycle according to the fluoride concentration (ppm F) and percentage of TMP are represented by the letter d.....	52
Figure 3	Mean (± se) of values of Ca (a), P (b) and Ca/P ratio (c) on hydroxyapatite synthesized and after pH cycle according to the F and TMP concentration. Correlation: concentration of calcium and phosphorus on hydroxyapatite (d). Distinct letters show significant differences between the % TMP for each fluoride concentration (Student-Newman-Keuls, p <0.05). (*) 0 ppm F = 100 ppm F = 250 ppm F; (&) 0 ppm F = 100 ppm F; (Φ) 0 ppm F = 250 ppm F; (#) 100 ppm F = 250 ppm F; (λ) 0 ppm F = 500 ppm F; (Ω) 100 ppm F = 500 ppm F; (ψ) 250 ppm F = 500 ppm F; (ω) 100 ppm F = 250 ppm F = 500 ppm F.....	53
Figure 4	Atomic % of Ca (a), P (b), F (c) and O (d) in HA according to the F concentration associated with TMP.....	54
Figure 5	Mean (± se) of alkali-soluble F on HA after treatment (a) and after pH cycle (b); acid-soluble F on HA after treatment (c) and after pH cycle (d). Distinct letters show significant differences between the % TMP for each fluoride concentration (Student-Newman-Keuls, p <0.05). (#) 100 ppm F = 250 ppm F; (ψ) 250 ppm F = 500 ppm F; (λ) 0 ppm F = 500 ppm F; (Φ) 100 ppm F = 250 ppm F = 500 ppm F; (Ω) 100 ppm F = 500 ppm F. Concentrations (mg/g) (mean ± SD) of alkali and acid soluble F in the synthetic HA were: 0.02 (0.0) and 0.01 (0.0), respectively.....	55

Figure 6	<p>Mean (\pm se) of F and TMP adsorbed to hydroxyapatite (a) adsorption of TMP (expressed through the amount of phosphorus), (b) adsorption of F. Distinct letters show significant differences between the %TMP for each fluoride concentration (Student-Newman-Keuls, $p < 0.05$). (*) All comparisons show similarity; (&) 100 ppm F = 250 ppm F = 500 ppm F; (λ) 250 ppm F = 500 ppm F; (Φ) no difference among the %TMP in 0 ppm F group.....</p>	56
----------	--	----

Capítulo 2 Biochemical analysis of hydroxyapatite solubility treated with fluoride and sodium trimetaphosphate..... 59

Figure 1	<p>a: XRD patterns of the synthetic HA and CRYSTMET database. b: HA spectra obtained for synthetic HA (Peaks 1,2: PO_4^{3-}, 3: OH^-, 4: HPO_4^{2-}, 5, 6 and 7, PO_4^{3-}; 8 and 9: CO_3^-; 10: H_2O).....</p>	74
----------	--	----

Figure 2	<p>XRD patterns of HA according to the groups evaluated associated with TMP. 0 ppm F (a); 1100 ppm F (b); 4500 ppm F (c); 9000 ppm F (d). The diameter values (nm) of the crystal after pH cycle according to the fluoride concentration (ppm F) and percentage of TMP are represented by the letter d.....</p>	75
----------	---	----

Figure 3	<p>Mean (\pm se) of values of Ca (a), P (b) and Ca/P ratio (c) on hydroxyapatite after pH cycle according to the fluoride and TMP concentration. Correlation between calcium and phosphorus concentrations on hydroxyapatite (d). Distinct letters show significant differences between the % TMP for each fluoride concentration (Student-Newman-Keuls, $p < 0.05$). (*) 4500 ppm F = 9000 ppm F; (&) 1100 ppm F = 9000 ppm F; (#) 1100 ppm F = 4500 ppm F; (ψ) 0 ppm F and 1100 ppm F; (Φ) 0 ppm F and 9000 ppm F; (Ω) 0 ppm F = 1100 ppm F = 9000 ppm F.....</p>	76
----------	--	----

Figure 4	<p>Mean (\pm se) of alkali-soluble F on HA after treatment (a) and after pH cycle (b); acid-soluble F on HA after treatment (c) and after pH cycle (d). Distinct letters show significant differences between the % TMP for each fluoride concentration (Student-Newman-Keuls, $p < 0.05$). (*) 4500 ppm F = 9000 ppm F; (&) 1100 ppm F = 9000 ppm F; (#) 1100 ppm F = 4500 ppm F. Concentrations (mg/g) (mean \pm SD) of acid-soluble and alkali-soluble in the synthetic HA were: 0.02 (0.0) and 0.01 (0.0),</p>
----------	--

	respectively.....	77
Figure 5	Atomic % of Ca (a), P (b), F (c) and O (d) in HA according to the F concentration associated with TMP. * Synthetic HA (% atomic): Ca= 20.55; P=13.33; O=66.12; F=0.....	78
Figure 6	Mean (\pm se) of F and TMP adsorbed to hydroxyapatite (a) adsorption of TMP (expressed through the amount of phosphorus), (b) adsorption of F. Distinct letters show significant differences between the %TMP for each fluoride concentration (Student-Newman-Keuls, $p < 0.05$). (*) All comparisons show similarity; (&) 1100 ppm F = 4500 ppm F = 9000 ppm F; (#) 0 ppm F = 1100 ppm F; (λ) 4500 ppm F = 9000 ppm F; (ψ) 0 ppm F = 1100 ppm F = 4500 ppm F.....	79
Capítulo 3	Effects of polyphosphates and fluoride on hydroxyapatite dissolution: a pH-stat investigation.....	82
Figure 1	Dissolution rate of HA for the three control runs before treatment (C1-3) and after treatment (Post 1-3) with 1100 ppm F. Dashed line= mean control rate. *Significantly different from mean baseline control.....	94
Figure 2	Dissolution rate of HA for the three control runs before treatment (C1-3) and after treatment (Post 1-3) with TMP and fluoride. Dashed line= mean control rate. *Significantly different from mean baseline control.....	95
Figure 3	Dissolution rate of HA for the three control runs before treatment (C1-3) and after treatment (Post 1-3) with HMP and fluoride. Dashed line= mean control rate. *Significantly different from mean baseline control.....	96
Figure 4	Graphic representation of HA dissolution rate reduction according to the treatments, saliva and post-treatment run. a= post-treatment 1 (30min), b=post-treatment 2 (60min) and c= post-treatment 3 (90min). Bars indicate the standard deviation of the mean. Distinct capital letters represent statistical difference between the groups without salivary pellicle. Different lowercase letters represent statistical difference between the groups with salivary pellicle (Holm-Sidak, $p < 0.001$).....	97

LISTA DE TABELAS

Capítulo 1	Effect of sodium trimetaphosphate and fluoride on hydroxyapatite solubility: an <i>in vitro</i> study.....	37
Table 1	Absorption coefficient obtained in the FTIR analysis according to the groups evaluated regarding the F and TMP concentration.....	57
Capítulo 2	Biochemical analysis of hydroxyapatite solubility treated with fluoride and sodium trimetaphosphate.....	59
Table 1	Absorption coefficient obtained in the FTIR analysis according to the groups evaluated regarding the F and TMP concentration.....	80

Lista de Abreviaturas

a.u.= Unidade aleatória

°C= Graus Celsius

μ= Micro

μL= Microlitro

μg F/g= Microgramas de fluoreto por grama

ppm F= partes por milhão de fluoreto

Ca= Cálcio

Ca(NO₃)₂ .H₂O= Nitrato de cálcio hidratado

DP= Desvio padrão

se= Erro padrão

F= Fluoreto

FA= Fluorapatita

FTIR= Espectroscopia no infravermelho transformada de Fourier

g= Gramas

g= Gravidade

KOH= Hidróxido de Potássio

h= Hora

H₂O= Água

HA= Hidroxiapatita

HCl= Ácido Clorídrico

HMP= Hexametáfosfato de sódio

L= Litro

min= Minuto

mL= Mililitro

mm= Milímetro

mm²= Milímetro quadrado

mmHg= Milímetro de Mercúrio

mol L⁻¹= Molaridade

nm= Nanômetro

NaF= Fluoreto de Sódio

NaOH= Hidróxido de sódio

NH_4OH = Hidróxido de amônio

P= Fosfato

pH= Potencial hidrogeniônico

s= Segundo

TISAB= Total ionic strength adjustment buffer (Tampão ajustador de força iônica)

TMP= Trimetafosfato de sódio

v1= Estiramento simétrico

v2 = Vibração angular

v3= Estiramento assimétrico

v4= Vibração angular

\pm = Mais ou menos

SUMÁRIO

SUMÁRIO

1. Introdução Geral.....	32
2. Capítulo 1 - Effect of sodium trimetaphosphate and fluoride on hydroxyapatite solubility: an in vitro study	
2.1. Abstract.....	37
2.2. Introduction.....	38
2.3. Materials and Methods.....	39
2.4. Results.....	43
2.5. Discussion.....	45
2.6. Conclusion.....	47
3. Capítulo 2 - Biochemical analysis of hydroxyapatite solubility treated with fluoride and sodium trimetaphosphate	
3.1. Abstract.....	59
3.2. Introduction.....	60
3.3. Materials and Methods.....	61
3.4. Results.....	65
3.5. Discussion.....	67
3.6. Conclusion.....	70
4. Capítulo 3 - Effects of polyphosphates and fluoride on hydroxyapatite dissolution: a pH-stat investigation	
4.1. Abstract.....	82
4.2. Introduction.....	83
4.3. Materials and Methods.....	84
4.4. Results.....	87
4.5. Discussion and Conclusion.....	88
Anexos.....	98

INTRODUÇÃO GERAL

1. Introdução Geral

O esmalte dentário é composto predominantemente de hidroxiapatita (HA) e pode estar susceptível a dois tipos de desmineralização: provocada por ácidos provenientes do biofilme dentário (microrganismos), denominada de cárie dentária, ou por ácidos advindos da alimentação, medicamentos, meio ambiente ou ácido gástricos, chamada de erosão dentária (Imfeld, 1996; Wiegand et al., 2007), os quais produzem lesões diferentes na estrutura do esmalte.

O fluoreto (F) é o principal agente utilizado no controle da cárie dentária mundialmente, sendo administrado por métodos de alcance comunitário, bem como de auto-aplicação e para uso pelo profissional (Pessan et al., 2011). Dentre os veículos mais utilizados, a água de abastecimento e os dentifrícios fluoretados são o mais amplamente difundidos. O principal efeito dos produtos fluoretados aplicados topicamente está relacionado à maior retenção de F na superfície dental na forma de fluoreto de cálcio (CaF_2), o qual age fornecendo F livre para atuar durante períodos de queda de pH, intervindo diretamente na dinâmica do processo desmineralização (Buzalaf et al., 2011). Embora uma marcante redução da incidência e prevalência da cárie dentária tenha sido observada no mundo, em regiões e populações específicas são encontradas acentuadas diferenças em relação à prevalência de cárie (Narvia et al., 2000; Antunes et al., 2004; Dye et al., 2007). Recentemente, a terapia com F também tem sido estudada e empregada no controle da progressão do desgaste dental erosivo (Ganss et al., 2013), o qual, apesar de ainda não ser caracterizado como um problema de saúde pública, vem acometendo crianças, adolescentes e adultos em diversas partes do mundo (Johansson et al., 2012).

Assim, considerando os hábitos modernos da população que têm aumentado o risco para o desenvolvimento dessas condições, a pesquisa atual tem focado no desenvolvimento de estratégias para melhorar a eficácia de produtos fluoretados, e ao mesmo tempo reduzir a exposição ao F, visto que a exposição excessiva ao F durante o período de formação dos dentes pode levar ao desenvolvimento de fluorose dental (Wong et al., 2011; Carey et al., 2014). Dentre as estratégias para se aumentar a eficácia de produtos fluoretados, a redução do pH de dentifrícios (Vilhena et al., 2010; de Almeida et al., 2014) e a adição de polifosfatos a diversos

tipos de produtos odontológicos (Takeshita et al., 2009, 2011; Moretto et al., 2013; Manarelli et al., 2011, Pancote et al., 2014, Camara et al., 2014) vem sendo estudada mais intensamente nos últimos anos. Estudos mostraram que o trimetafosfato de sódio (TMP) e o hexametáfosfato de sódio (HMP) apresentam efeitos protetores tanto para cárie quanto para a erosão (Takeshita et al., 2009, 2011; Moretto et al., 2013; Manarelli et al., 2011, Pancote et al., 2014, Camara et al., 2014).

O TMP é um polifosfato cíclico condensado e, de acordo com a literatura, preserva a estabilidade e integridade da superfície do mineral do esmalte (Gonzalez, 1971). Estudos recentes mostram que produtos com uma proporção adequada de TMP:F podem proporcionar um efeito protetor maior que em produtos fluoretados convencionais, tanto nos processos erosivos (Moretto et al., 2010, 2013; Manarelli et al., 2011; Pancote et al., 2014) quanto na cárie dentária (Takeshita et al., 2009, 2010; Danelon et al., 2014; Manarelli et al., 2014). Acredita-se que o mecanismo de ação esteja relacionado com a adsorção deste composto à superfície do esmalte, limitando a difusão de ácidos para o esmalte (Van Dijk et al., 1980; Takeshita et al., 2011, Manarelli et al., 2014). Takeshita et al. (2009) demonstraram que a associação de 1% de TMP a um dentifrício com 500 ppm F promoveu um efeito protetor contra a desmineralização do esmalte *in vitro* semelhante à um dentifrício convencional contendo 1100 ppm F. O mesmo dentifrício apresentou efeito protetor contra a erosão/abrasão semelhante ao de um dentifrício contendo 5000 ppm F (Moretto *et al.*, 2010). Recentemente, um estudo clínico avaliou a progressão de cárie em crianças utilizando um dentifrício de baixa concentração de F (500 ppm F) associado a 1%TMP e um dentifrício padrão comercial (1100 ppm F), tendo demonstrado uma superioridade do dentifrício contendo TMP em crianças com experiência prévia de cárie (Amaral et al., 2014)

O HMP é também um polifosfato cíclico que tem a capacidade de reduzir a solubilidade do esmalte, apresentando alta afinidade com a apatita do esmalte (Van Dijk et al., 1980; Andreola et al., 2004; Castellini et al., 2005). Conceição (2013) avaliou *in situ* um gel contendo 1% de NaF associado ao HMP, tendo demonstrado que esta associação promoveu menor desgaste dental erosivo e menor perda mineral do esmalte comparado a um gel de mesma concentração de F, sem adição de HMP. Camara et al. (2013) avaliaram o efeito de dentifrícios contendo 250 ppm F

associado a 0,5% de HMP *in vitro*, tendo obtido um efeito anticariogênico similar ao de um dentífrico convencional (1100 ppm F).

No entanto, tanto para o TMP como para o HMP, parece haver uma proporção apropriada de polifosfato:F para que a efetividade máxima seja obtida, o que pode estar relacionado ao mecanismo de ação destes polifosfatos associados ao F. Este parece ocorrer devido a uma formação de uma "barreira" na superfície do esmalte, que pode fornecer proteção contra a perda mineral em desafios cariogênicos e erosivos (Camara et al, 2013; Souza et al, 2013; Manarelli et al. 2014). Neste sentido, o F e TMP parecem competir pelos mesmos sítios de ligação na hidroxiapatita (Souza et al., 2013). No entanto, os protocolos mencionados acima não fornecem informações detalhadas sobre a interação entre o F e TMP ou HMP com a estrutura do esmalte. Dado que o mecanismo de ação do F associado ao TMP ou HMP não está completamente elucidado, seria interessante avaliar a interação direta desses compostos com a HA, que é o principal componente mineral do esmalte através de análises bioquímicas e estruturais.

Com base no proposto acima, o objetivo deste estudo foi avaliar diferentes concentrações de F presentes em formulações para uso tópico mais comumente apresentadas em produtos de saúde bucal, como soluções para bochecho, dentífricos, géis e vernizes (0, 110, 250, 500, 1100, 4500, 9000 ppm F), associadas ao TMP (0-10%) na estrutura HA após serem submetidos a um ciclo de pH (simulando um desafio cariogênico), bem como os efeitos de TMP na deposição de fluoreto alcali-solúvel e ácido-solúvel, bem como as concentrações de cálcio (Ca) e fosfato (P) presentes da HA após o processo. Além disso, a interação da HA com soluções contendo F e polifosfatos em um modelo erosivo também foi estudada, utilizando o sistema "pH stat" para avaliar o efeito imediato e prolongado destes agentes terapêuticos associado ou não ao F sobre a dissolução de discos de hidroxiapatita. Este protocolo foi utilizado em estudos anteriores (Barbour et al., 2005; Barbour et al., 2008; Jones et al, 2013) como um modelo para tecidos dentários em estudos de outros compostos e demonstraram propriedades qualitativamente semelhante ao esmalte (Shellis et al., 2010). Considerando-se que a saliva pode ter uma forte influência sobre a erosão dental e em testes de agentes anti-erosivos (Buzalaf et al, 2012; Jones et al., 2013), os efeitos TMP e HMP na

dissolução de discos de HA, com e sem formação da película salivar, foram avaliados.

Para responder aos questionamentos acima propostos, o presente trabalho foi dividido em 3 capítulos, a saber:

- **Capítulo 1:** *Effect of sodium trimetaphosphate and fluoride on hydroxyapatite solubility: an in vitro study* (artigo redigido de acordo com as normas do periódico Journal of Materials Science: Materials in Medicine);

- **Capítulo 2:** *Biochemical and structural analysis of hydroxyapatite solubility treated with fluoride and sodium trimetaphosphate* (artigo redigido de acordo com as normas do periódico Journal of Materials Science: Materials in Medicine);

- **Capítulo 3:** *Effects of polyphosphates and fluoride on hydroxyapatite dissolution: a pH-stat investigation* (artigo redigido de acordo com as normas do periódico Caries Research).

*Referências da Introdução Geral estão no Anexo A.

CAPÍTULO 1

Effect of sodium trimetaphosphate and fluoride on hydroxyapatite solubility: an *in vitro* study

2.1 Abstract

This study aimed to evaluate the effect of sodium trimetaphosphate (TMP) associated with fluoride (F) on hydroxyapatite (HA) biochemical and physical properties after a pH-cycle. Synthetic HA powder (1.0 g, n=6) was suspended in TMP solutions varying at 0-10% associated with 0, 100, 250 and 500 ppm F and submitted to a pH cycle. The concentration of alkali- and acid-soluble F, Ca and P were determined in/on HA and P and F in the supernatant. Samples were analyzed by energy-dispersive X-ray spectroscopy (EDX), Fourier transformed infrared spectroscopy (FTIR) and X-ray diffraction (XRD). Data were submitted to ANOVA and Student-Newman-Keuls' test ($p < 0.05$). The highest Ca/P ratios were observed for HA treated with TMP at 0.4%-0.8% combined with 250 ppm F, and between 0.6%-2% with 500 ppm F ($p < 0.05$). The increase of TMP led to a reduced acid-soluble F incorporation in HA for all groups ($p < 0.05$). Additionally, the increase in TMP concentrations led to higher P adsorption to HA for the 0 and 100 ppm F solutions, but lower for the 250 and 500 ppm F solutions ($p < 0.05$). A reduction of the size of the HA crystallites was seen with increasing TMP concentrations. The FTIR spectra showed alterations in the bands corresponding to phosphates and to carbonate for all groups when compared to the HA synthesized. Thus, F and TMP in combination can precipitate a HA lower soluble and the action mechanism seems to be related with the TMP adsorption on enamel surface by binding to HA.

Keywords: hydroxyapatite; polyphosphates; fluoride; dissolution.

*Capítulo escrito de acordo com as instruções do periódico Journal of Materials Science: Materials in Medicine

2.2 Introduction

Calcium phosphates have been used as biomaterials and have been considered as tissue engineering scaffolds because their similarity to the mineral phase of hard tissue in the body. HA is a calcium phosphate widely used due its unique properties as biodegradation and bioactivity [1]. These properties added to its high capacity to adsorption and/or absorption molecules may provide an excellent support for prolonged action of anticancer drugs for the treatment of bone tumors. Moreover, the chemical and structural features of HA allow its use in medical field as biocompatible material in implants and prosthesis. In dentistry, HA has been used to avoid bone loss after the restoration or extraction of a tooth, for example. In addition, titanium implants coated with HA have been used to replace the root [2].

In human tooth enamel, hydroxyapatite (HA - $\text{Ca}_{10}(\text{PO}_4)_6(\text{OH})_2$) crystals are arranged into highly organized prisms to form the main unit. In the oral cavity, dental enamel can be damaged by the local cariogenic bacteria in biofilm (caries) or non-bacterially derived erosive challenges (such as acidic beverages) [3]. The maintenance of HA in dental structures by decreasing its dissolution can be achieved by the use of fluoride-containing products, such as mouthrinses, toothpastes, fluoride varnishes, gels and restoratives materials [4].

Several studies have suggested that TMP reduces the demineralization process, and that an ideal TMP:F molar ratio allows an enhancement of the effects of F-containing products [5-9]. When TMP and F are co-administered, the adsorption of TMP on the enamel surface can change the selective permeability and facilitate the diffusion of ions Ca and F [8] into the enamel [10]. However, the mechanism of action of the TMP has not been completely clarified. Nonetheless, the studies assessing the effects of F and TMP in the dynamics of dental caries and erosion cited above have not considered the direct interactions between F and TMP with dental enamel, which would be helpful to provide new insights on the mechanisms of action of TMP. Thus, the aim of this study was to evaluate the effect of low-F solutions associated with TMP at varying concentrations on biochemical and physical properties of HA after pH cycle. The F concentrations studied are those present in products of home and commercial use, such as mouthrinses (100 and 250 ppm F) and dentifrices (500 ppm F). The study's null hypothesis was that the biochemical and physical properties of

HA would not be influenced by the presence of TMP and F, either alone or in combination.

2.3 Materials and Methods

Synthesis of HA

HA powder was prepared based on the protocol by Qu and Wei [12]. Briefly, 300 mL of 1 mol/L calcium nitrate solution ($\text{Ca}(\text{NO}_3)_2 \cdot \text{H}_2\text{O}$, Sigma-Aldrich Corp. St. Louis, MO, USA) and 600 mL of 0.3 mol/L diammonium phosphate solution ($(\text{NH}_4)_2\text{HPO}_4$, 600 mL, Sigma-Aldrich Corp. St. Louis, MO, USA) were prepared and had their pH raised to 10–12 by adding NH_4OH (29.5%). Afterwards, the diammonium phosphate solution was added slowly to the calcium nitrate solution (2–5 mL/min), under constant agitation at 37°C. The precipitates were aged for 7 days at 37°C and the pH was adjusted diary at around 10 in order to allow the growth and a formation of a single crystalline phase. The system remained open in order to precipitate a carbonated HA similar to that presented in the dental tissue. Then, the precipitate was filtered using a Buchner funnel attached to a vacuum system (–600 mmHg), washed with anhydrous ethanol and with deionized water (250 ml/0.5 g HA) to remove the contaminant ions (NH_4^+ and NO_3^-) [9]. The precipitate was dried for 24 h at 70°C and then ground into a fine powder (particle size less than 53 μm) using a ball mill (Pulverisette 7, Fritsch, Germany). Six samples of approximately 0.5 g were separated for characterization through energy-dispersive X-ray spectroscopy (EDX), infrared spectroscopy (FTIR) and X-ray diffraction (XRD) and to perform the F, calcium (Ca) and phosphorus (P) analysis (Anexo B).

Treatment and pH Cycle

Solutions (100 mL, n=6) containing TMP ($\text{Na}_3\text{P}_3\text{O}_9$, Sigma-Aldrich Co., USA) at 0, 0.1, 0.2, 0.4, 0.6, 0.8, 1.0, 2.0, 4.0, 6.0, 8.0, and 10%, associated with 0, 100, 250 and 500 ppm F (NaF, Merck, Darmstadt, Germany) were prepared. At first, the synthetic HA powder (1.0 g) was suspended in each of the prepared solutions during 2 min under constant agitation to 37°C. Afterwards, the precipitate was collected by filtration using a Buchner funnel attached to a vacuum system (–600 mmHg), washed repeatedly with deionized water (250 ml/0.5 g HA) and dried for 24 h at 37°C. The precipitate was then ground again into a fine powder using a ball mill (Pulverisette 7,

Fritsch, Germany). During the treatment of synthetic HA powder, an aliquot of the suspension was collected, centrifuged for 1 min at $2900 \times g$. (Combi – 514R) in order to calculate the P and F adsorption in the HA. After the treatment, HA samples (0.5 g) of each group was suspended in deionized water and the pH of the suspensions was slowly reduced to 4.0 using 1 mol L^{-1} nitric acid (HNO_3 , Merck, Darmstadt, Germany) under agitation. After 30 min, the pH of each solution was raised to 7.0 by the addition of 1 mol L^{-1} sodium hydroxide (NaOH, Merck, Darmstadt, Germany) which was maintained during 30 min. Samples of synthetic HA powder ($n= 6$) were suspended in deionized water as a negative control. After completion of this process, the precipitates were separated by filtration, washed with deionized water, dried for 24 h at 37°C and ground into a fine powder as described above. Thus, HA was analyzed for F, Ca, and P concentration and by EDX, FTIR and XRD (Anexo C).

Calcium and phosphorus analysis in hydroxyapatite

For Ca and P determination, 5 mg of HA powder was weighed into pre-weighed micro-centrifuge tubes and 2.0 mL of 1 mol L^{-1} HCl was added. After agitation for 1 h (Shaker, SK-300, Lab. Companion, Kimpo City, Korea), the samples were diluted (1:10) and partly neutralized to avoid the HA powder precipitation. Aliquots of 5 μL were taken from the samples and added to 50 μL of deionized water and Arsenazo solution. For calibration, standards containing 40 to 200 $\mu\text{g Ca/mL}$ were used. The Ca analysis was performed using a spectrophotometer (Microplate Spectrophotometer EONC, Biotek, USA) with a wavelength of 650 nm by adopting the Arsenazo III colorimetric method described by Vogel et al. [13]. Phosphorus was measured by the molybdate method colorimetric method described by Fiske and Subbarow [14] with a wavelength of 660 nm and using aliquots of 20 μL from the samples, which were subsequently added to a mixture of 50 μL molybdate solution and 20 μL of reactive reducer. Standards containing 1.5 to 24 $\mu\text{g P/mL}$ were used. The Ca and P analyses were realized in duplicate (Anexo D).

Fluoride analysis (alkali-soluble and acid-soluble F)

For fluoride analysis, 5 mg of HA powder post-treatment and post-cycled was weighed into pre-weighed micro-centrifuge tubes, and 2.0 mL of 1 mol L^{-1} KOH was added for alkali-soluble F extraction, according to the method described by Caslavská et al. [15]. After 24 h of continuous agitation (Shaker, SK-

300, Lab. Companion, Kimpo City, Korea), the samples were centrifuged (Combi – 514R) for 20 min at $2900 \times g$. A 0.5 mL aliquot of the supernatant was neutralized with 0.5 mL of TISAB II (total ionic strength adjustment buffer) modified with 1 mol L^{-1} HCl (0.82 mL HCl/L). Alkali-soluble F was determined by using a specific electrode 9409BN (Thermo Scientific, Beverly, MA, USA) and reference electrode (Analyser, Sao Paulo, Brazil) connected to an ion analyzer (Orion 720A⁺ Thermo Scientific, Beverly, MA, USA). For determination of acid-soluble F, the precipitate was washed three times with deionized water and once with methanol. After methanol evaporation (overnight at $60 \text{ }^{\circ}\text{C}$), 1 mL of 1 mol L^{-1} HCl was added, and the samples were homogenized for 30 s by vortexing, and subsequently agitated for 1 h at room temperature. 0.5 mL aliquot of these samples was then added to 0.5 mL of TISAB II modified with 20 g NaOH/L. Samples were analyzed for acid-soluble F as described for alkali-soluble F. The F analyses were performed in duplicate [11] (Anexo E).

Phosphorous and fluoride analysis in suspension of HA treatment

F and P concentrations were determined in supernatants removed from the suspensions during the HA treatment. Phosphorus was determined using an aliquot of 100 μL of sample and standards, plus 50 μL molybdate and 20 μL of reactive reducer through the colorimetric method described by Fiske & Subbarow [14]. The fluoride was determined by a specific electrode 9409BN (Thermo Scientific, Beverly, MA, USA) and inverted reference electrode (Orion 900100) coupled to an ion analyzer (Orion 720 A⁺, Thermo Scientific, Beverly, MA, USA). The electrode was calibrated with standards containing 0.25 to 4.00 $\mu\text{g F / ml}$ and 4.0 to 64.0 $\mu\text{g F / ml}$ under the same conditions of samples. Aliquots of 40 μL of samples and the same volume of TISAB II were dispensed on the active tip of the reference electrode. Analyses were performed in duplicate. Afterwards, the adsorption of F and TMP to hydroxyapatite was calculated from the initial concentrations of these compounds in the solutions and the concentration during the HA treatment.

Energy-dispersive X-ray spectroscopy (EDX)

Samples ($n=1$) of HA were prepared and placed in sample holder to the EDX analysis in order to quantify the atomic percentage Ca, P, F and oxygen (O). It was used a Scanning Electron Microscope (SEM), ZEISS brand, model EVO-LS15

coupled with an energy-dispersive X-ray spectroscopy (EDX), Oxford Instrument's brand, model INCA X-act with resolution of 133eV.

X-Ray Diffraction (XRD)

Samples (n=1) of each fluoride group of HA associated with TMP concentrations at 0, 0.4, 1, 6 and 10%, were prepared and placed in sample holder to the XDR analysis. Powder XRD was performed at room temperature, using Cu-K α radiation (Ultima IV X-ray diffractometer, Rigaku Corp., Osaka, Japan) generated at a voltage of 40 kV and a current of 20 mA. The scanning range (2θ) was from 10 to 60° with a step size of 0.02°. The CRYSTMET database (Toth Information Systems Inc., Ottawa, Canada) was used for phase identification. The crystallite sizes were estimated using the Scherrer equation ($d = K \lambda / \beta \cos \theta_B$), where d is the diameter dimension of the crystalline particle, K (0.9) is the slope factor, λ is the wavelength of the incident X-ray (1.542 Å), β is the line broadening at half the maximum intensity (FWHM), θ_B is the Bragg angle obtained from the XRD pattern.

FTIR Spectroscopy (FTIR)

Groups selected for XDR analysis were mixed with powder potassium bromide (KBr), in the proportion of 1 mg of sample to 600 mg of KBr (n=1). Soon after, a pellet was prepared with 170 mg of this mixture (sample plus KBr). The infrared absorbance spectra were recorded by the absorbance method in an FTIR spectrophotometer (Nexus 670, Nicolet Instrument Corporation Madison, USA) using 128 scans at 4 cm⁻¹ resolution in the spectral range between 400 and 4000 cm⁻¹. The intensity of the absorption band was divided by the pellet thickness, and the coefficient of absorption (α ; in cm⁻¹) was measured regarding the baseline joining the points of lowest absorbance on the peak using the subtraction of a straight line. The error of α measurement was of the 0.005 order.

Data analysis

For statistical analysis, SigmaPlot 12.0 was used, and the significance limit was set at 5%. Ca, P, Ca/P ratio, alkali and acid soluble F, F and P data showed normal (Shapiro Wilk test) and homogeneous (Cochran's test) distribution and were subjected to two-way ANOVA followed by Student-Newman-Keuls' test. Correlation

between Ca and P in HA (Pearson's test) was calculated to quantify the relationships between these ions. EDX data were described as atomic percentage of the elements. Data from structural analysis were described as a function of the presence of specific bands obtained from diverse treatment submitted to the pH cycle. FTIR data were analyzed as absorption coefficient and data obtained from XRD were analysed through diameter values of crystallite sizes.

2.4 Results

The XRD pattern obtained for the synthetic HA is shown in Figure 1a. This pattern was compared with that available at the CRYSTMET database, confirming that the material obtained by the method described above consists only of HA. The diffractograms obtained for all samples were similar to the pattern seen at CRYSTMET, but differences in the size of crystals were observed (Figure 2). A reduction of the crystallites was seen with increased TMP concentrations in the most of groups. The treatment of HA with the 500 ppm F solution associated to 1% TMP (Figure 2d) promoted an increase of its crystallinity when compared to the synthetic HA (Figure 1a). Solutions containing F without TMP led to an increase of the HA crystals in comparison to synthetic HA and an increase of the F concentration in the groups without TMP promoted an increase in the size of the crystallites.

The infrared absorption spectra of the HA synthesized are presented in the Figure 1b. The characteristic bands of the HA corresponding to the functional groups of the phosphates (PO_4^{3-}) and hydroxyl (OH^-) were observed at all spectra. The phosphate presented absorption bands between 960 and 1000 cm^{-1} (symmetric stretching - ν_1), 1000 and 1200 cm^{-1} (asymmetric stretching - ν_3) 540 and 580 (angular vibration - ν_4) and, 600 and 620 cm^{-1} (angular vibration - ν_4). The OH^- band was observed in the region of 630-650 cm^{-1} . Alterations in the intensity of most of these bands were observed when the HA, treated with F and TMP, was submitted to the pH cycle process (Table 1). The intensities of the phosphate bands to all groups were lower when compared to the synthetic HA except for the band at 964 cm^{-1} , where the most of the samples presented an increase in the intensity of this band. Furthermore, it was observed that an increase at the TMP concentration promoted a reduction in the intensity of the phosphate bands, except for 500 ppm F.

The bands at 1418 and 1451 cm^{-1} are related to the vibrational mode ν_3 (stretching) of the carbonate group that presented lower intensity at the groups with F and TMP compared with the synthetic HA (Table 1). With the increase of TMP concentration, there was a reduction in the intensity of these bands. For all groups, a reduction in the intensity of the OH^- band at 634 cm^{-1} can be observed in relation to the HA synthesized. Monohydrogen phosphate (HPO_4^{2-}) ions can be detected from the peaks at 875 and 868 cm^{-1} at the carbonated HA. In the groups with F and TMP, it was observed a reduction of this band in relation to the synthetic HA.

Figure 3 shows Ca and P concentrations in HA, and Ca/P ratio among the groups tested. Increases in the percentage of TMP in the solutions led to lower Ca content in HA for all groups ($p < 0.05$) (Anexo F). A similar pattern was seen for P concentrations in HA. This behavior can be seen in Figures 3a and 3b. Ca/P ratios were greatly influenced by both F and TMP in the solutions. For the F-free solution, TMP did not affect Ca/P ratio at any concentration tested ($p > 0.05$). On the other hand, a dose-dependent trend between TMP and Ca/P ratio was observed for the F solutions. Samples with TMP concentration between 0.4% and 1% presented significantly higher values of Ca/P ratio for the 250 ppm F, as well as between 0.6% and 2% for the 500 ppm F solution ($p < 0.05$). A strong positive correlation ($r = 0.820$, $p < 0.001$) was observed between Ca and P in the HA structure (Figure 3d). EDX analysis showed the % atomic of Ca, P, F and O (Figure 4), showing that traces of fluoride were observed according to the fluoride and TMP concentration tested (Anexo G).

Regarding alkali-soluble and acid-soluble F, the overall pattern showed that fluoride levels in both post-treated and post-cycled HA were related to F concentrations in the solutions, regardless the TMP concentrations (Figure 5). For post-treated, HA alkali-soluble F was significantly reduced for TMP concentrations between 0% and 0.8% when compared with higher TMP concentrations for the 250 and 500 ppm F solutions, while only minor changes were observed for the 100 ppm F solution (Figure 5a). Acid-soluble F concentrations were inversely related to TMP concentrations in the solutions (Figure 5c) for all F concentrations tested. For post-cycled HA, alkali-soluble F increased according to TMP concentrations for the 250 and 500 ppm F solutions, while only the 100 ppm F solution with TMP at 6% presented a slight increase. Samples of HA treated with 500 ppm F and TMP

between 2% and 10% showed the highest alkali-soluble F among all samples. Alkali-soluble F values in post-cycle samples were lower than those for the post-treatment samples.

Estimated F and TMP adsorption to HA is shown in Figure 6. Increase of TMP concentration led to a higher P adsorption in the HA structure for the 0 and 100 ppm F, while lower adsorption was seen for the solutions with the highest concentrations of fluoride (250 and 500 ppm F) ($p < 0.05$) (Figure 6a). Fluoride adsorbed was proportional to the F concentration presented in the solutions and related to the alkali-soluble F on HA ($p < 0.05$) (Figures 6b).

2.5 Discussion

This study evaluated the structural and biochemical alterations of HA treated with F and TMP using a pH cycle model, in order to provide additional data for a better understanding on the mechanisms of action of this phosphate. The present results showed that biochemical and physical properties of HA can be significantly modified by the presence of F and TMP in combination, in comparison with F or TMP alone, thus leading to the rejection of the study's null hypothesis.

The pH-cycle method used showed a reduction in the Ca/P ratio of the control group (no TMP or F). Although this protocol was able to promote an alteration in the Ca/P ratio of control and experimental groups (Figure 3), there was no change in the basic crystalline arrangement (Figure 2). In the present study, regarding the increase in the percentage of TMP in the treatment solutions there was a trend to reduction in the P concentration for all groups when compared to that of the HA. According to Rodríguez-Lorenzo et al. [16], this reduction could be related to the occurrence of P in the form of HPO_4^{2-} ($866\text{-}879\text{ cm}^{-1}$) in the sample, which occupies PO_4^{3-} sites. The HPO_4^{2-} band ($866\text{-}879\text{ cm}^{-1}$) is related to the formation of a calcium-deficient HA (Ca/P 1.5-1.6) [17] as HA synthesized in this experiment. The peak intensity in this region is higher when the Ca/P ratio or Ca concentration [18,19] is lower in the HA. These data are in line with the results obtained by FTIR and chemical analysis. The peak intensity in this region was higher in the groups without F when compared to that containing F and TMP and it was associated with a lower Ca/P ratio (Table 1). On the other hand, the decrease in the intensity of the carbonate (ν_3) bands

observed in the groups with F and TMP are related to well-mineralized apatites phases [20].

According to Freund et al. [21], the absorption band at 631 cm^{-1} reacts to the introduction of F into the OH^- chains. In particular, this band shifts markedly to higher wavenumber and decreases in intensity. In addition, new bands appear nearby. The treatment of the HA with F and TMP promoted no displacement of this absorption band in the present study. Furthermore, new bands were not observed in the spectra of the groups (Table 1) and there was no change in the basic crystalline arrangement as shown in Figure 2. It indicates that the F and TMP did not modified the structure of the HA after the pH cycle. However, it can be adsorbed on the HA as it was observed in this study (Figure 6). Thus, it would be interesting evaluate more accurately these chemical interactions in order to understand how TMP could be adsorbed. F has shown to increase the crystallinity and the Ca/P ratio, what is in line with previous data showing that HA samples treated with 1100 ppm F presented a higher crystallinity and Ca/P ratio than the HA treated with deionized water [11]. In the present study, Ca/P ratios increased according to the F concentration in the solutions, being dose-dependent. The solution containing 250 ppm F associated with TMP between 0.4 and 1% showed the highest Ca/P ratio for this F concentration which are in agreement with an *in vitro* study conducted by Missel et al. [22], that observed an improved reduction of bovine enamel demineralization when 250 ppm F was associated with TMP at 0.25 and 0.5% in dentifrices. Furthermore, the solution containing 500 ppm F associated with TMP between 0.6 and 2% also showed the highest Ca/P ratio for this F concentration and, mainly, promoted an increase in the crystallinity of the HA (Figure 2), what is also in line with *in vitro* data showing that HA treated with 500 ppm F associated to 1 and 3% TMP increased twice the alkali-soluble F content and precipitated an HA with a Ca/P ratio more similar to synthetic HA [23].

After pH-cycle, the formation of alkali-soluble F on HA was increased for the 500 ppm F group associated to TMP at higher concentrations (2 to 10%). This observation helps to explain why the addition of 3% TMP to low-fluoride dentifrices (500 $\mu\text{g F/g}$) led to an anticaries action similar to that of standard dentifrice using a pH-cycle model and bovine enamel specimens [24]. The authors also showed that this association increased fluoride and calcium present in enamel, showing results

similar to those of a standard dentifrice (containing 1100 ppm F). However, in the present study, a reduction of acid-soluble F incorporation on the HA for all F concentrations associated with TMP was observed, what is in agreement with results obtained using a similar protocol [25]. The effect of TMP and F has been related with the TMP adsorption on enamel surface that seems to involve the same binding sites as those for F and could, thus, interfere with its action depending on the TMP concentration. TMP form a “barrier” on the enamel surface that could limit acid diffusion and allow the deposition of F as CaF_2 , which is helpful in the remineralization process and would be released during acid challenges [26].

HA is usually produced from wet chemical synthesis, due to its simplicity, low cost, and easy application in industrial production [27]. It is important mention that in this study an *in vitro* model was used to simulate dissolution and precipitation for the evaluation of the effect of TMP and/or F on HA. However, this is a chemical model and therefore it presents limitations, especially related to the inability to reproduce the complex intraoral conditions. Such as, the saliva and the acquired pellicle are extremely important in the de- and remineralization process as well for adsorption of ions and molecules to the HA structure.

2.6 Conclusion

To conclude, the combination of F and TMP promoted changes in the biochemical and physical properties of HA. An appropriate TMP: F molar ratios can precipitate a more crystalline HA and with lower amount of impurities. It was also observed that a lower TMP adsorption on the HA structure occurred in the presence of F.

Acknowledgments

The authors thank the FAPESP for the financial support (process 2011/07788-7) and for the scholarship (process 2011/17234-9) for the first author and Élton J. Souza for the EDX measurements.

References

1. Li Y, Kong F, Weng W. Preparation and characterization of novel biphasic calcium phosphate powders (α -TCP/HA) derived from carbonated amorphous calcium phosphates. *J Biomed Mater Res Part B: Appl Biomater.* 2009;89B: 508-17.
2. Krajewski A, Mazzocchi M, Buldini PL, Ravaglioli A, Tinti A, Taddei P, Fagnano C. Synthesis of carbonated hydroxyapatites: efficiency of the substitution and critical evaluation of analytical methods. *J Mol Struct.* 2005;744-747:221-228.
3. Johansson AK, Omar R, Carlsson GE, Johansson A. Dental erosion and its growing importance in clinical practice: from past to present. *Int J Dent* 2012; 2012: 632907.
4. Pessan JP, Toumba KJ, Buzalaf MA. Topical use of fluorides for caries control. *Monogr Oral Sci.* 2011;22:115-32.
5. Manarelli MM, Vieira AEM, Matheus AA, Sasaki KT, Delbem ACB. Effect of mouth rinses with fluoride and trimetaphosphate on enamel erosion: an in vitro study. *Caries Res.* 2011;45:506-9.
6. Favretto CO, Danelon M, Castilho FCN, Vieira AEM, Delbem ACB. In vitro evaluation of the effect of mouth rinse with trimetaphosphate on enamel demineralization. *Caries Res.* 2013;47:532-8.
7. Danelon, M, Takeshita, EM, Sasaki, KT, Delbem, ACB. In situ evaluation of a low fluoride concentration gel with sodium trimetaphosphate in enamel remineralization. *Am J Dent.* 2013;26:15-20.
8. Takeshita EM, Castro LP, Sasaki KT, Delbem ACB. In vitro evaluation with low fluoride content supplemented with trimetaphosphate. *Caries Res.* 2009;43:50-6.
9. Moretto MJ, Magalhães AC, Sasaki KT, Delbem ACB, Martinhon CCR. Effect of different fluoride concentrations of experimental dentifrices on enamel erosion and abrasion. *Caries Res.* 2010;44:135-40.
10. Van Dijk JW, Borggreven JM, Driessens FC. The effect of some phosphates and a phosphonate on the electrochemical properties of bovine enamel. *Arch Oral Biol.* 1980;25:591-5.

11. Delbem ACB, Alves KMRP, Sasaki KT, Moraes JCS. Effect of Iron II on Hydroxyapatite Dissolution and Precipitation in vitro. *Caries Res.* 2012;46:481–7.
12. Qu H, Wei M. Synthesis and characterization of fluorine-containing hydroxyapatite by a pH-cycling method. *J Mater Sci Mater Med.* 2005;16:129-33.
13. Vogel GL, Chow LC, Brown WE: A microanalytical procedure for the determination of calcium, phosphate and fluoride in enamel biopsy samples. *Caries Res.* 1983;17:23-31.
14. Fiske CH, Subarrow Y: The colorimetric determination of phosphorus. *J Biol Chem.* 1925;66:375-400.
15. Caslavská V, Moreno EC, Brudevold F. Determination of the calcium fluoride formed from in vitro exposure of human enamel to fluoride solutions. *Arch Oral Biol.* 1975;20:333-9.
16. Rodríguez-Lorenzo LM, Hart JN, Gross KA. Influence of fluorine in the synthesis of apatites: synthesis of solid solutions of hydroxyl-fluorapatite. *Biomaterials.* 2003;24:3777-85.
17. Wilson RM, Elliott JC, Dowker SEP. Formate incorporation in the structure of Ca-deficient apatite: Rietveld structure refinement. *J Solid State Chem.* 2003;174: 132-40.
18. Wilson RM, Elliott JC, Dowker SEP, Rodríguez-Lorenzo LM: Rietveld refinements and spectroscopic studies of the structure of Ca-deficient apatite. *Biomaterials.* 2005;26:1317-27.
19. Elliott JC. Hydroxyapatite and nonstoichiometric apatites. In Elliott JC, editor. *Structure and chemistry of the apatites and other calcium orthophosphates.* Amsterdam: Elsevier 1994. pp 111-86.
20. Antonakosa A, Liarokapisa E, Leventouri T. Micro-Raman and FTIR studies of synthetic and natural apatites. *Biomaterials.* 2007;28:3043-54.
21. Freund F and Knobel RM. Distribution of fluorine in hydroxyapatite studied by infrared spectroscopy. *J Chem Soc Dalton Trans.* 1977.1136-1140.
22. Missel EMC, Delbem ACB, Vieira AEM, Sasaki KT, Cruz NVS, Percinoto C. Avaliação de dentifrícios com concentração reduzida de fluoreto associada ao

- trimetafosfato de sódio na desmineralização do esmalte. *Braz Oral Res.* 2010;24:247-83.
23. Souza JAS, Takeshita EM, Zaze ACSF, Sasaki KT, Moraes JCS, Delbem ACB. Effect of trimetaphosphate and fluoride association on hydroxyapatite dissolution and precipitation in vitro. *Braz Oral Res.* 2011;29:90.
24. Takeshita EM, Exterkate RAM, Delbem ACB, ten Cate JM. Evaluation of different fluoride concentrations supplemented with trimetaphosphate on enamel de- and remineralization in vitro. *Caries Res.* 2011;45:494-7.
25. Souza JAS, Amaral JG, Moraes JCS, Sasaki KT, Delbem ACB. Effect of Sodium Trimetaphosphate on Hydroxyapatite Solubility: An In Vitro Study. *Braz Dent J.* 2013;24:235-40.
26. Manarelli MM, Delbem AC, Lima TM, Castilho FC, Pessan JP. In vitro Remineralizing Effect of Fluoride Varnishes Containing Sodium Trimetaphosphate. *Caries Res* 2014; 48: 299-305.
27. Liu C, Huang Y, Shen W, Cui J. Kinetics of hydroxyapatite precipitation at pH 10 to 11. *Biomaterials.* 2001;22(4):301-6.

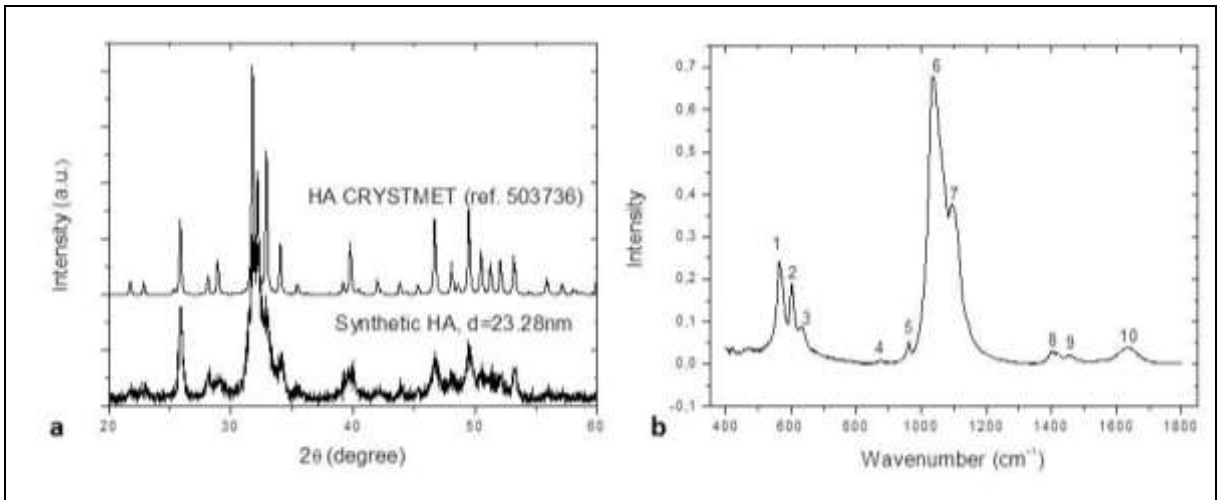


Figure 1. a: XRD patterns of the synthetic HA and CRYSTMET database. b: HA spectra obtained for synthetic HA (Peaks 1,2: PO_4^{3-} ; 3: OH^- ; 4: HPO_4^{2-} ; 5, 6 and 7, PO_4^{3-} ; 8 and 9: CO_3 ; 10: H_2O).

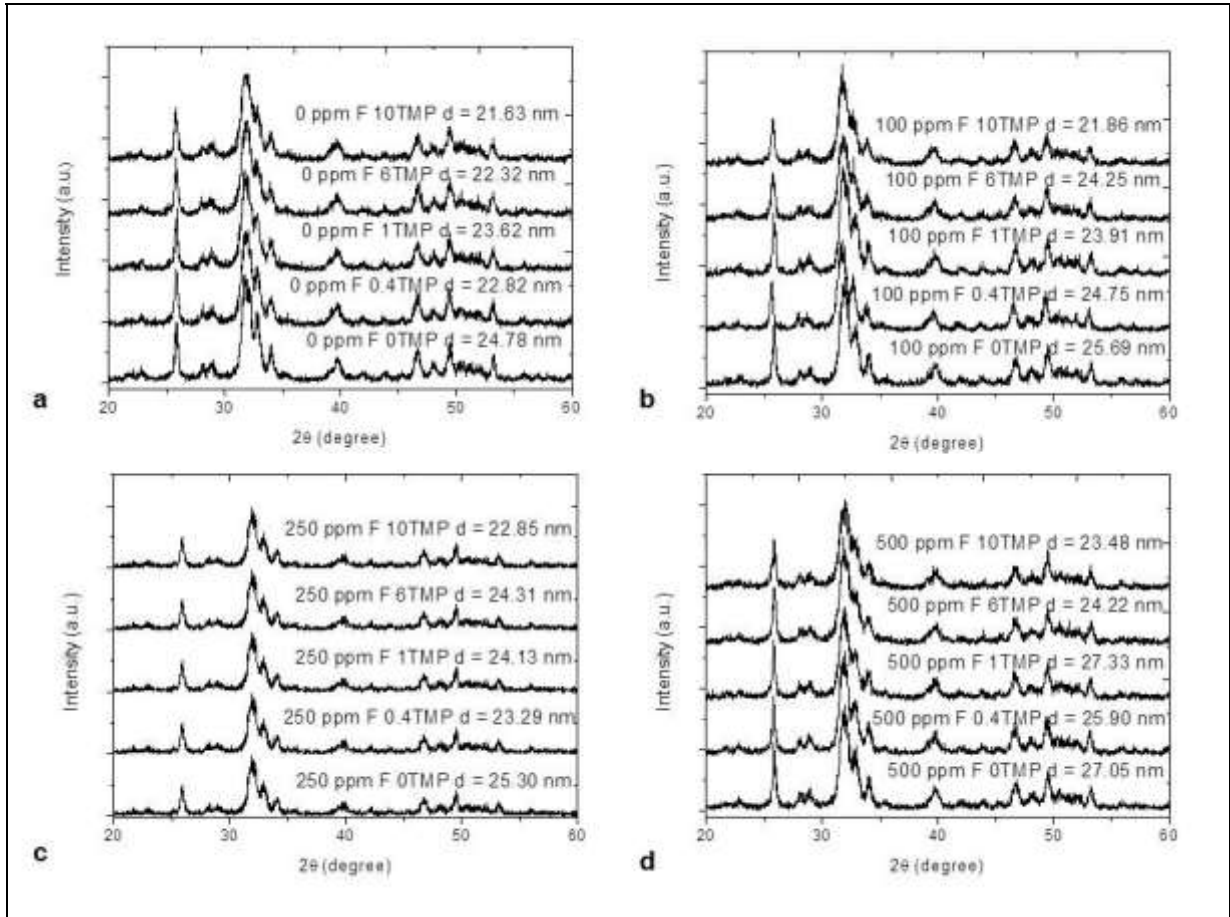


Figure 2. XRD patterns of HA according to the groups evaluated associated with TMP. 0 ppm F (a); 100 ppm F (b); 250 ppm F (c); 500 ppm F (d). The diameter values (nm) of the crystal after pH cycle according to the fluoride concentration (ppm F) and percentage of TMP are represented by the letter d.

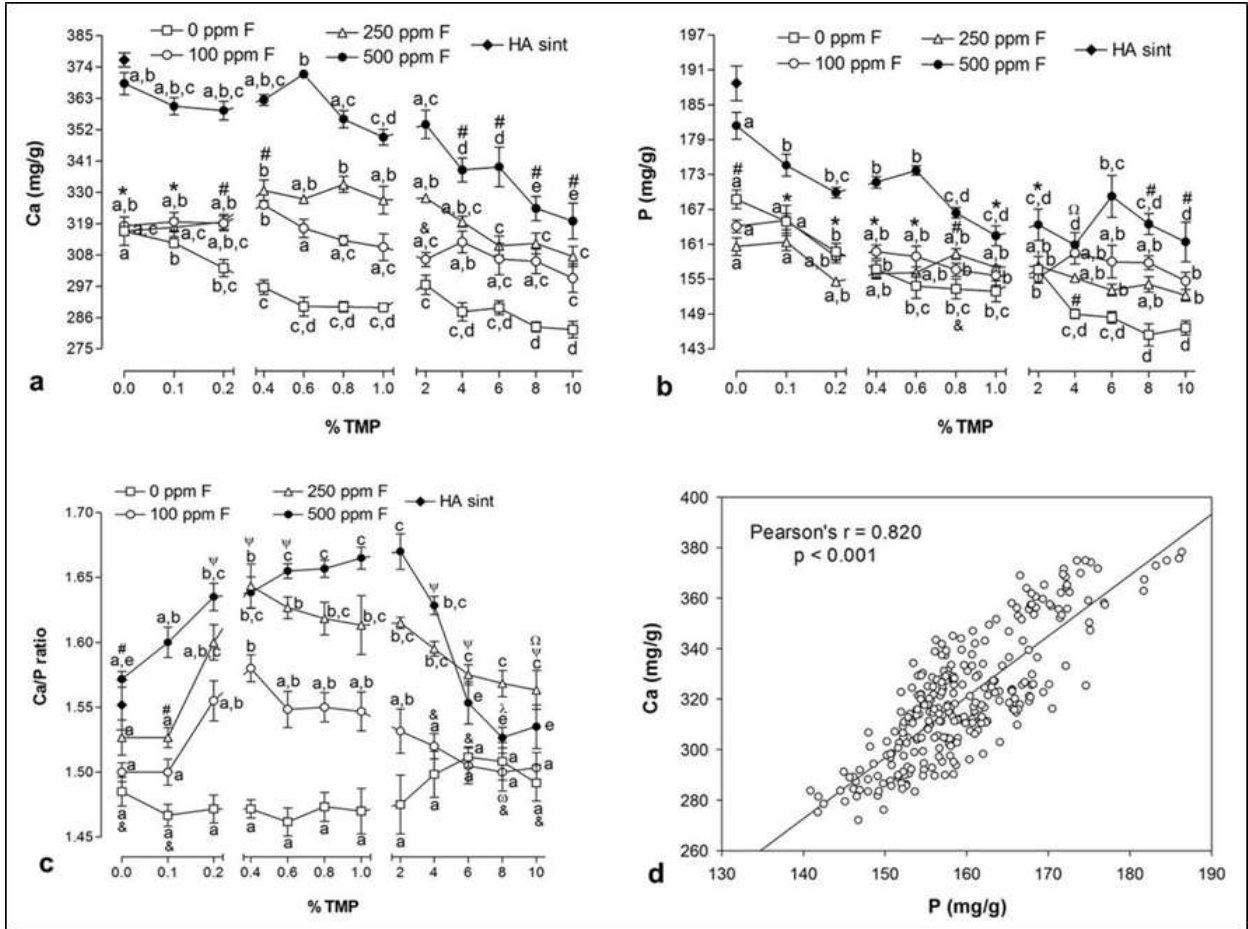


Figure 3. Mean (\pm se) of values of Ca (a), P (b) and Ca/P ratio (c) on hydroxyapatite synthesized and after pH cycle according to the F and TMP concentration. Correlation: concentration of calcium and phosphorus on hydroxyapatite (d). Distinct letters show significant differences between the % TMP for each fluoride concentration (Student-Newman-Keuls, $p < 0.05$). (*) 0 ppm F = 100 ppm F = 250 ppm F; (&) 0 ppm F = 100 ppm F; (Φ) 0 ppm F = 250 ppm F; (#) 100 ppm F = 250 ppm F; (λ) 0 ppm F = 500 ppm F; (Ω) 100 ppm F = 500 ppm F; (Ψ) 250 ppm F = 500 ppm F; (ω) 100 ppm F = 250 ppm F = 500 ppm F.

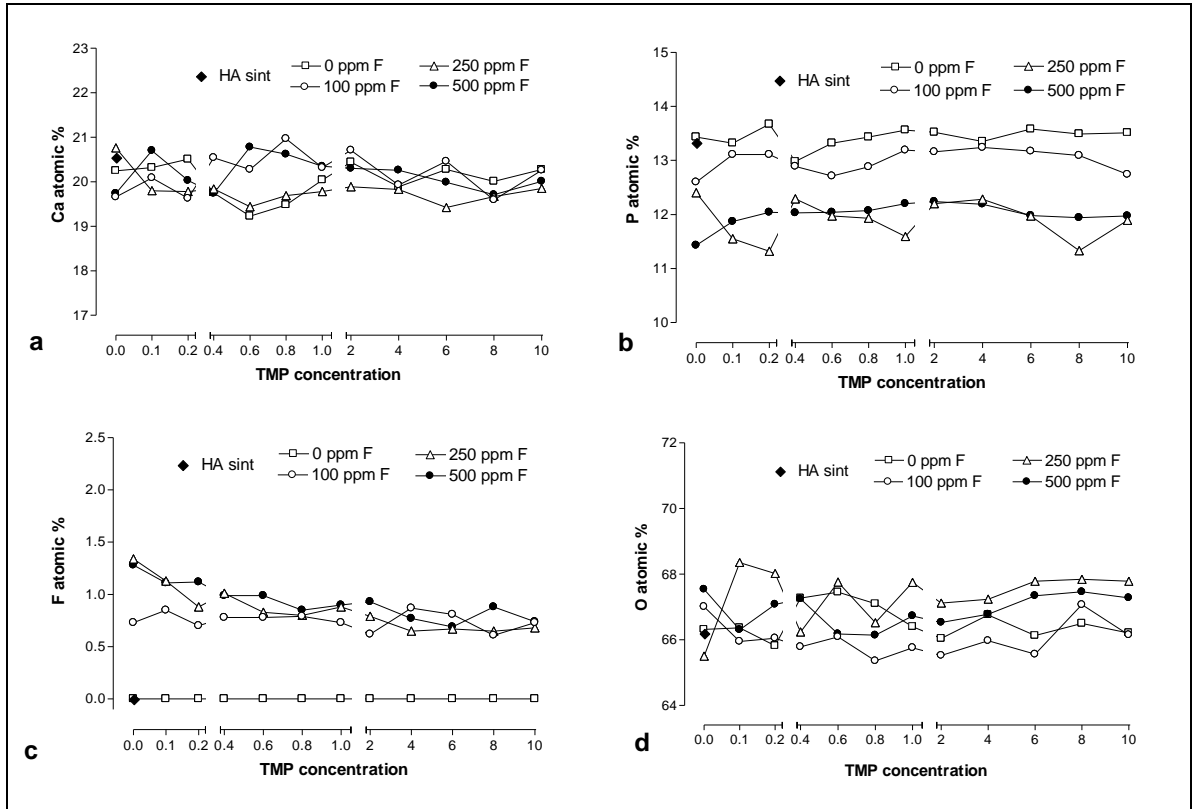


Figure 4. Atomic % of Ca (a), P (b), F(c) and O (d) in HA according to the F concentration associated with TMP.

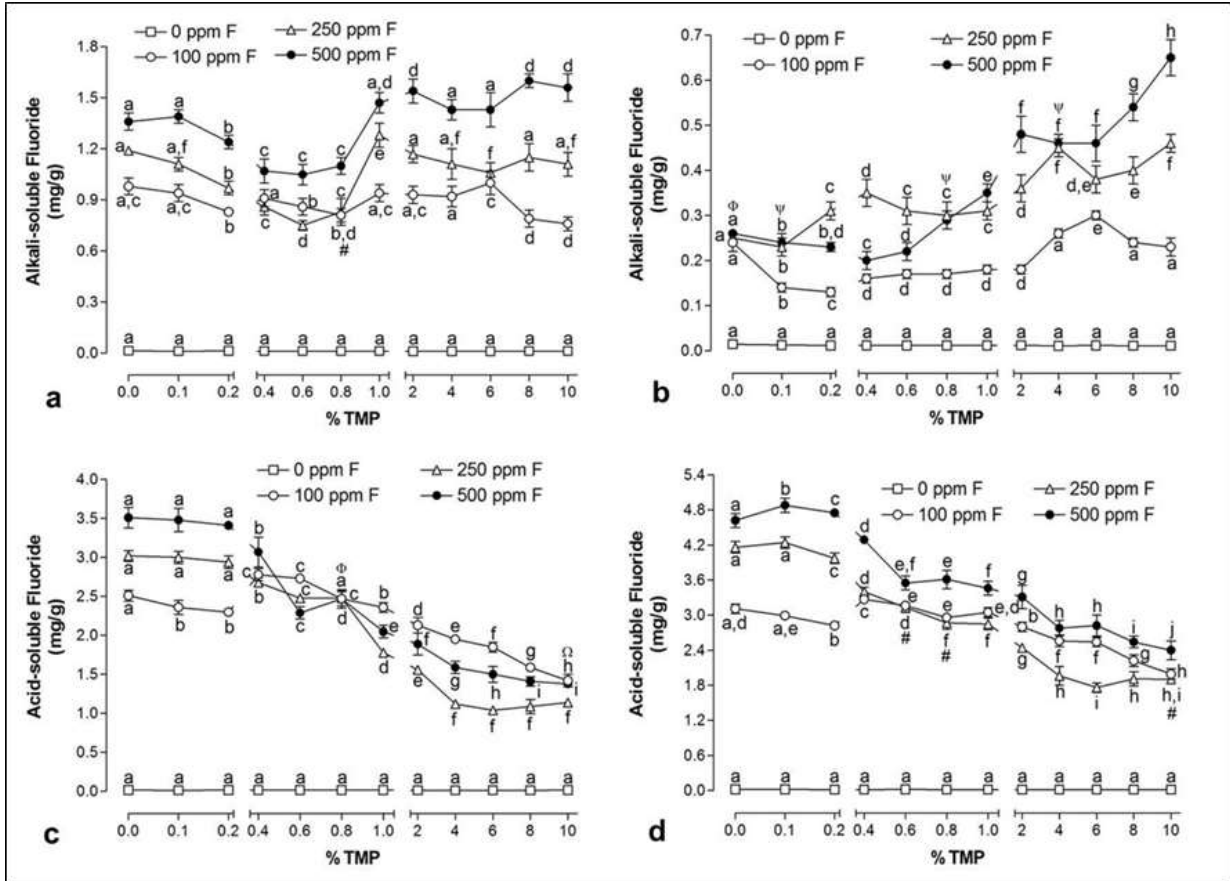


Figure 5. Mean (\pm se) of alkali-soluble F on HA after treatment (a) and after pH cycle (b); acid-soluble F on HA after treatment (c) and after pH cycle (d). Distinct letters show significant differences between the % TMP for each fluoride concentration (Student-Newman-Keuls, $p < 0.05$). (#) 100 ppm F = 250 ppm F; (ψ) 250 ppm F = 500 ppm F; (λ) 0 ppm F = 500 ppm F; (Φ) 100 ppm F = 250 ppm F = 500 ppm F; (Ω) 100 ppm F = 500 ppm F. Concentrations (mg/g) (mean \pm SD) of alkali and acid soluble F in the synthetic HA were: 0.02 (0.0) and 0.01 (0.0), respectively.

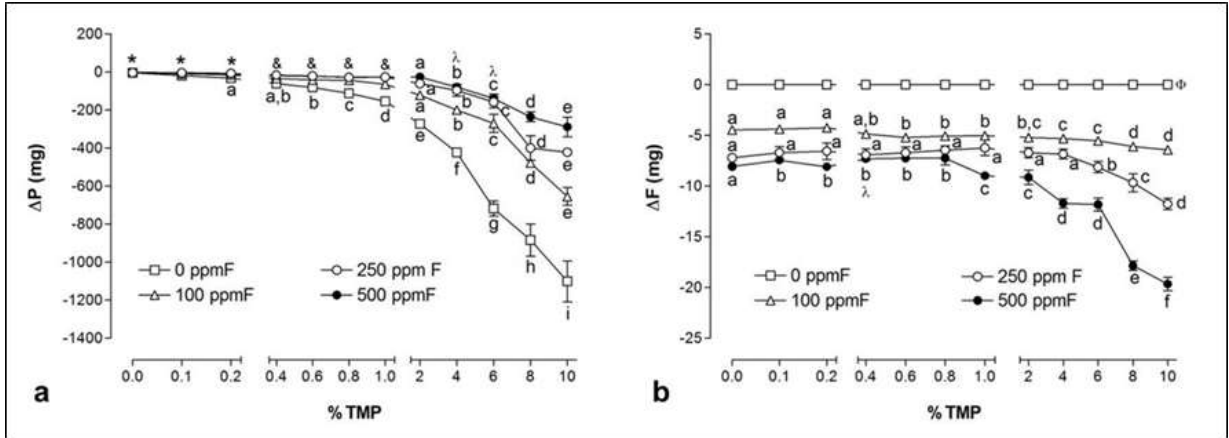


Figure 6. Mean (\pm se) of F and TMP adsorbed to hydroxyapatite (a) adsorption of TMP (expressed through the amount of phosphorus), (b) adsorption of fluoride. Distinct letters show significant differences between the %TMP for each fluoride concentration (Student-Newman-Keuls, $p < 0.05$). (*) All comparisons show similarity; (&) 100 ppm F = 250 ppm F = 500 ppm F; (λ) 250 ppm F = 500 ppm F; (Φ) no difference among the %TMP in 0 ppm F group.

Table 1. Absorption coefficient obtained in the FTIR analysis according to the groups evaluated regarding the F and TMP concentration after pH cycle

Groups		Wavenumber (cm ⁻¹)								
ppm F	TMP%	565	603	634	874	964	1,039	1,094	1,418	1,451
	Synthetic H _A	4.879	3.740	1.650	0.151	0.695	17.459	8.920	0.590	0.457
0	0	4.132	3.056	1.253	0.220	1.175	13.264	7.366	0.427	0.351
	0.4	4.100	3.180	1.300	0.100	0.881	13.230	7.312	0.302	0.205
	1	3.488	2.800	1.272	0.120	0.828	10.939	6.283	0.263	0.218
	6	3.812	2.936	1.248	0.102	0.815	12.179	6.827	0.280	0.243
	10	3.997	3.183	1.529	0.197	0.887	12.165	6.966	0.234	0.196
100	0	4.911	4.159	1.614	0.152	0.965	16.464	9.426	0.541	0.473
	0.4	4.389	3.440	1.210	0.121	0.945	14.459	7.967	0.368	0.349
	1	3.682	3.166	1.234	0.103	0.758	11.922	6.624	0.289	0.243
	6	3.951	3.393	1.318	0.064	0.767	12.730	7.054	0.301	0.262
	10	4.259	3.445	1.405	0.089	0.732	13.350	7.227	0.319	0.261
250	0	4.732	3.972	1.637	0.191	0.929	14.803	7.871	0.433	0.365
	0.4	3.810	3.177	1.454	0.078	0.671	11.610	6.422	0.405	0.370
	1	4.412	3.647	1.604	0.143	0.742	13.302	7.223	0.384	0.318
	6	3.353	2.725	1.250	0.058	0.586	9.861	5.735	0.261	0.261
	10	3.860	3.201	1.540	0.084	0.638	10.595	6.297	0.327	0.327
500	0	3.185	2.712	1.193	0.058	0.522	9.260	5.412	0.305	0.286
	0.4	3.804	3.093	1.312	0.103	0.717	12.131	6.525	0.378	0.339
	1	3.379	2.746	1.173	0.056	0.561	10.459	5.889	0.351	0.302
	6	3.559	2.803	1.314	0.103	0.619	11.128	5.379	0.316	0.248
	10	3.742	3.144	1.515	0.066	0.519	11.016	6.266	0.349	0.299

* 565, 603, 964, 1039 and 1094 cm⁻¹ correspond to phosphate bands; 874 cm⁻¹ correspond to monohydrogen phosphate (HPO₄²⁻); the carbonate vibrational mode is located at regions of 1418 and 1451 cm⁻¹ and the OH band was observed at 634 cm⁻¹.

CAPÍTULO 2

Biochemical and structural analysis of hydroxyapatite solubility treated with fluoride and sodium trimetaphosphate

3.1 Abstract

This study aimed to evaluate the effect of sodium trimetaphosphate (TMP) associated with fluoride (F) on structure and dissolution of hydroxyapatite (HA). Synthetic HA powder (1.0 g) was suspended (n=6) in solutions containing TMP varying at 0-10% associated with 0, 1100, 4500 and 9000 ppm F. The precipitates were filtered, dried (24 h at 37°C), ground and submitted to a pH cycle. Samples were analyzed by Fourier transformed infrared spectroscopy (FTIR), X-ray diffraction (XRD) and energy-dispersive X-ray spectroscopy (EDX). The concentration of F, Ca and P were determined in HA, and P and F in the supernatants. Data were submitted to ANOVA, followed by Student-Newman-Keuls' test ($\alpha=0.05$). Higher Ca/P ratios were observed with TMP at 2- 4% for the 1100 ppm F solution, and at 4-8% for the 4500 and 9000 ppm F solutions ($p<0.05$). The overall trend was that alkali-soluble F deposition was directly related to TMP concentrations in the treatment solutions, while acid-soluble incorporation was inversely related to TMP concentrations ($p<0.05$). The increase of TMP provided a greater P adsorption in the HA structure for the 0 and 1100 ppm F solutions ($p<0.05$). XRD data indicated that HA powder crystallinity is altered according to the addition of F:TMP and all diffractograms and FTIR spectra obtained showed a similar pattern that for pure HA. In conclusion, when TMP and F are co-administered, TMP interferes with F deposition on HA and an ideal TMP:F ratio can provide an enhancement of the fluoride products and precipitate a HA with low solubility.

Keywords: hydroxyapatite, polyphosphates, fluoride, dissolution.

*Capítulo escrito de acordo com as instruções do periódico Journal of Materials Science: Materials in Medicine

3.2 Introduction

Tooth enamel is predominantly composed by hydroxyapatite (HA), which is a calcium phosphate and can be susceptible to basically two types of demineralization, either caused by dental biofilm acids (dental caries) and arising from acids from food, medicines, environment or gastric acids (known as dental erosion) [1,2]. There is no question that fluoride (F) has been the cornerstone in strategies to prevent dental caries [2]. Moreover, recent reports have shown that F has been studied on the prevention and treatment of dental erosion [3].

Nonetheless, considering modern habits of the population and the increasing of risk factors for the development of these oral diseases, current research is focused on the development of strategies to improve the efficacy of topically applied fluoridated products [4], at the same time as reducing F exposure, as this ion has been related to an increasing of dental fluorosis in young children [5]. A large number of new or improved F products have been released at marketplace, which include toothpastes, fluoride varnishes, gels, restoratives materials and mouthrinses.

Among the promising products that have been studied, several formulations containing F and sodium trimetaphosphate (TMP) are described in the literature. *In vitro* [6-13], *in situ* [14,15] and clinical studies [16] demonstrated that TMP-containing fluoridated dentifrices, gels, mouthrinses and varnishes have a higher protective effect for both dental caries and erosion when compared with products without TMP. However, the protocols used in the above-mentioned studies do not provide detailed information regarding the interaction between the F:TMP with the tooth structure. Given that the mechanisms of action of F and TMP in association has not yet been completely elucidated, it would be interesting to evaluate the direct interaction of these compounds with HA, which is the main mineral component of enamel. Biochemical and structural analysis in HA powder would be one way to provide new insights into the mechanisms of action of F and TMP when associated in formulations for topical use.

Thus, the aim of this study was to evaluate the effect of the most commonly F concentrations presented in oral health products, as dentifrices, gels and varnishes (0, 1100, 4500, 9000 ppm F), associated with TMP varying at 0-10% on HA structure after submitted to a pH cycle, in order to verify changes that might occur on HA structure, as well as the effects of TMP on the deposition of alkali- and acid-soluble

F. Combined to this, knowing the ideal F:TMP ratio can be helpful in developing new products for oral hygiene.

3.3 Materials and Methods

Synthesis of HA

HA powders were synthesized according to the protocol by Qu and Wei's [17]. Initially, 1 mol L⁻¹ (300 mL) calcium nitrate solution (Ca(NO₃)₂·H₂O, Sigma-Aldrich Corp. St. Louis, MO, USA) and 0.3 mol L⁻¹ (600 mL) diammonium phosphate solution ((NH₄)₂HPO₄, Sigma-Aldrich Corp. St. Louis, MO, USA) were prepared and the pH of each solution was raised to 10–12 by adding NH₄OH (29.5%). Diammonium phosphate solution was added slowly to the calcium nitrate solution (2–5 mL/min), under constant agitation at 37 °C, in order to precipitate the fully-crystallized HA. The precipitates were aged for 7 days at 37 °C while the pH was checked every day and maintained at around 10 for the growth and formation of a single crystalline phase. During synthesis, the system remained open in order to precipitate a carbonated HA similar to that found in dental tissue. The precipitate was collected by filtration using a Buchner funnel attached to a vacuum system (–600 mmHg), washed repeatedly with deionized water (250 ml/0.5 g HA) and anhydrous ethanol in order to remove the contaminated ions (NH₄⁺ and NO₃⁻) [18], and subsequently dried for 24 h at 70 °C. The precipitate was then ground into a fine powder, all samples had the particle size reduced to less than 53 µm using a ball mill (Pulverisette 7, Fritsch, Germany). Six samples of approximately 0.5 g were separated for biochemical and structural analysis (Anexo B).

Treatment and pH Cycle

Solutions (100 mL, n=6) of TMP (Na₃P₃O₉, Sigma-Aldrich Co., USA) were prepared at 0, 0.1, 0.2, 0.4, 0.6, 0.8, 1.0, 2.0, 4.0, 6.0, 8.0, and 10%, associated with 0, 1100, 4500 and 9000 ppm F (NaF, Merck, Darmstadt, Germany), totaling 48 combinations. Following, synthetic HA powder were submitted to the treatment and subsequently to one pH cycle.

Treatment. The synthetic HA powder (1.0 g) was suspended under agitation in each of the prepared solutions during 2 min at 37°C. Afterwards, the precipitate was collected by filtration using a Buchner funnel attached to a vacuum system (–600

mmHg), washed repeatedly with deionized water (250 ml/0.5 g HA) and dried for 24 h at 37°C. The precipitate was then ground again into a fine powder with the aid of a ball mill (Pulverisette 7, Fritsch, Germany). An aliquot of supernatant was collected to evaluate the F and P concentration in order to calculate the P and F adsorption in the HA.

pH Cycle. After the treatment with the solutions, HA powder of each group was suspended in deionized water and the pH of the suspensions was slowly reduced to 4.0 using 1 mol L⁻¹ nitric acid (HNO₃, Merck, Darmstadt, Germany) under agitation. After 30 min of equilibration, the pH of each solution was raised to 7.0 by the addition of 1 mol L⁻¹ sodium hydroxide (NaOH, Merck, Darmstadt, Germany). Samples of synthetic HA powder (n= 6) were suspended in deionized water and used as negative control. After completion of this process, the precipitates were immediately separated by filtration, washed with deionized water, dried for 24 h at 37 °C and ground into a fine powder as described above (Anexo C).

HA powder was analyzed in duplicate for F, calcium (Ca) and phosphorus (P) concentrations; for energy-dispersive X-ray spectroscopy (EDX), X-ray diffraction (XRD) and Fourier transform infrared spectroscopy (FTIR).

Calcium and phosphorus analysis in hydroxyapatite

For Ca and P determination, 5 mg of HA powder was weighed into pre-weighed micro-centrifuge tubes and 2.0 mL of 1 mol L⁻¹ HCl was added. After agitation for 1 h (Shaker, SK-300, Lab. Companion, Kimpo City, Korea), Ca analysis was performed using a spectrophotometer (Microplate Spectrophotometer EONC, Biotek, USA) with a wavelength of 650 nm by adopting the Arsenazo III colorimetric method [19]. Aliquots of 5 µL were taken from the samples (diluted 1:10 and partly neutralized) and added to 50 µL of deionized water and Arsenazo. For calibration, standards containing 40 to 200 µg Ca/mL were used. Phosphorus was measured by the molybdate method (colorimetric method) using aliquots of 20 µL from the samples, which were subsequently added to a mixture of 50 µL molybdate solution and 20 µL of reactive reducer, as described by Fiske and Subbarow [20], at a wavelength of 660 nm and standards containing 1.5 to 24 µg P/mL were used (Anexo D).

Fluoride analysis (alkali- and acid-soluble)

For fluoride analysis, 5 mg of the treated and cycled HA powder was weighed into pre-weighed micro-centrifuge tubes, and 2.0 mL of 1 mol L⁻¹ KOH was added for alkali-soluble extraction, according to the protocol described by Caslavská et al. [21], with some modifications. After 24 h of continuous agitation (Shaker, SK-300, Lab. Companion, Kimpo City, Korea), the samples were centrifuged for 20 min at 2900 × g. A 0.5 mL aliquot of the supernatant was neutralized with 0.5 mL of TISAB II (total ionic strength adjustment buffer) modified with 1 mol L⁻¹ HCl (0.82 mL HCl/L). Alkali-soluble F concentration was determined by using a specific electrode (Orion 9409BN, Thermo Scientific, Beverly, MA, USA) and reference electrode (Orion 900100) connected to an ion analyzer (Orion 720⁺, Thermo Scientific, Beverly, MA, USA).

For determination of acid-soluble F [22], the precipitate was washed three times with deionized water and once with methanol. After methanol evaporation (overnight at 60 °C), 1 mL of 1 mol L⁻¹ HCl was added, and the samples were homogenized for 30 s by vortexing, and subsequently agitated for 1 h at room temperature. 0.5 mL aliquot of these samples was then added to 0.5 mL of TISAB II modified with 20 g NaOH/L. Samples were analyzed for acid-soluble F as described for alkali-soluble F (Anexo E)

Phosphorous and fluoride analysis in suspension during HA treatment

F and P concentrations were determined in aliquots removed from the suspensions during treatment. Phosphorus was determined using an aliquot of 100 µL of sample and standards, added to 50 µL molybdate and 20 µL of reactive reducer through the colorimetric method described by Fiske & Subbarow [20]. Fluoride was determined by a specific electrode (Orion 9409BN, Thermo Scientific, Beverly, MA, USA) and an inverted reference electrode (Orion 900100) coupled to an ion analyzer (Orion 720 A⁺, Thermo Scientific, Beverly, MA, USA). The electrode was calibrated with standards containing 0.25 to 4.00 µg F / ml and 4.0 to 64.0 µg F / ml under the same conditions of samples. Aliquots of 40 µL of samples and the same volume of TISAB II were dispensed on the active tip of the reference electrode. Analyses were performed in duplicate. Afterwards, the adsorption of F and TMP to hydroxyapatite

was calculated from the initial concentrations of these compounds in the solutions and the concentration after pH-cycle.

Structural analyses (FTIR and XRD)

HA samples (n=1) of all F concentrations tested associated with TMP at 0, 1, 4 and 10% were submitted to the FTIR and XRD analysis. These concentrations were selected based on the results obtained in the biochemical analysis of HA. For FTIR analysis, all samples had the particle size reduced to less than 53 μm using a ball mill (Pulverisette 7, Fritsch, Germany) in order to allow lower IR irradiation scattering, especially at high wavenumber. Samples (1 mg) were mixed to 600 mg of a dry potassium bromide (KBr) and a pellet was prepared. The infrared absorbance spectra were recorded by a transmitted radiation method through a FTIR spectrophotometer (Nexus 670, Nicolet Instrument Corporation, Madison, USA) using 128 scans at 4 cm^{-1} resolution in the spectral range between 400 and 4000 cm^{-1} . The intensity of the absorption band was divided by the pellet thickness, and the coefficient of absorption (α) was measured regarding the baseline joining the points of lowest absorbance on the peak using the subtraction of a straight line. Thus, α value obtained was compared among the groups evaluated. The error of α measurement was of the 0.005 order.

XRD analysis was performed at room temperature using a $\text{CuK}\alpha$ radiation (Ultimate IV X-ray diffractometer, Rigaku Corp., Osaka, Japan) generated at a voltage of 40 kV and a current of 20 mA. The scanning range (2θ) was from 10 to 60° with a step size of 0.02°. The CRYSTMET database (Toth Information Systems Inc., Ottawa, Canada) was used for phase identification. The crystallite sizes were estimated using the Scherrer equation ($d = K \lambda / \beta \cos \theta_B$), where d is the diameter dimension of the crystalline particle, K (0.9) is the slope factor, λ is the wavelength of the incident X-ray (1.542 Å), β is the line broadening at half the maximum intensity (FWHM), θ_B is the Bragg angle obtained from the XRD pattern.

Energy-dispersive X-ray spectroscopy (EDX)

The EDX, an analytical technique used for chemical characterization, allowed assessing the atomic percentage of the elements Ca, P, oxygen (O), and F; it was performed in order to complement and support the discussion of the results obtained

by structural as well as biochemical analysis. HA powders were dropped onto a specific holder and the characterization was carried out using a scanning electron microscope (Carl Zeiss, model EVO LS-15, NTS, LTD, Germany) at a voltage of 20kV (\times 500-1000 magnification) associated with energy-dispersive X-ray spectrophotometer (Oxford Instrument, Inca X-act) with 133eV resolution.

Data analysis

For statistical analysis, SigmaPlot 12.0 was used, and the significance limit was set at 5%. Ca, P, Ca/P ratio, alkali- and acid-soluble F of HA, and F and P data in the suspensions showed normal (Shapiro Wilk test) and homogeneous (Cochran's test) distributions and were subjected to two-way ANOVA followed by Student-Newman-Keuls' test. Correlation between Ca and P in HA (Pearson's test) was calculated to quantify the relationships between these ions under all conditions studied. FTIR and XDR were described according to the presence of specific bands obtained from different treatment submitted to the pH cycle. FTIR data were analyzed as absorption coefficient and data obtained from XRD were used to evaluate the diameter values of crystallite sizes. EDX data were described as atomic percentage of the elements.

3.4 Results

The diffractograms obtained for the HA synthetic were compared with the HA XRD pattern in the CRYSTMET data base, confirming that the powder synthesized by the method used in the present study consists of HA (Figure 1a). The synthetic HA powder spectra (Figure 1b) show typical peaks of a carbonated HA in the regions of 565 (ν_4), 603 (ν_4), 874 (ν_2), 964 (ν_1), 1039 (ν_{3c}) and 1094 (ν_{3a}) cm^{-1} , which correspond to phosphate bands; the carbonate vibrational mode is located at regions of 1418 and 1451 cm^{-1} (ν_3) and the OH band was observed at 634 cm^{-1} (ν_4). The FTIR data are presented in the Table 1.

All diffractograms obtained showed a similar pattern to that presented in the CRYSTMET data base for HA, confirming that the HA presented the same crystalline arrangement after the cycle process. The diameter values (nm) of the crystal after pH cycle according to the fluoride concentration (ppm F) and percentage of TMP are shown in Figure 2. These data indicated that the HA powder crystallinity may be

altered according to the addition of F and TMP. No displacement of the position of any absorption peak was observed. The FTIR analyses indicate an overall reduction of P intensity compared to the synthetic HA, a reduction in the intensity of carbonate and OH⁻ band with the presence of F. These data are also presented in the Table 1.

Ca, P and Ca/P ratios for HA synthetic and in the groups tested are presented in Figure 3. An increase in the percentage of TMP in the solutions led to lower Ca content in HA for all groups, except for the 9000 ppm F solutions. A similar behavior was seen for P concentrations. Regarding Ca/P ratios, no significant differences were observed for the F-free solution at any TMP concentration tested ($p < 0.05$). TMP concentrations at 2% and 4% promoted higher Ca/P ratios for the 1100 ppm F solution, while TMP concentrations at 4-8% led to the highest Ca/P ratios for the 4500 and 9000 ppm F solutions, respectively ($p < 0.05$). A strong correlation was observed between Ca and P in the HA structure, as shown in Figure 2d ($r = 0.889$, $p < 0.001$ (Anexo H)).

Figure 4 presents alkali-soluble and acid-soluble for both treated and post-cycled HA. No significant changes were observed for alkali-soluble and acid-soluble in HA treated with F-free solutions ($p > 0.05$) for both substrates. For F-containing solutions, alkali-soluble in treated HA tended to increase according to TMP concentrations for the 1100 ppm F groups, while no accentuated changes were observed for the 4500 and 9000 ppm F solutions. A decrease in acid-soluble according to the TMP concentration of 0-10% was observed for all groups. Post-cycled HA treated with 9000 ppm F and TMP at 4% and 8% had the highest alkali-soluble concentrations among the groups tested ($p < 0.001$). However, alkali-soluble showed lower values than for the post-treatment samples. Figure 5 shows the atomic % of Ca, P, F and O in HA according to the F concentration), showing that traces of fluoride were observed after the pH cycle (Anexo I).

Estimated F and TMP adsorbed by HA are shown in Figure 6. Overall, increases in TMP concentrations led to increase of P adsorption in the HA structure for the 0 and 1100 ppm F, but the adsorption was lower for solutions with 4500 and 9000 ppm F (Figure 6a). Fluoride adsorbed by HA was proportional to the F concentration presented in the solutions (Figure 6b).

3.5 Discussion

Studies have suggested that an ideal TMP:F ratio allows enhancement of the effects of oral health products by reducing demineralization of sound enamel, promoting an improved remineralization of caries lesions, as well as by reducing enamel erosive wear [6-15]. The present study was conducted in order to provide new insights into the mechanisms of this phosphate when associated with F, by assessing the biochemical and structural changes of HA treated with F and TMP using a pH cycle model.

HA used in this study was precipitated by a wet-chemical process and has similar characteristics to bone and tooth tissue [23]. This pH cycle model and HA powder was used in this study in order to obtain a greater interaction between fluoride and HA crystals [22], in contrast with *in vitro* models using bovine or human enamel slabs. This protocol did not include artificial or human saliva, which contains ions and buffers that are essential in the de- and remineralization processes under intra-oral conditions. Although this may be considered as a limitation of the protocol used, this was deliberately done so that the only sources of Ca e P were HA itself and TMP, without any other source that could potentially interfere with the data interpretation. The method used promoted a reduction in the Ca/P ratio for the control group (without TMP and F) and this fact was mainly related to loss of Ca from HA, which is in agreement with the study by Souza et al. [24] using a similar protocol involving HA powder and pH cycling. The FTIR analyses (Table 1) indicate a general reduction of P intensity compared to the synthetic HA, which were observed in the biochemical data (Figure 3).

The increase of HA crystallinity and the Ca/P ratio through the use of fluoride is well known, as its effect on reducing the demineralization and improving the remineralization of enamel [22,25]. Samples treated with 1100 ppm F presented a higher Ca/P ratio than the HA treated with deionized water, also in line with previous observations from our research group [22]. In addition to, the diameter value (nm) obtained for the crystallite treated with 1100 ppm F was higher compared to the HA treated with deionized water (Figure 2), which suggest a higher crystallinity. In this protocol the 0, 1100, 4500 and 9000 ppm F without TMP presented a proportional increase of Ca/P ratio according to the F concentration. The solution containing 1100 ppm F associated with TMP between 2 and 4% showed the highest Ca/P ratio for

this F concentration which are in agreement with an in vitro study conducted by Castro et al. [26], who observed an improved reduction of demineralization process of bovine enamel specimens using a pH cycling model when 1100 ppm F was associated with TMP at 3%. For the solutions with higher F concentrations, improved Ca/P ratios were observed for TMP concentrations between 4 and 8%, which correspond to those evaluated in the study by Manarelli et al. [12] using TMP-containing fluoride varnishes and demineralized bovine enamel.

Considering the results of this study and data from literature [12,24], the synergistic action of F and TMP seems to differ from data reported by Gonzalez et al. [27]. Manarelli et al. [12] observed that after the application of varnishes containing 2.5% NaF + 5% TMP and 5% NaF + 5%TMP, the incorporation of F in the enamel, as well as the alkali-soluble formation on enamel surface, were significantly reduced in comparison with varnishes with the same fluoride concentrations, without TMP. The study conducted by Souza et al., [24] also observed a reduction of alkali-soluble and acid-soluble F when TMP was associated with F. In the present study, a reduction of acid-soluble F in HA was observed for all F concentrations associated with TMP, which is in agreement with Manarelli et al. [12] and Souza et al. [24]. Nonetheless, the alkali-soluble F concentration in/on HA in this study was increased for 1100 ppm F and slightly increased for higher F concentrations (4500 and 9000 ppm F). This finding differs that the results observed by Manarelli et al., [12], however could be due the different modes of administration used by Manarelli et al., [12] (varnish) and in the present study (aqueous solutions), as HA powder does not have a solid surface (as tooth enamel) and therefore HA crystals were free to react promptly with the TMP and F [24]. Thus, the enhanced effect of F-containing products associated with TMP has been related with the TMP adsorption on enamel surface [12] which seems to involve the same binding sites as those for F and can, therefore, interfere with its action depending on the TMP concentration. When in the oral environment, TMP can release Na⁺ ions from its molecule and become negatively charged, adsorbing to enamel by binding to Ca²⁺ from HA, and thus, limiting the sites available for the loosely bound fluoride (represented in this study by the alkali-soluble F) deposition. Other negatively charged sites of TMP would be then available for Ca²⁺ and CaF₂ retention. This TMP “barrier” on the enamel surface could

limit acid diffusion, as well as allow the deposition of CaF_2 that would be released during cariogenic challenges and might participate in the remineralization process.

Although this model was able to produce changes in the biochemical analysis, there was no change for all groups regarding the crystalline structure (Figure 2) and no displacement of the position of any absorption peak was observed in the FTIR analysis, indicating that there was no replacement of F or TMP in the hydroxyapatite. Regarding the FTIR spectra data, it was observed slightly a reduction in the intensity of OH^- and CO_3^- with the presence of F or TMP. The spectra obtained showed changes in the absorption coefficient of carbonate, especially in the 1418 and 1451 cm^{-1} bands, which suggest a lower soluble HA, especially in the TMP:F ratio that present improved results [28]. However, the spectra did not allow the conclusion on how TMP could be adsorbed. One possibility that still need be investigated more accurately would be the probability of F and TMP bind at sites of Ca on HA. It would be interesting to use methods that allow assess more accurately these chemical interactions. It is important to highlight that the FTIR does not give an accurate quantification of intensity changes, thus data should be considered in association with another analysis. In case of ion incorporation, we should observe a displacement peak in the XRD and FTIR [29], which did not occurred in this study. However, the biochemical and EDX analysis showed traces of F in the samples (Figures 3 and 5). One possibility is that F would be inside the crystal structure, considering that the synthesis process used led to the formation of amorphous HA, which represents the dental enamel structure and this crystal provides peaks with lower definition in the analysis.

Besides the implications on dental caries and erosion, the present results could potentially be relevant for medicine and other areas of dentistry, due to the widespread use of HA in those fields over recent years [30]. Hydroxyapatite (HA), fluor-hydroxyapatite (FHA) with varying levels of fluoride ion substitution and fluorapatite (FA) are synthesized as possible implant coating or bone-grafting materials [31] and a large number of techniques has being developed for the HA synthesis powder due to increasing applications [17,31]. For instance, studies have evaluated fluoride incorporation into HA, providing more stability and biocompatibility, but have noted that if all of the OH^- groups in HA are replaced by F, the resulting

material is not osteoconductive [17]. Thus, the development of an adequate and stable HA synthetic crystal may also be important for other areas.

3.6 Conclusion

Based on the obtained results and within the limitations of the protocol used, it can be concluded that TMP interferes with F deposition on HA when it is co-administered with F, and with ideal TMP:F molar ratio may be possible obtain an enhancement of the fluoride products and precipitate a HA with low solubility. In addition to, TMP has been shown to have little or no action on tooth enamel in the absence of fluoride.

Acknowledgements

The authors thank the FAPESP for the financial support (process 2011/07788-7) and the PhD scholarship (process 2011/17234-9) for the first author and Éilton J. Souza for the EDX measurements.

References

1. Shellis RP, Featherstone JD, Lussi A. Understanding the chemistry of dental erosion. *Monogr Oral Sci.* 2014;25:163-79
2. Pessan JP, Toumba KJ, Buzalaf MA. Topical use of fluorides for caries control. *Monogr Oral Sci.* 2011;22:115-32.
3. Ganss C, Schulze K, Schlueter N. Toothpaste and erosion. *Monogr Oral Sci.* 2013;23:88-99.
4. Carey CM. Focus on fluorides: update on the use of fluoride for the prevention of dental caries. *J Evid Base Dent Pract.* 2014;14: 95-102.
5. Wong MC, Clarkson J, Glenny AM, Lo EC, Marinho VC, Tsang BW, Walsh T, Worthington HV. Cochrane reviews on the benefits/risks of fluoride toothpastes. *J Dent Res.* 2011;90:573-9.
6. Takeshita EM, Castro LP, Sasaki KT, Delbem ACB. In vitro evaluation with low fluoride content supplemented with trimetaphosphate. *Caries Res.* 2009;43:50-6.

7. Takeshita EM, Exterkate RA, Delbem AC, ten Cate JM. Evaluation of different fluoride concentrations supplemented with trimetaphosphate on enamel de- and remineralization in vitro. *Caries Res.* 2011;45:494-7.
8. Moretto MJ, Magalhães AC, Sasaki KT, Delbem AC, Martinhon CC. Effect of different fluoride concentrations of experimental dentifrices on enamel erosion and abrasion. *Caries Res.* 2010;44:135-40.
9. Danelon M, Takeshita EM, Peixoto LC, Sasaki KT, Delbem AC. Effect of fluoride gels supplemented with sodium trimetaphosphate in reducing demineralization. *Clin Oral Investig.* 2014;18:1119-27.
10. Manarelli, MM, Delbem ACB, Lima TMT, Castilho FCN, Pessan JP. Effect of fluoride varnish supplemented with sodium trimetaphosphate on enamel erosion and abrasion. *Am J Dent.* 2013;26:307-12.
11. Favretto CO, Danelon M, Castilho FC, Vieira AE, Delbem AC. In vitro evaluation of the effect of mouth rinse with trimetaphosphate on enamel demineralization. *Caries Res.* 2013;47:532-8.
12. Manarelli MM, Delbem AC, Lima TM, Castilho FC, Pessan JP. In vitro Remineralizing Effect of Fluoride Varnishes Containing Sodium Trimetaphosphate. *Caries Res.* 2014;48:299-305.
13. Pancote LP, Manarelli MM, Danelon M, Delbem ACB. Effect of fluoride gels supplemented with sodium trimetaphosphate on enamel erosion and abrasion. In vitro study. *Arch Oral Biol.* 2014; 59:336-40.
14. Danelon, M, Takeshita, EM, Sasaki, KT, Delbem, ACB. In situ evaluation of a low fluoride concentration gel with sodium trimetaphosphate in enamel remineralization. *Am J Dent.* 2013;26:15-20.
15. Moretto MJ, Delbem AC, Manarelli MM, Pessan JP, Martinhon CC. Effect of fluoride varnish supplemented with sodium trimetaphosphate on enamel erosion and abrasion: an in situ/ex vivo study. *J Dent.* 2013;41:1302-6.
16. Amaral JG, Freire IR, Martinhon CCR, Pessan JP, Delbem ACB. Low-fluoride dentifrices with polyphosphates on dental caries: longitudinal clinical study. *J Dental Res.* 2014;93B(Poster #188931).
17. Qu H, Wei M. Synthesis and characterization of fluorine-containing hydroxyapatite by a pH-cycling method. *J Mater Sci: Mater Med.* 2005;16:129-33

18. Li Y, Kong F, Weng W. Preparation and characterization of novel biphasic calcium phosphate powders (α -TCP/HA) derived from carbonated amorphous calcium phosphates. *J Biomed Mater Res Part B: Appl Biomater.* 2009;89: 508-17.
19. Vogel GL, Chow LC, Brown WE. A microanalytical procedure for the determination of calcium, phosphate and fluoride in enamel biopsy samples. *Caries Res.* 1983;17:23-31.
20. Fiske CH, Subarrow Y. The colorimetric determination of phosphorus. *J Biol Chem.* 1925;66:375-400.
21. Caslavskva V, Moreno EC, Brudevold F. Determination of the calcium fluoride formed from in vitro exposure of human enamel to fluoride solutions. *Arch Oral Biol.* 1975;20:333-9.
22. Delbem ACB, Alves KMRP, Sasaki KT, Moraes JCS. Effect of Iron II on Hydroxyapatite Dissolution and Precipitation in vitro. *Caries Res.* 2012;46:481–87.
23. Fulmer MT, Martin RI, Brown PW: Formation of calcium deficient hydroxyapatite at near-physiological temperature. *J Mater Sci: Mater Med.* 1992; 3:299-305.
24. Souza JAS, Amaral JG, Moraes JCS, Sasaki KT, Delbem ACB. Effect of Sodium Trimetaphosphate on Hydroxyapatite Solubility: An In Vitro Study. *Braz Dent J.* 2013;24:235-40.
25. ten Cate JM. Fluorides in caries prevention and control: empiricism or science. *Caries Res.* 2004;38:254-7.
26. Castro LP, Danelon M, Delbem ACB, Percinoto C. In vitro evaluation of conventional dentifrice supplemented with sodium trimetaphosphate on the bovine enamel demineralization. *Braz Oral Res.* 2013;27:166-99.
27. Gonzalez M, Jeansonne BG, Feagin FF. Trimetaphosphate and fluoride actions on mineralization at the enamel-solution interface. *J Dent Res.* 1973; 52:261-266.
28. Antonakosa A, Liarokapisa E, Leventouri T. Micro-Raman and FTIR studies of synthetic and natural apatites. *Biomaterials.* 2007;28:3043-54.
29. Freund F and Knobel RM. Distribution of Fluorine in Hydroxyapatite studied by Infrared Spectroscopy. *J Chem. Soc, Dalton Trans.* 1977;11:1136-40.

30. Rintoul L, Wentrup-Byrne E, Suzuki S, Grøndahl L. FT-IR spectroscopy of fluoro-substituted hydroxyapatite: strengths and limitations. *J Mater Sci: Mater Med.* 2007;18:1701-9.
31. Tredwin CJ, Young AM, Neel EAA, Georgiou G, Knowles JC. Hydroxyapatite, fluor-hydroxyapatite and fluorapatite produced via the sol-gel method: dissolution behaviour and biological properties after crystallization. *J Mater Sci: Mater Med.* 2014;25:47–53.

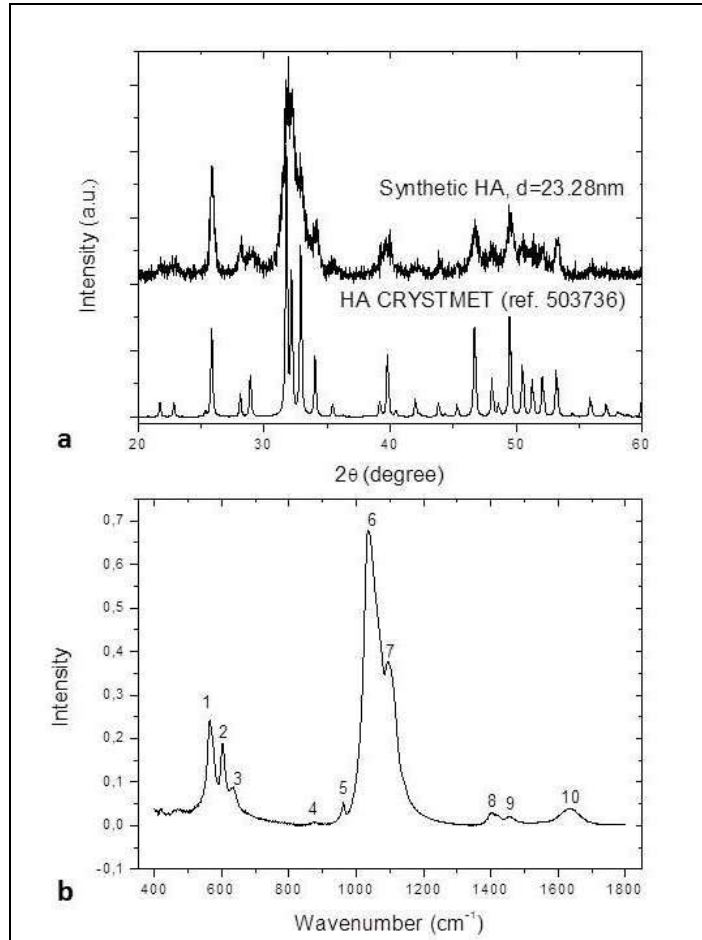


Figure 1. a: XRD patterns of the synthetic HA and CRYSTMET database. b: IR spectra obtained for synthetic HA (Peaks 1,2: PO_4^{3-} ; 3: OH^- ; 4: HPO_4^{2-} ; 5, 6 and 7, PO_4^{3-} ; 8 and 9: CO_3^{2-} ; 10: H_2O).

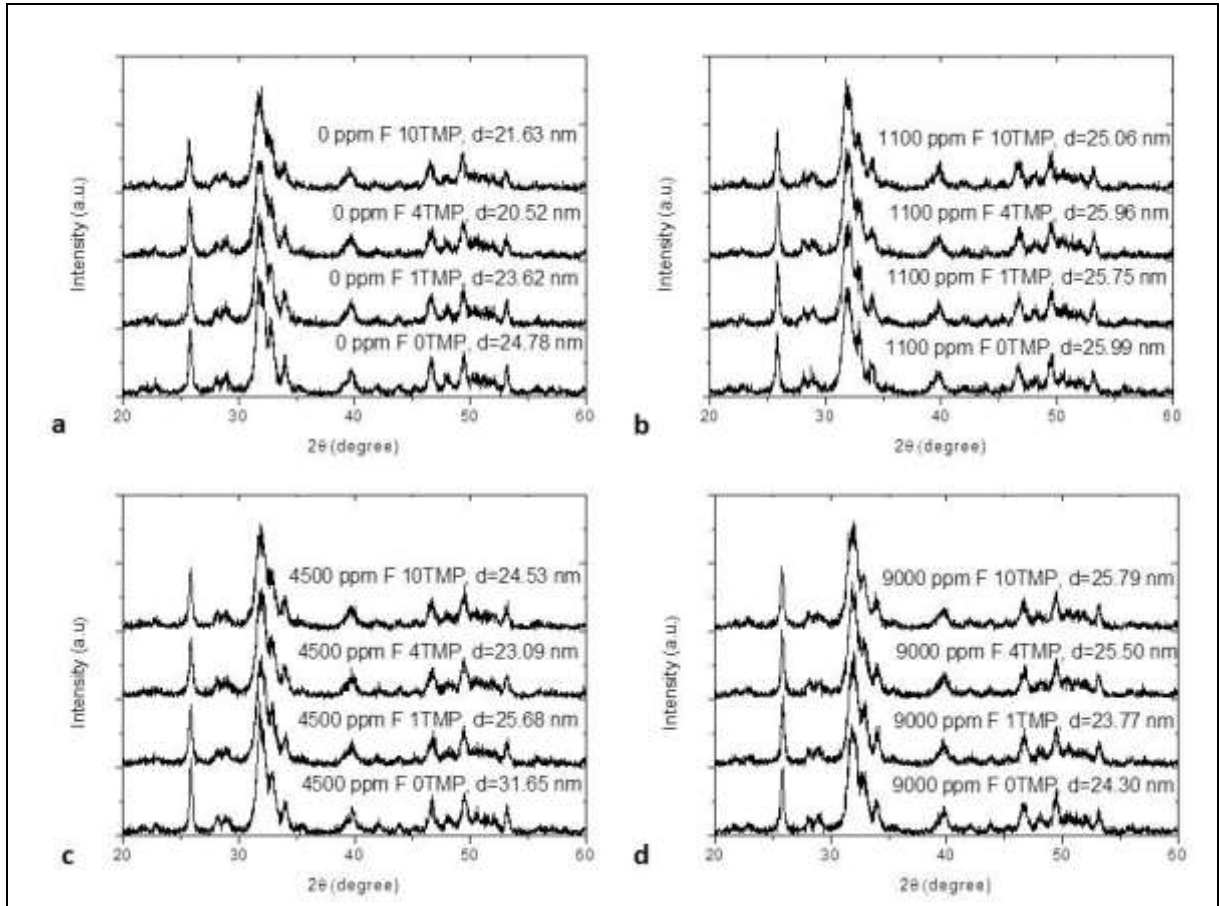


Figure 2. XRD patterns of HA according to the groups evaluated associated with TMP. 0 ppm F (a); 1100 ppm F (b); 4500 ppm F (c); 9000 ppm F (d). The diameter values (nm) of the crystal after pH cycle according to the fluoride concentration (ppm F) and percentage of TMP are represented by the letter d.

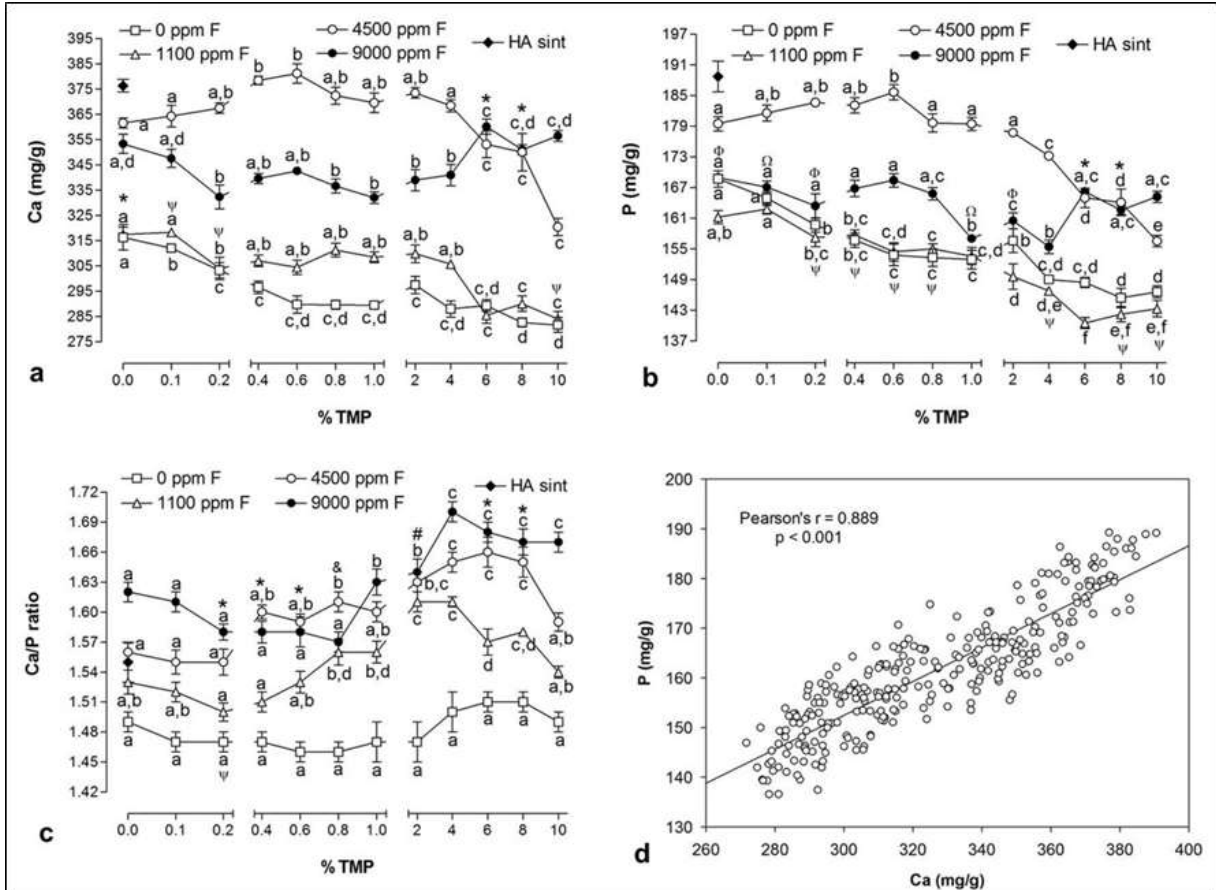


Figure 3. Mean (\pm se) of values of Ca (a), P (b) and Ca/P ratio (c) on hydroxyapatite after pH cycle according to the F and TMP concentration. Correlation between calcium and phosphorus concentrations on hydroxyapatite (d). Distinct letters show significant differences between the % TMP for each fluoride concentration (Student-Newman-Keuls, $p < 0.05$). (*) 4500 ppm F = 9000 ppm F; (&) 1100 ppm F = 9000 ppm F; (#) 1100 ppm F = 4500 ppm F; (ψ) 0 ppm F and 1100 ppm F; (Φ) 0 ppm F and 9000 ppm F; (Ω) 0 ppm F = 1100 ppm F = 9000 ppm F.

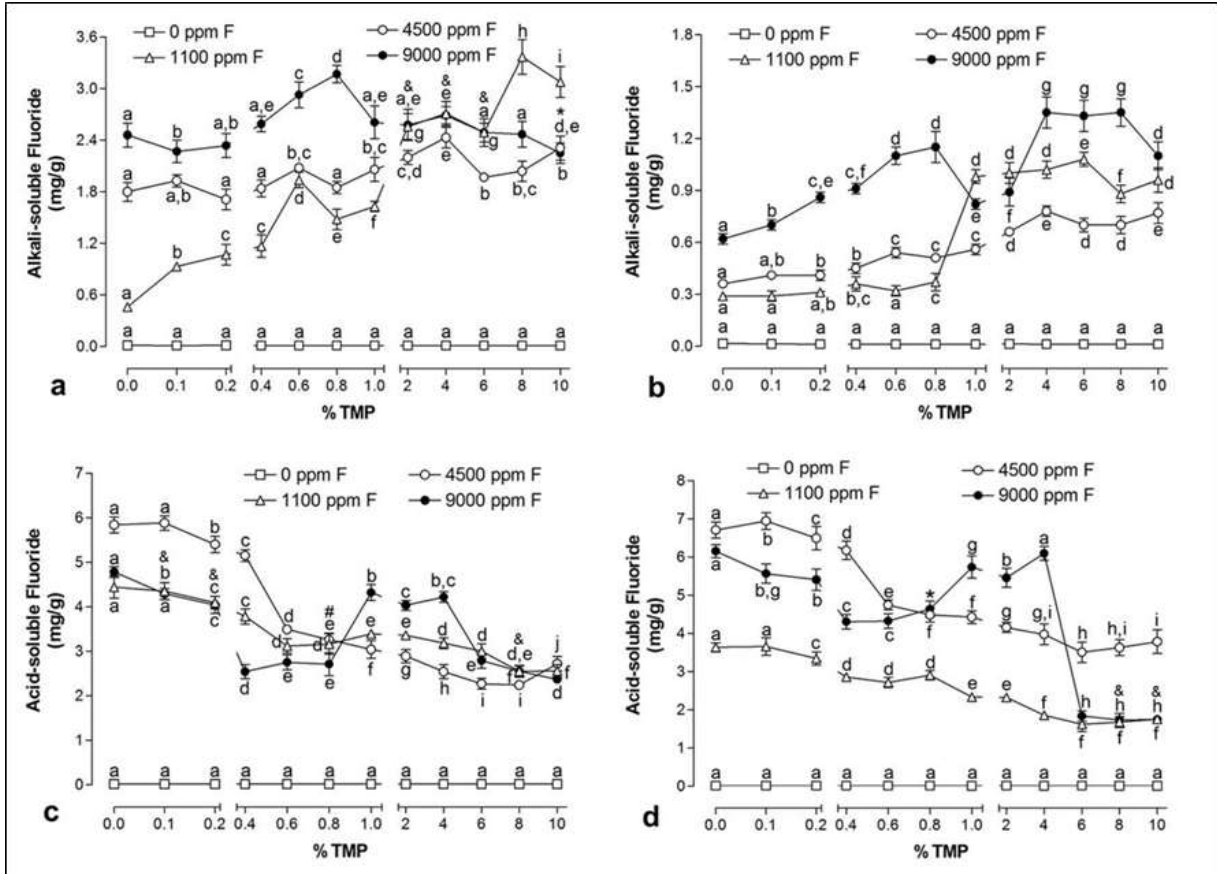


Figure 4. Mean (\pm se) of alkali-soluble F on HA after treatment (a) and after pH cycle (b); acid-soluble F on HA after treatment (c) and after pH cycle (d). Distinct letters show significant differences between the % TMP for each fluoride concentration (Student-Newman-Keuls, $p < 0.05$). (*) 4500 ppm F = 9000 ppm F; (&) 1100 ppm F = 9000 ppm F; (#) 1100 ppm F = 4500 ppm F. Concentrations (mg/g) (mean \pm SD) of acid-soluble and alkali-soluble in the synthetic HA were: 0.02 (0.0) and 0.01 (0.0), respectively.

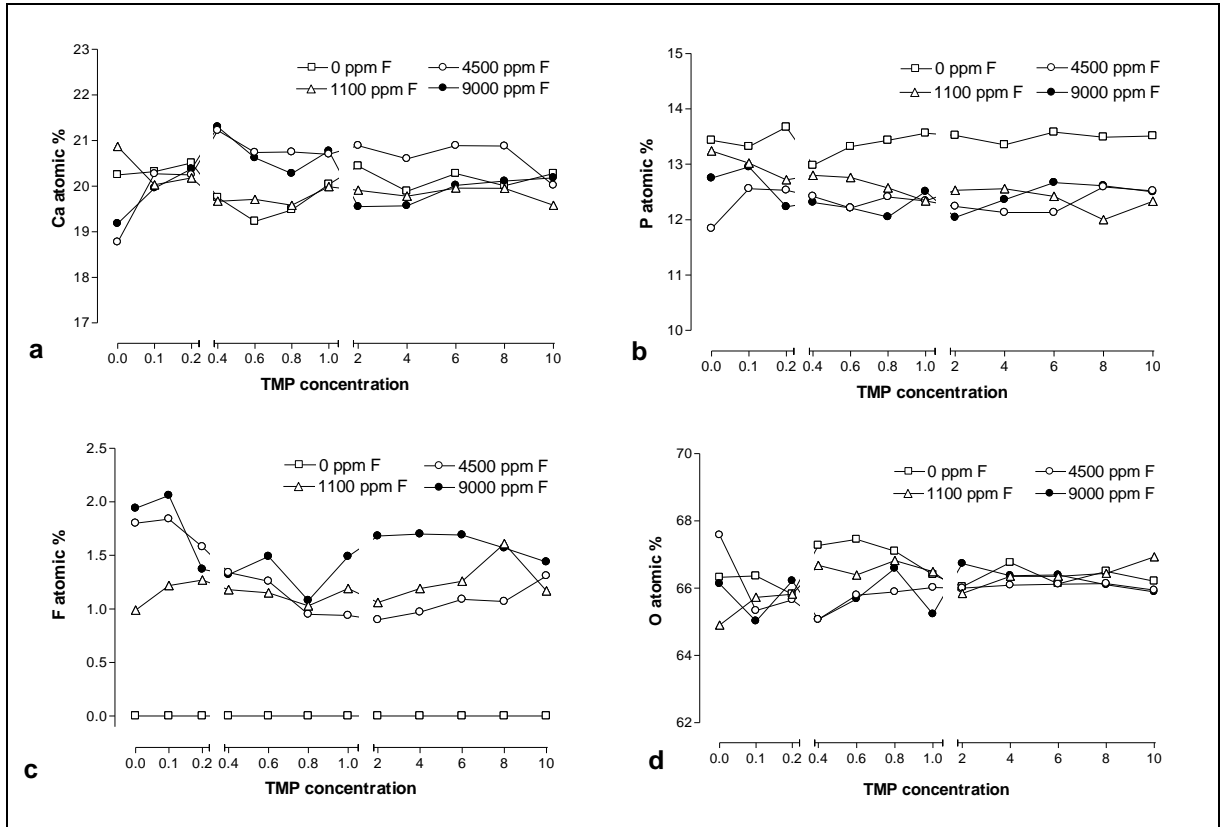


Figure 5. Atomic % of Ca (a), P (b), F (c) and O (d) in HA according to the F concentration associated with TMP.

* Synthetic HA (% atomic): Ca= 20.55; P=13.33; O=66.12; F=0.

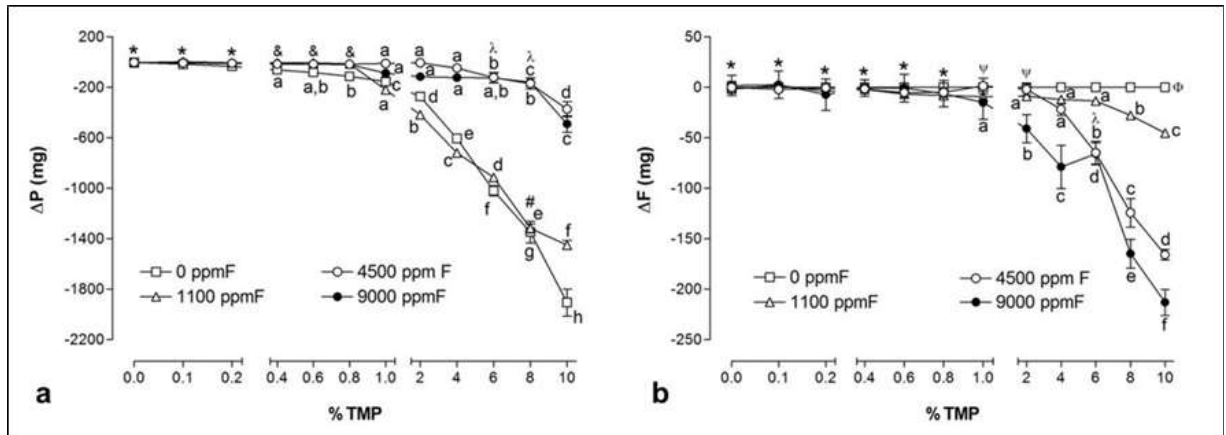


Figure 6. Mean (\pm se) of F and TMP adsorbed to hydroxyapatite (a) adsorption of TMP (expressed through the amount of phosphorus), (b) adsorption of F. Distinct letters show significant differences between the %TMP for each fluoride concentration (Student-Newman-Keuls, $p < 0.05$). (*) All comparisons show similarity; (&) 1100 ppm F = 4500 ppm F = 9000 ppm F; (#) 0 ppm F = 1100 ppm F; (λ) 4500 ppm F = 9000 ppm F; (ψ) 0 ppm F = 1100 ppm F = 4500 ppm F.

Table 1. Absorption coefficient obtained in the FTIR analysis according to the groups evaluated regarding the F and TMP concentration after pH cycle

Groups		Wavenumber (cm ⁻¹)								
ppm F	TMP%	565	603	634	874	964	1039	1094	1418	1451
Synthetic H _A		4.879	3.740	1.650	0.151	0.695	17.456	8.920	0.590	0.457
0	0	4.132	3.056	1.253	0.220	1.175	13.264	7.366	0.427	0.351
	1	3.488	2.800	1.272	0.120	0.828	10.939	6.283	0.263	0.218
	4	3.881	2.996	1.303	0.133	0.763	12.193	6.848	0.295	0.244
	10	3.997	3.183	1.529	0.197	0.887	12.165	6.966	0.234	0.196
1100	0	3.825	3.202	1.012	0.123	0.825	12.237	6.880	0.515	0.423
	1	3.972	3.328	1.062	0.166	0.863	15.201	8.096	0.670	0.570
	4	2.885	2.433	1.091	0.119	0.668	11.021	6.170	0.433	0.310
	10	3.640	2.956	1.068	0.162	0.858	12.491	6.870	0.483	0.405
4500	0	3.229	2.656	1.060	0.131	0.738	10.059	5.532	0.376	0.334
	1	3.308	2.634	0.855	0.117	0.708	11.198	5.052	0.407	0.373
	4	3.385	2.727	1.085	0.127	0.687	10.704	5.877	0.350	0.313
	10	3.298	2.790	1.267	0.076	0.582	9.649	5.613	0.256	0.269
9000	0	4.057	3.342	1.321	0.137	0.803	12.108	6.668	0.423	0.392
	1	3.558	2.951	1.239	0.121	0.675	10.402	5.756	0.333	0.307
	4	4.066	3.381	1.265	0.087	0.803	12.609	6.987	0.358	0.334
	10	3.922	2.989	1.235	0.080	0.578	11.078	5.971	0.301	0.290

* 565, 603, 964, 1039 and 1094 cm⁻¹ correspond to phosphate bands; 874 cm⁻¹ correspond to monohydrogen phosphate (HPO₄²⁻); the carbonate vibrational mode is located at regions of 1418 and 1451 cm⁻¹ and the OH⁻ band was observed at 634 cm⁻¹.

CAPÍTULO 3

Effects of polyphosphates and fluoride on hydroxyapatite dissolution: a pH-stat investigation

4.1 Abstract

This study investigated the immediate and sustained effect of sodium trimetaphosphate (TMP) and sodium hexametaphosphate (HMP) associated or not with fluoride (F) on hydroxyapatite (HA) discs dissolution using an erosion-like model, in the presence and absence of a salivary pellicle. Baseline dissolution rates were determined for HA discs from the mean of three 30-min assays prior to treatment using a pH-stat system (0.3% citric acid, pH 3.2). In the first set of experiments, HA discs were treated with 1100 ppm F, 1% and 8% of HMP or TMP and 1100 ppm F associated with 1% and 8% of HMP or TMP, totaling 9 groups (n=8). In a second phase, HA discs were kept in pooled human saliva at 37° C for 2h before treatment with deionised water and 1100 ppm F associated with 1% and 8% of HMP or TMP, totaling 5 groups (n=8). The post-treatment dissolution rate was determined from three consecutive 30-min assays. Data were analysed using 2 and 3-way ANOVA followed by Fisher and Holm-Sidak methods, respectively ($\alpha=0.05$). All test solutions promoted reduction in HA dissolution rate when compared to baseline control in the first post-treatment run ($p<0.001$). However, the duration of inhibitory effect was greater when 8% HMP and 1 or 8% HMP associated with F were assessed, remaining 40%, 19% and 22% higher than baseline after 90 minutes, respectively ($p<0.001$). The presence of salivary pellicle led to higher protection for all groups when compared to discs without pellicle ($p<0.001$). In conclusion, the reduction of HA dissolution rate, as well as the duration of this effect were influenced by fluoride, type and concentration of phosphate salt and the presence of a salivary pellicle.

Keywords: erosion; fluoride; polyphosphates; salivary pellicle; hydroxyapatite.

*Capítulo escrito de acordo com as instruções do periódico Caries Research

4.2 Introduction

Dental erosion has been recognized as an increasing dental problem among children, adolescents and adults [Johansson et al., 2012]. Thus, there is a growing interest in the development and evaluation of treatments which can reduce the severity and offer protection against dental erosion.

Fluoride (F) has been widely used as a complementary preventive measure with the aim of reducing mineral loss [Magalhães et al., 2011]. Nonetheless, the protective effect of fluoride against erosion is controversial and favorable results on the inhibition of erosion have been achieved in the presence of high fluoride concentrations, showing that low and moderate F concentrations are unable to provide a significant preventive effect against erosion [Larsen and Richards, 2002]. Moreover, conventional formulations used daily such as dentifrices have presented a limited effectiveness on dental erosion [Magalhães et al., 2011]. In order to design more effective formulations, several active ingredients other than fluorides, or in addition to, have been studied [Hooper et al., 2007; Barbour et al., 2008; Takeshita et al., 2009, 2013; Jager et al., 2013; Yamashita et al., 2013; da Camara et al., 2014; Buzalaf et al., 2014].

Promising results have led to an increasing interest in polyphosphates with and without fluoride in this context [Moretto et al., 2010, 2013; Manarelli et al., 2013; Pancote et al., 2014]. Among these, sodium trimetaphosphate (TMP) and sodium hexametaphosphate (HMP) have been shown to have protective effects in both caries and erosion [Takeshita et al., 2009, 2013; Moretto et al., 2010, 2013; Manarelli et al., 2011, 2013, 2014; Danelon et al., 2012, 2013 a/b; Pancote et al., 2014; da Camara et al., 2014]. TMP is a cyclic condensed phosphate and, according to the literature, it would preserve the stability and integrity of the enamel mineral surface during enamel erosion [Gonzalez, 1971]. It can remain bound to enamel for a longer period in comparison to other polyphosphates [McGaughey and Stowell, 1977]. Sodium hexametaphosphate (HMP) is a cyclic phosphate which has the ability to reduce enamel solubility [van Dijk et al., 1980; Andreola et al., 2004; Castellini et al., 2005]. For both TMP and HMP, an appropriate ratio of phosphate/F should be maintained to achieve favorable effects; it seems to be related to a formation of a "barrier" on the enamel surface which can provide protection against mineral loss in cariogenic and erosive challenges [Camara et al., 2014; Souza et al., 2013]

Considering that the mechanisms of action of TMP and HMP are still not fully elucidated, the assessment of their effects alone or in combination with fluoride would be instructive, especially regarding the interactions of these with the tooth mineral. In this sense, a pH stat system can be used to evaluate the immediate and sustained effect of therapeutic agents on the dissolution of hydroxyapatite discs. This model has been used in previous studies [Barbour et al., 2005, 2008; Jones et al., 2013] as a model for dental tissues in studies of other inhibitors and have been shown to react to solution factors such as pH in a qualitatively similar way as enamel [Shellis et al., 2010].

Based on the above, the purpose of the present study was to evaluate the demineralisation-inhibiting properties of these phosphates alone or associated with fluoride. Considering that saliva may have a strong influence on dental erosion and on tests of anti-erosive agents [Buzalaf et al., 2012; Jones et al., 2013], the effects of TMP and HMP on dissolution of both native surfaces and of surfaces previously coated with salivary pellicle were assessed. The study hypothesis was that HA dissolution would be significantly reduced by the presence of fluoride associated or not with TMP or HMP, and that this effect would be enhanced by the presence of salivary acquired pellicle.

4.3 Material and Methods

Hydroxyapatite discs and solutions preparation

Discs of compressed hydroxyapatite (HA) (mean diameter 12.7 mm and thickness 1.39 mm) were acquired from HiMed Inc., Old Bethpage, N.Y., USA. Prior to use in the pH-stat, discs were exposed to gently stirred 0.3% citric acid, pH 3.2, for 30 min at room temperature, washed in deionised water and finally air-dried to ensure consistency of response and remove loose HA particles. Before use in pH-stat, each disc was coated with nail varnish on the underside to leave a constant exposed area (126.6 mm²) available for reaction using an established procedure [Barbour et al., 2008]. Then, discs were fixed with sticky wax to the tip of a glass tube to be inserted into the inlet port in a reproducible position.

Solutions were prepared using deionised water and reagents were acquired from Sigma-Aldrich (Poole, Dorset, UK). Solutions of citric acid were prepared at 0.3% concentrations with pH value of 3.20 (adjusted using NaOH). Fluoride (NaF;

Poole, Dorset, UK) and phosphates (sodium trimetaphosphate – TMP and sodium hexametaphosphate – HMP; Poole, Dorset, UK) solutions were prepared in the following concentrations: 1100 ppm F, 1% and 8% of HMP or TMP and 1100 ppm F associated with 1% and 8% of HMP or TMP.

Measurement of Dissolution Rate

A pH-stat system (718 Stat Titrino: Metrohm UK, Runcorn, Cheshire, UK) with a 50-mL double-walled glass reaction vessel and a lid with 3 inlet ports was used to determine the dissolution rate of hydroxyapatite. The reaction temperature was 37 °C maintained using a water-jacketed reaction vessel and a water bath (Type GD120; Grant Instruments, Cambridge, UK). For each dissolution measurement, 30 ml of 0.3% citric acid solution was introduced into the reaction vessel and pH electrode and burette tip adapted. After the system had reached thermal equilibrium, the pH was adjusted to 3.2 by adding 1M NaOH and then performing final fine adjustment using the pH-stat. The reaction was initiated by immersing the HA disc into the reaction vessel and addition of titrant (50 mM HCl) was recorded for 30 min. A baseline measurement of dissolution rate was determined for each disc from the mean of three 30-min assays prior to treatment, so each disc served as its own control. Afterwards, HA discs were exposed to the chosen treatment, reattached to the glass specimen and post-treatment measurements of dissolution rate were made at 30, 60 and 90 minutes (Anexo J).

The rate of dissolution was calculated as the slope of the linear portion from the graphic obtained of acid volume versus time ($\text{mL}\cdot\text{s}^{-1}$). This was converted to $\text{nmol of HA min}^{-1}\cdot\text{mm}^{-2}$ using the area of the HA disc and a pH- and acid-dependent factor converting micromoles of acid to micromoles of hydroxyapatite [Shellis et al., 2010].

Deposition of salivary pellicle

Saliva was collected from two healthy volunteers participating in a saliva bank from University of Bristol. Volunteers were directed to decline the donation of saliva in the following situations: (1) they had recently taken any medication, (2) habitual smoker, (3) pregnant or (4) if they had any upper respiratory tract infections in recent times. As required, each volunteer chewed a square of Parafilm to stimulate salivary flow and expectorated saliva into a tube until reach the 20-ml level of a polystyrene

universal tube. These samples were pooled and centrifuged using a Centaur 1 (MSE, London, UK) at 4000 g for 15 min at ambient temperature. The supernatant was immediately used to treat HA specimens (2mL/ HA disc).

Treatment

Phase 1 (Native discs). After determining the mean baseline dissolution rate, HA discs (n=72) were divided into 9 groups (n=8) and treated for 2 min by immersion (with gentle stirring) in the following solutions: 1100 ppm F (1100); 1% and 8% HMP (1%HMP; 8%HMP); 1% and 8% TMP (1%TMP; 8%TMP); 1,100 ppm F with 1% HMP (1100 1%HMP); 1100 ppm F with 8% HMP (1100 8%HMP); 1100 ppm F with 1% TMP (1100 1%TMP) and 1100 ppm F with 8% TMP (1100 8%TMP). After rinsing in deionised water, three measurements of post-treatment were performed at 30, 60 and 90 min by the same way those baseline measurements.

Phase 2 (Saliva coated discs). For the saliva-coated HA discs, restriction in the number of experimental groups was necessary due to the nature of the experiment regarding the saliva amount. These groups chosen were based on those that showed the best overall results in phase one. Four groups were chosen from the non-saliva-treated discs to observe the influence of salivary pellicle with phosphates and fluoride. A group treated with deionised water (DIW) was included as a control to observe the effect of saliva alone. Groups with phosphates that led to higher reduction of dissolution rate were selected as following: 1100 1% HMP; 1100 8% HMP; 1100 1% TMP; and 1100 8% TMP. After obtaining the control measurements of dissolution rate, discs (n=40) were immersed in pooled saliva supernatant for 2h and incubated at 37°C. After this, the discs were stored in a damp environment until the treatment with the solutions selected. HA discs were therefore treated with the selected groups by the same way for non-saliva discs. Finally, the post-treatment dissolution rate was measured on each disc at three post-treatment times, as described above.

Statistical Analysis

For statistical analysis, SigmaPlot 12.0 software was used and the significance limit was set at 5%. Data from non-saliva and saliva coated discs exhibited a normal distribution (determined using the Shapiro-Wilks test). Treatment solutions, time

(baseline control, post-treatment 1, 2 and 3) and presence or absence of saliva were considered as variation factors. A control value was determined for each specimen by averaging the three control runs before treatment. Then, data of groups from non-saliva coated discs were submitted to 2-way ANOVA, followed by Fisher test. When saliva was considered as variable, the 3-way ANOVA was employed and the post hoc test used was Holm-Sidak test.

4.4 Results

In phase 1, exposure to 1100 ppm F promoted a significant reduction in the dissolution rate (12%) when compared with baseline values ($p=0.041$) in the first post-treatment run. This reduction decreased beyond the first 30 min and did not persist over time (Figure 1).

Exposure to TMP at concentrations of 1 and 8% exhibited a similar profile of dissolution rate (Figure 2a and 2b) and reduced dissolution rate at 9% ($p=0.009$) and 13% ($p=0.016$), respectively, in the first post treatment run. This reduction persisted over time for the 8%TMP, presenting 10% of reduction in the third post-treatment run ($p=0.048$). When either 1 or 8% TMP concentrations were associated to fluoride (1100 ppm), a significant reduction in HA dissolution was seen for 1100 8%TMP over time, being 22% lower than the baseline values ($p<0.001$) in the first post-treatment run and 8% ($p=0.048$) in the third post-treatment run (Figure 2c and 2d).

The maximum reduction of dissolution rate in this study was observed for HMP. When 1 and 8% of HMP were assessed, the reduction of dissolution rate was, respectively, 24% ($p<0.001$) and 61% ($p<0.001$) at the first post-treatment run, 17% ($p=0.004$) and 41% ($p<0.001$) at the second post-treatment run, and 4% ($p=0.374$) and 40% ($p<0.001$) at the third post-treatment, showing a significant reduction of dissolution rate versus baseline over time for HMP at 8% (Figure 3a and 3b). For the 1100 1%HMP and 1100 8%HMP, the reduction rates were very similar, but persisted higher for the 1100 8% HMP in the second post-treatment ($p<0.001$) (Figure 3c and 3d)

Figure 4 shows the results from the saliva coated discs regarding the percentage reduction in the dissolution rate. There was a significant reduction of dissolution rate ($p<0.001$) for all groups evaluated in the presence of salivary pellicle, when compared with their treatment with DIW or with their counterparts not covered

by salivary pellicle. Also, the presence salivary pellicle alone resulted in a significant reduction of the hydroxyapatite dissolution rate compared to the baseline rate ($p < 0.001$), as seen for discs treated with DIW. The higher reduction of dissolution rate and persistence of effect over time in the presence of saliva was observed when HMP (1 and 8%) was associated with fluoride. There was a higher persistence of effect over time for the 1100 associated with 8% HMP ($p < 0.001$).

4.5 Discussion

TMP and HMP associated with fluoride have been shown to have a synergistic effect for both dental caries and erosion [Takeshita et al., 2009, 2013; Moretto et al., 2010, 2013, Manarelli et al., 2011, 2013, 2014; da Camara et al., 2014]. As pH-stat method has been used successfully as a technique to study dental erosion, providing information about interactions with hydroxyapatite and the persistence of the inhibitory effect during repeated erosive challenges, in this study this method was employed to investigate the effect of these phosphates with or without fluoride.

In the present study, both phosphate salts evaluated inhibited dissolution of HA by different levels. The reduction of dissolution rate of HA treated with fluoride did not persist significantly further than the first post-treatment run, which is in agreement with Jones et al., [2013]. Although the fluoride concentration used in the present study was higher (1100 ppm F) than that used by Jones et al., [2013] (300 ppm F), no additional effect on HA dissolution was observed. The protective effect of fluoride against dental erosion is probably given by a formation of a layer of KOH-soluble calcium fluoride [Magalhães et al., 2011], indicating that the adsorbed fluoride could be reduced by the acid challenge over time [Jones et al., 2013].

Regarding the polyphosphates evaluated, higher inhibitory effect was found when compared with 1100, especially for HMP. For TMP alone, a similar dissolution profile was observed for both concentrations evaluated, showing a sustained inhibition over time for the 8% TMP. When TMP was associated with fluoride, a higher immediate and a sustained effect for the 1100 8% TMP was observed (Figure 2a and 2b). Based on the current results [Manarelli et al., 2014, Pancote et al., 2014] and on previous studies, it becomes clear that the synergistic action between F and TMP can increase enamel remineralisation and reduce enamel demineralisation, as well as the mineral loss in erosive challenges. Such effects, however, are not

associated with formation of high amounts of Alkali-soluble, as described for fluoride. This effect seems to be related to a formation of a "barrier" of TMP on the enamel surface, which limits the diffusion of acid into the enamel as well as the deposition of Alkali-soluble on this barrier, and the retention of ions (Ca^{++} and CaF^+) in the TMP molecule, which would be released during pH challenges [Cochrane et al, 2008; Manarelli et al., 2014].TMP in the absence of fluoride has shown a little or no action on dental enamel [Takeshita et al., 2009].

As has been stated for TMP, HMP has been shown to provide a less soluble hydroxyapatite as well as reduce the ion diffusion into the enamel [van Dijk et al.1980]. Camara et al. [2014] suggested that HMP is capable of binding to surface enamel and remain bound and also demonstrated that, in the absence of fluoride, a significant reduction of mineral loss was observed 0.5% HMP was used, when compared to placebo, suggesting that HMP (negatively charged) can adsorb at the positive sites of enamel surfaces forming a "coat" after treatment that acts as a protective layer on the enamel. In the present study a higher reduction of dissolution rate was found for the 8% HMP concentration (with or without fluoride), which differ that data found by Camara et al. [2014] that showed higher mineral loss with increased HMP concentration in association with fluoride (250 ppm F) when an *in vitro* caries model was used. In the present study HA dissolution was assessed using an erosion-like model with a different F concentration, which might have influenced in the different results obtained. Regarding HMP and TMP structure, these salts have six and three phosphorus atoms, respectively, what might help explain the greater results obtained with HMP; when in the oral environment, HMP could form a stronger "barrier" on enamel surface and provide a higher amount of binding sites for the retention of ions (Ca^{++} and CaF^+) in comparison with TMP.

Considering the influence of saliva on the effect of anti-erosive agents, the presence of a salivary pellicle was considered in the second set of experiments. An exposure time of 2h to saliva ensured an effect on HA discs and allowed to investigate the interactions with polyphosphates in this study. According to literature a significant effect can be obtained for exposure times ≥ 60 min [Wetton et al., 2006; Jones et al., 2013]. As expected, the formation of a salivary pellicle resulted in a significant reduction of the hydroxyapatite dissolution rate (33%), which is in line with a previous study conducted with the same methods of analysis [Jones et al., 2013],

showing a reduction in HA dissolution of 41%. Furthermore, the presence of salivary pellicle led to higher protection for all groups when compared to discs without pellicle (Figure 4). The profile obtained was similar to those obtained for native discs; however all tested solutions with fluoride and associated to HMP or TMP promoted an additional effect in the presence of saliva and polyphosphates. Nonetheless this effect (immediate and sustained) was greater for the solutions containing HMP, showing that the salivary pellicle did not reduce or hinder the polyphosphates action. These data are in agreement with a study conducted by Danelon et al. [2014], which demonstrated that the effect of TMP was not modified by the presence of acquired enamel pellicle.

To conclude, confirming this study hypothesis, the reduction of HA dissolution rate as well as the duration of this effect was influenced by the type of phosphate salt and not reduced by the presence of a salivary pellicle. This is important from a clinical point of view, since the tooth surfaces *in vivo* are coated with salivary pellicle under normal conditions.

Acknowledgements

The authors thank the CAPES for the PhD scholarship (process BEX 9221-12-3) for the first author.

References

- Andreola F, Castellini E, Manfredini T, Romagnoli M. The role of sodium hexametaphosphate in the dissolution process of kaolinite and kaolin. *J Eur Ceram Soc* 2004; 24: 2113–24.
- Barbour ME, Shellis RP, Parker DM, Allen GC, Addy M. An investigation of some food-approved polymers as agents to inhibit hydroxyapatite dissolution. *Eur J Oral Sci.* 2005; 113: 457-61.
- Barbour ME, Shellis RP, Parker DM, Allen GC, Addy M. Inhibition of hydroxyapatite dissolution by whole casein: the effects of pH, protein concentration, calcium, and ionic strength. *Eur J Oral Sci.* 2008; 116: 473-8.
- Buzalaf MA, Hannas AR, Kato MT. Saliva and dental erosion. *J Appl Oral Sci* 2012; 20: 493-502.

- Buzalaf MA, Magalhães AC, Wiegand A. Alternatives to fluoride in the prevention and treatment of dental erosion. *Monogr Oral Sci* 2014; 25: 244-52.
- Camara DM, Miyasaki ML, Danelon M, Sassaki KT, Delbem AC. Effect of low-fluoride toothpastes combined with hexametaphosphate on in vitro enamel demineralization. *J Dent*. 2014; 42: 256-62.
- Castellini E, Lusvardi G, Malavasi G, Menabue L. Thermodynamic aspects of the adsorption of hexametaphosphate on kaolinite. *J Colloid Interface Sci* 2005; 292: 322–29.
- Cochrane NJ, Saranathan S, Cai F, Cross KJ, Reynolds EC: Enamel subsurface lesion remineralization with casein phosphopeptide stabilized solutions of calcium, phosphate and fluoride. *Caries Res* 2008; 42: 88–97.
- Danelon M, Camara DM, Miyasaki ML, Scarpa JB, Delbem ACB, Sassaki KT. Effect of fluoride gels supplemented with hexametaphosphate in inhibiting demineralization. *J Dent Res* 2012; 91(Sp Iss B): 162761.
- Danelon M, Takeshita EM, Peixoto LC, Sassaki KT, Delbem AC. Effect of fluoride gels supplemented with sodium trimetaphosphate in reducing demineralization. *Clin Oral Investig*. 2013b; DOI 10.1007/s00784-013-1102-4.
- Danelon M. Efeito de dentifrícios fluoretados e suplementados com nanopartículas de trimetafosfato de sódio sobre a desmineralização, remineralização e erosão dentária [tese]. Araçatuba: Universidade Estadual Paulista; 2014.
- Danelon, M, Takeshita, EM, Sassaki, KT, Delbem, ACB. In situ evaluation of a low fluoride concentration gel with sodium trimetaphosphate in enamel re-mineralization. *Am J Dent* 2013a;26:15-20.
- Ganss C, Schulze K, Schlueter N. Toothpaste and erosion. *Monogr Oral Sci*, v. 23, p. 88-99, 2013.
- Gonzalez M. Effect of trimetaphosphate ions on the process of mineralization. *J Dent Res* 1971; 50: 1056-64.
- Hooper SM, Newcombe RG, Faller R, Eversole S, Addy M, West NX. The protective effects of toothpaste against erosion by orange juice: studies in situ and in vitro. *J Dent* 2007; 35: 476–481.
- Jaeggi T, Lussi A. Prevalence, incidence and distribution of erosion. *Monogr Oral Sci* 2006; 20: 44 - 65.

- Jager DH, Vissink A, Timmer CJ, Bronkhorst E, Vieira AM, Huysmans MC. Reduction of erosion by protein-containing toothpastes. *Caries Res* 2013; 47:135-40.
- Johansson AK, Omar R, Carlsson GE, Johansson A. Dental erosion and its growing importance in clinical practice: from past to present. *Int J Dent* 2012; 2012: 632907.
- Jones SB, Rees GD, Shellis RP, Barbour ME. The effect of monoalkyl phosphates and fluoride on dissolution of hydroxyapatite, and interactions with saliva. *Caries Res* 2013; 47: 355-63.
- Larsen MJ, Richards A. Fluoride is unable to reduce dental erosion from soft drinks. *Caries Res* 2002; 36: 75-80.
- Magalhães AC, Wiegand A, Rios D, Buzalaf MA, Lussi A. Fluoride in dental erosion. *Monogr Oral Sci* 2011; 22: 158-170.
- Manarelli MM, Delbem AC, Lima TM, Castilho FC, Pessan JP. In vitro Remineralizing Effect of Fluoride Varnishes Containing Sodium Trimetaphosphate. *Caries Res* 2014; 48: 299-305.
- Manarelli MM, Vieira AE, Matheus AA, Sasaki KT, Delbem AC. Effect of mouth rinses with fluorides and trimetaphosphate on enamel erosion: an in vitro study. *Caries Res* 2011; 46: 506-9.
- Manarelli, MM, Delbem ACB, Lima TMT, Castilho FCN, Pessan JP. Effect of fluoride varnish supplemented with sodium trimetaphosphate on enamel erosion and abrasion. *Am J Dent* 2013; 26: 307-12.
- McGaughey C, Stowell EC. Effects of polyphosphates on the solubility and mineralization of HA: relevance to a rationale for anticaries activity. *J Dent Res* 1977; 56: 579-87.
- Moretto MJ, Delbem AC, Manarelli MM, Pessan JP, Martinhon CC. Effect of fluoride varnish supplemented with sodium trimetaphosphate on enamel erosion and abrasion: an in situ/ex vivo study. *J Dent* 2013; 41: 1302-6.
- Moretto MJ, Magalhães AC, Sasaki KT, Delbem AC et al. Effect of different fluoride concentrations of experimental dentifrices on enamel erosion and abrasion. *Caries Res* 2010; 44: 135-40.
- Pancote LP, Manarelli MM, Danelon M, Delbem ACB. Effect of fluoride gels supplemented with sodium trimetaphosphate on enamel erosion and abrasion. In vitro study. *Arch Oral Biol* 2014; 59: 336-40.

Shellis RP, Barbour ME, Jones SB, Addy M. Effects of pH and acid concentration on erosive dissolution of enamel, dentine, and compressed hydroxyapatite. *Eur J Oral Sci* 2010; 118: 475-82.

Souza JA, Amaral JG, Moraes JC, Sasaki KT, Delbem AC. Effect of sodium trimetaphosphate on hydroxyapatite solubility: an in vitro study. *Braz Dent J* 2013; 24: 235-40.

Takeshita EM, Castro LP, Sasaki KT, Delbem ACB. In vitro evaluation with low fluoride content supplemented with trimetaphosphate. *Caries Res* 2009; 43: 50-6.

Takeshita EM, Exterkate RA, Delbem AC, ten Cate JM. Evaluation of different fluoride concentrations supplemented with trimetaphosphate on enamel de- and remineralization in vitro. *Caries Res* 2011; 45: 494-97.

van Dijk JW, Borggreven JM, Driessens FC. The effect of some phosphates and a phosphonate on the electrochemical properties of bovine enamel. *Arch Oral Biol* 1980; 25: 591-95.

Wetton S, Hughes J, West N, Addy M. Exposure time of enamel and dentine to saliva for protection against erosion: a study in vitro. *Caries Res* 2006; 40: 213-17.

Yamashita JM, Torres NM, Moura-Grec PG, Marsicano JA, Sales-Peres A, Sales-Peres SH. Role of arginine and fluoride in the prevention of eroded enamel: an in vitro model. *Aust Dent J* 2013; 58: 478-82.

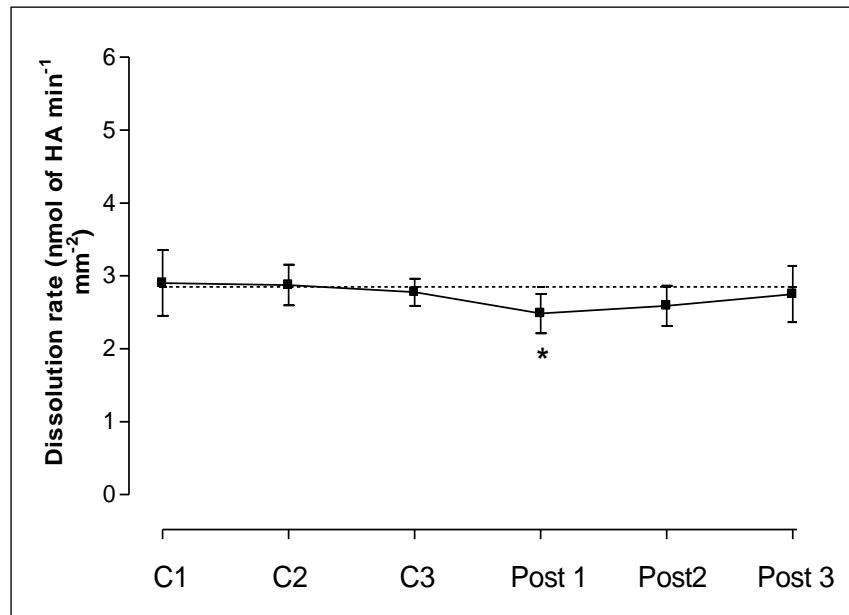


Figure 1. Dissolution rate of HA for the three control runs before treatment (C1-3) and after treatment (Post 1-3) with 1100 ppm F. Dashed line= mean control rate. *Significantly different from mean baseline control.

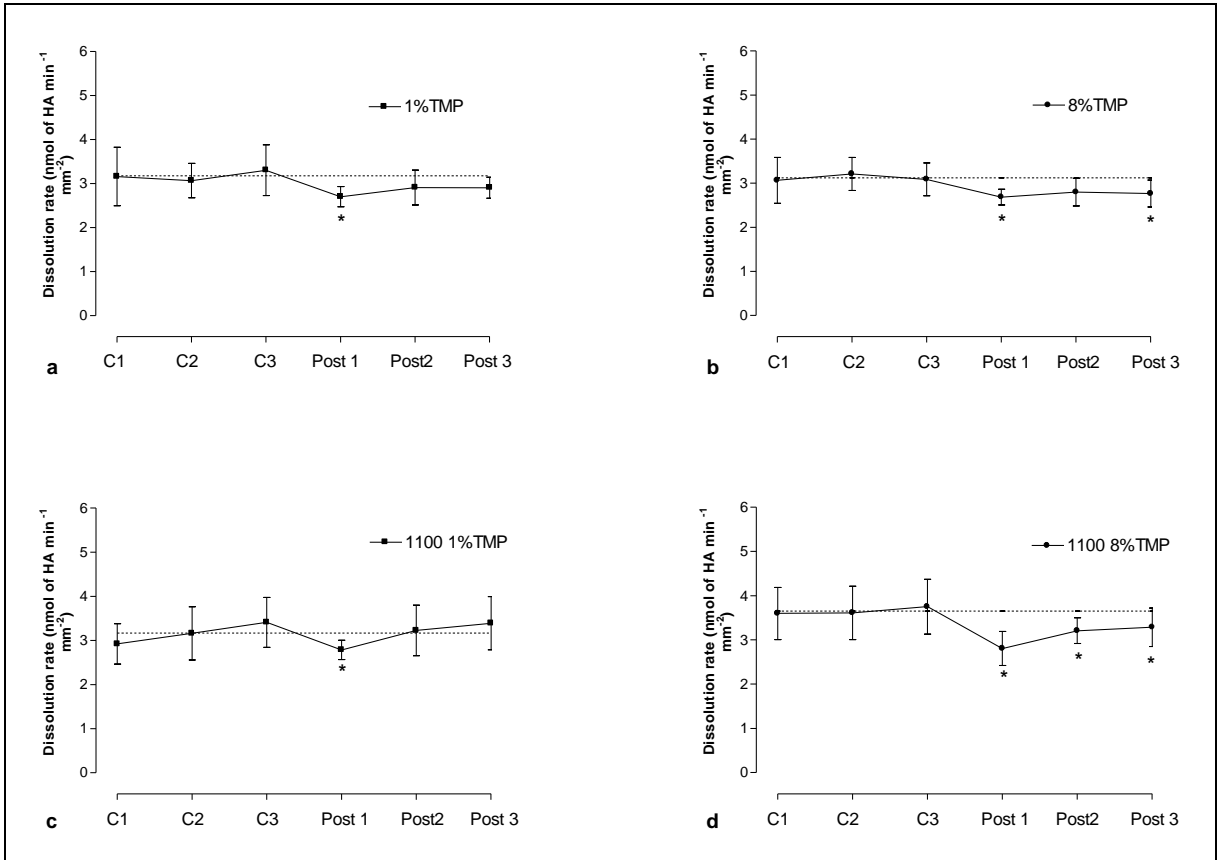


Figure 2. Dissolution rate of HA for the three control runs before treatment (C1-3) and after treatment (Post 1-3) with TMP and fluoride. Dashed line= mean control rate. *Significantly different from mean baseline control.

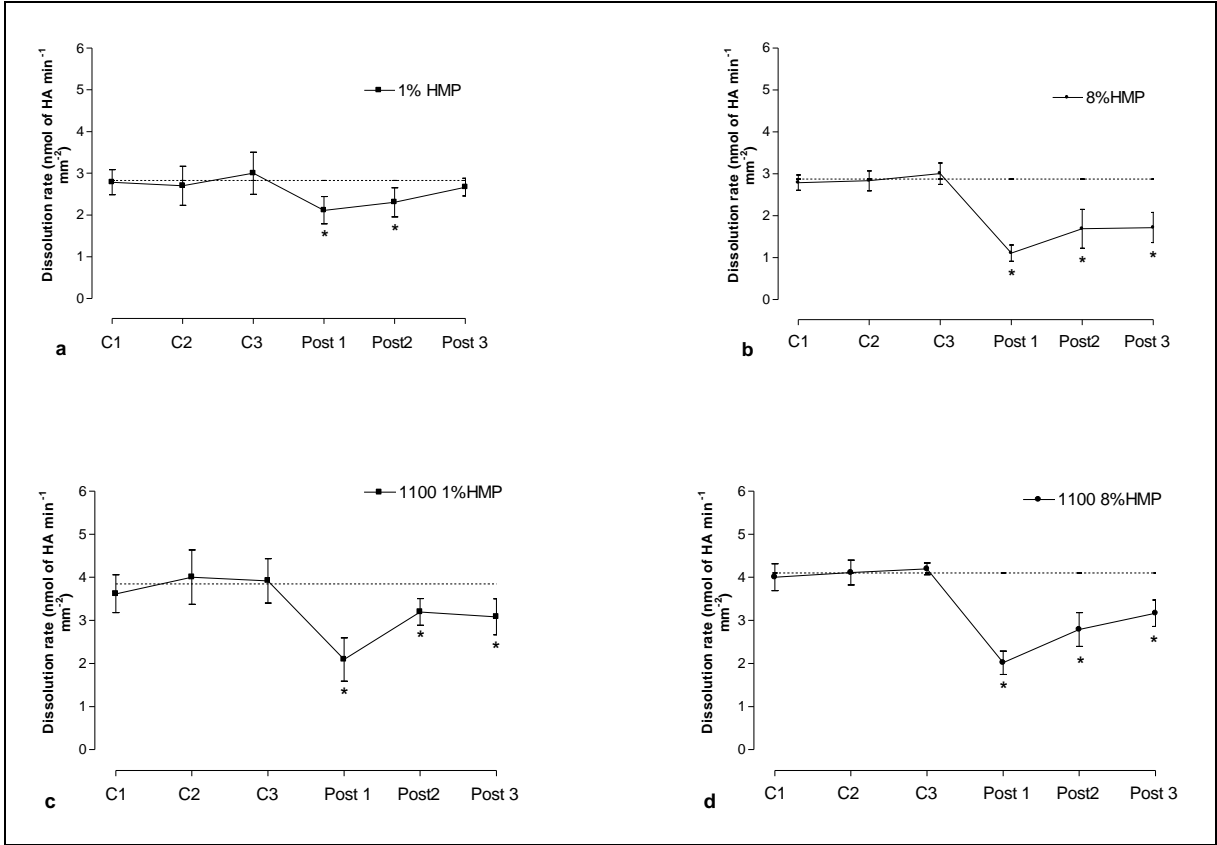


Figure 3. Dissolution rate of HA for the three control runs before treatment (C1-3) and after treatment (Post 1-3) with HMP and fluoride. Dashed line= mean control rate. *Significantly different from mean baseline control.

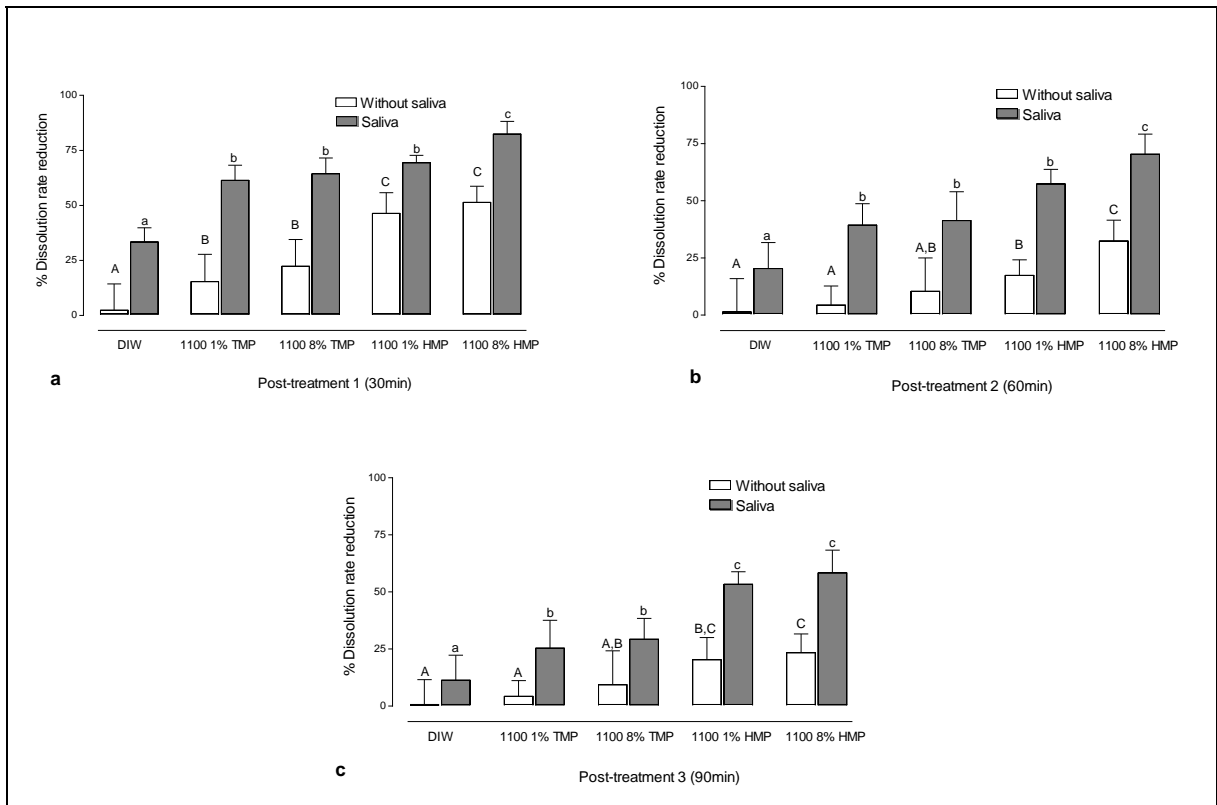


Figure 4. Graphic representation of HA dissolution rate reduction according to the treatments, saliva and post-treatment run. a= post-treatment 1 (30min), b=post-treatment 2 (60min) and c= post-treatment 3 (90min). Bars indicate the standard deviation of the mean. Distinct capital letters represent statistical difference between the groups without salivary pellicle. Different lowercase letters represent statistical difference between the groups with salivary pellicle (Holm-Sidak, $p < 0.001$).

ANEXOS

Jackeline Gallo do Amaral

ANEXO A**REFERÊNCIAS DA INTRODUÇÃO GERAL**

Amaral JG, Freire IR, Martinhon CCR, Pessan JP, Delbem ACB. Low-fluoride dentifrices with polyphosphates on dental caries: longitudinal clinical study. *J Dental Res* 2014; 93B (Poster #188931).

Andreola F, Castellini E, Manfredini T, Romagnoli M. The role of sodium hexametaphosphate in the dissolution process of kaolinite and kaolin. *J Eur Ceram Soc* 2004; 24: 2113–24.

Antunes JLF, Narvai PC, Nugent ZJ. Measuring inequalities in the distribution of dental caries. *Community Dent Oral Epidemiol.* 2004; 32:41-8.

Barbour ME, Shellis RP, Parker DM, Allen GC, Addy M. An investigation of some food-approved polymers as agents to inhibit hydroxyapatite dissolution. *Eur J Oral Sci* 2005; 113: 457-61.

Barbour ME, Shellis RP, Parker DM, Allen GC, Addy M. Inhibition of hydroxyapatite dissolution by whole casein: the effects of pH, protein concentration, calcium, and ionic strength. *Eur J Oral Sci* 2008; 116: 473-8.

Buzalaf MA, Hannas AR, Kato MT. Saliva and dental erosion. *J Appl Oral Sci* 2012; 20: 493-502.

Buzalaf MA, Pessan JP, Honório HM, ten Cate JM. Mechanisms of action of fluoride for caries control. *Monogr Oral Sci.* 2011; 22: 97-114.

Camara DM, Miyasaki ML, Danelon M, Sasaki KT, Delbem AC. Effect of low-fluoride toothpastes combined with hexametaphosphate on in vitro enamel demineralization. *J Dent* 2014; 42: 256-62.

Carey CM. Focus on fluorides: update on the use of fluoride for the prevention of dental caries. *J Evid Base Dent Pract* 2014; 14: 95-102.

Castellini E, Lusvardi G, Malavasi G, Menabue L. Thermodynamic aspects of the adsorption of hexametaphosphate on kaolinite. *J Colloid Interface Sci* 2005; 292: 322–9.

Conceição JM. Avaliação de géis fluoretados, suplementados ou não com hexametafosfato de sódio, no processo de erosão do esmalte dentário. Estudo in situ. [dissertação] Araçatuba: Universidade Estadual Paulista; 2013.

Danelon M, Takeshita EM, Peixoto LC, Sasaki KT, Delbem AC. Effect of fluoride gels supplemented with sodium trimetaphosphate in reducing demineralization. *Clin Oral Investig* 2014; 18: 1119-27.

de Almeida Baldini Cardoso C, Manguiera DF, Olympio KP, Magalhães AC, Rios D, Honório HM, Vilhena FV, Sampaio FC, Buzalaf MA. The effect of pH and fluoride concentration of liquid dentifrices on caries progression. *Clin Oral Investig* 2014; 18: 761-7.

Dye BA, Tan S, Smith V, Lewis BG, Barker LK, Thornton-Evans G, et al: Trends in oral health status: United States, 1988-1994 and 1999-2004. *Vital Health Stat* 2007; 248: 1-92.

Ganss C, Schulze K, Schlueter N. Toothpaste and erosion. *Monogr Oral Sci.* 2013; 23: 88-99.

Gonzalez M. Effect of trimetaphosphate ions on the process of mineralization. *J Dent Res* 1971; 50: 1056-64.

Imfeld T: Dental erosion. Definition, classification and links. *Eur J Oral Sci* 1996; 104: 151-5.

Johansson AK, Omar R, Carlsson GE, Johansson A. Dental erosion and its growing importance in clinical practice: from past to present. *Int J Dent* 2012; 2012: 632907.

Jones SB, Rees GD, Shellis RP, Barbour ME. The effect of monoalkyl phosphates and fluoride on dissolution of hydroxyapatite, and interactions with saliva. *Caries Res* 2013; 47: 355-63.

Manarelli MM, Delbem AC, Lima TM, Castilho FC, Pessan JP. In vitro Remineralizing Effect of Fluoride Varnishes Containing Sodium Trimetaphosphate. *Caries Res* 2014; 48: 299-305.

Manarelli MM, Vieira AE, Matheus AA, Sasaki KT, Delbem AC. Effect of mouth rinses with fluoride and trimetaphosphate on enamel erosion: an in vitro study. *Caries Res* 2011; 45: 506-9.

Moretto MJ, Delbem AC, Manarelli MM, Pessan JP, Martinhon CC. Effect of fluoride varnish supplemented with sodium trimetaphosphate on enamel erosion and abrasion: an in situ/ex vivo study. *J Dent* 2013; 41: 1302-6.

Moretto MJ, Magalhães AC, Sasaki KT, Delbem AC et al. Effect of different fluoride concentrations of experimental dentifrices on enamel erosion and abrasion. *Caries Res* 2010; 44: 135-40.

Narvai PC, Castellanos RA, Frazão P: Prevalência de cárie em dentes permanentes de escolares no Município de São Paulo, SP, 1970-1996. *Rev Saúde Pública* 2000; 34: 196-200.

Pancote LP, Manarelli MM, Danelon M, Delbem ACB. Effect of fluoride gels supplemented with sodium trimetaphosphate on enamel erosion and abrasion. In vitro study. *Arch Oral Biol* 2014; 59: 336-40.

Pessan JP, Toumba KJ, Buzalaf MA. Topical use of fluorides for caries control. *Monogr Oral Sci* 2011; 22:115-32.

Shellis RP, Barbour ME, Jones SB, Addy M. Effects of pH and acid concentration on erosive dissolution of enamel, dentine, and compressed hydroxyapatite. *Eur J Oral Sci* 2010; 118: 475-82.

Souza JA, Amaral JG, Moraes JC, Sasaki KT, Delbem AC. Effect of sodium trimetaphosphate on hydroxyapatite solubility: an in vitro study. *Braz Dent J* 2013; 24: 235-40.

Takeshita EM, Castro LP, Sasaki KT, Delbem ACB. In vitro evaluation with low fluoride content supplemented with trimetaphosphate. *Caries Res* 2009; 43: 50-6.

Takeshita EM, Exterkate RA, Delbem AC, ten Cate JM. Evaluation of different fluoride concentrations supplemented with trimetaphosphate on enamel de- and remineralization in vitro. *Caries Res* 2011; 45: 494-7.

van Dijk JW, Borggreven JM, Driessens FC. The effect of some phosphates and a phosphonate on the electrochemical properties of bovine enamel. *Arch Oral Biol* 1980; 25: 591-5.

Vilhena FV, Olympio KP, Lauris JR, Delbem AC, Buzalaf MA. Low-fluoride acidic dentifrice: a randomized clinical trial in a fluoridated area. *Caries Res* 2010; 44:478-84.

Wiegand A, Kowing L, Attin T. Impact of brushing force on abrasion of acid-softened enamel. *Arch Oral Biol* 2007; 52: 1043-7.

Wong MC, Clarkson J, Glenny AM, et al. Cochrane reviews on the benefits/risks of fluoride toothpastes. *J Dent Res* 2011; 90: 573-9.

ANEXO B

SÍNTESE DA HIDROXIAPATITA



1. A solução de fosfato de amônio dibásico foi adicionada à solução de nitrato de cálcio lentamente (2 a 5 mL/minuto), por meio de um funil de separação sob agitação constante, a 37° C.

2. Os precipitados foram separados por filtração, utilizando funil de Buchner acoplado a um sistema de vácuo (-600 mm Hg).



3. Moinho de Bola utilizado para triturar os grãos de hidroxiapatita (Planetary Micro Mill Pulverisette, Fritsh).

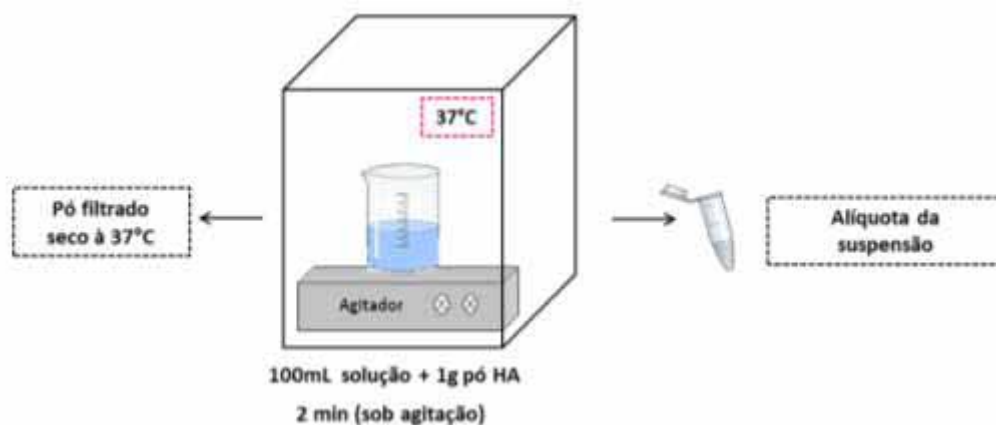
4. Peneira granulométrica para obtenção de uma hidroxiapatita com grãos de 53 µm.



ANEXO C

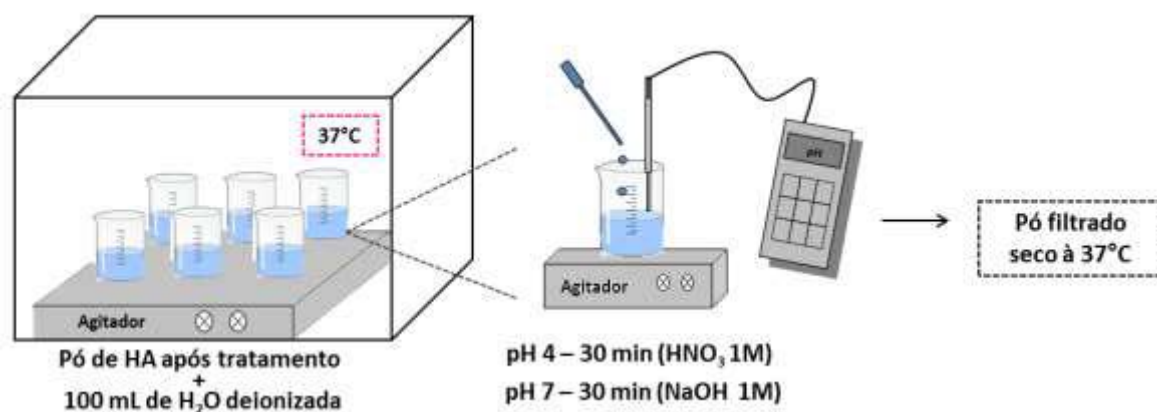
TRATAMENTO E CICLO DE pH DO PÓ DE HIDROXIAPATITA

Tratamento



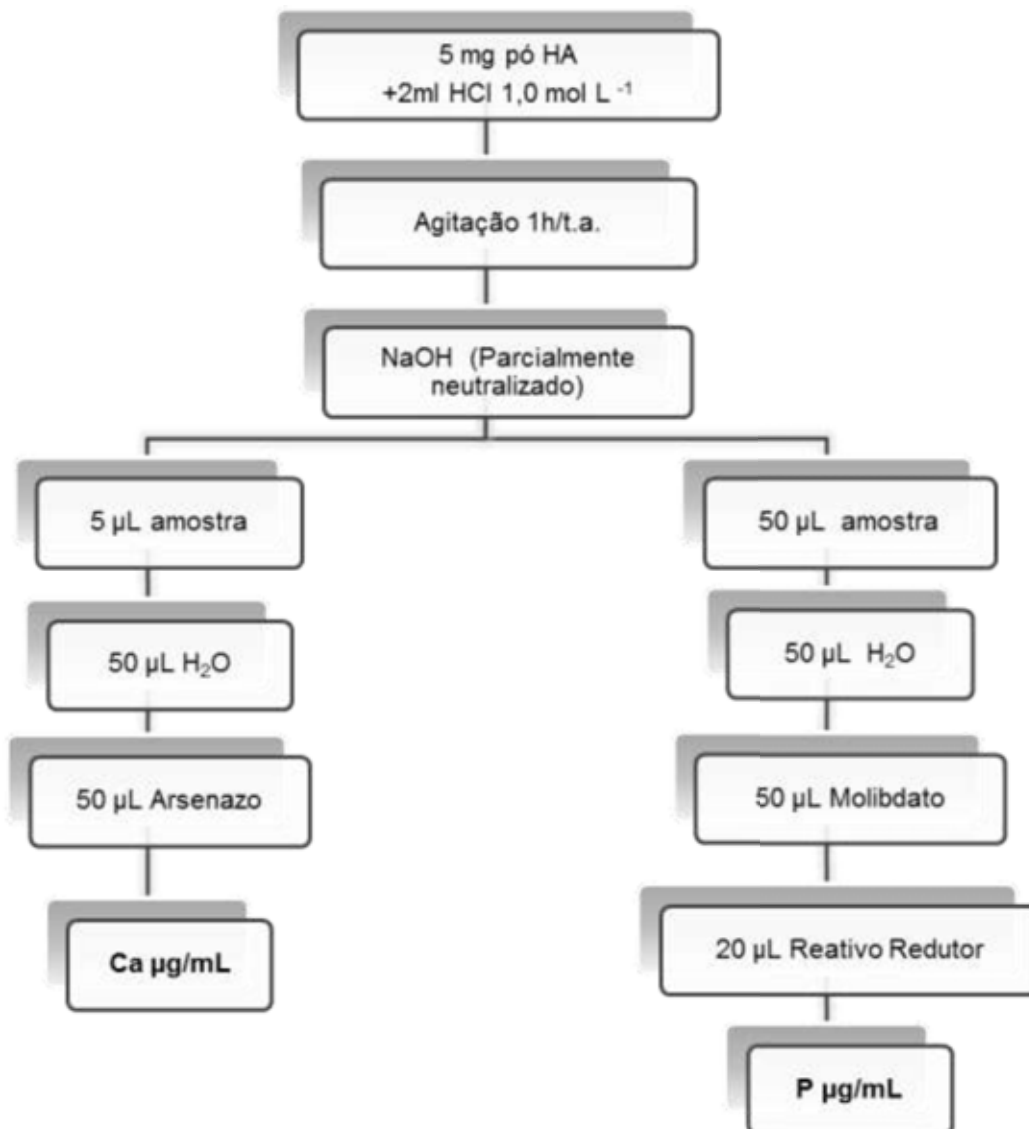
Após o tratamento foi realizada a dosagem de F e P na alíquota da suspensão. O pó foi filtrado e seco (como descrito no anexo B) e submetido ao ciclo de pH.

Ciclo de pH



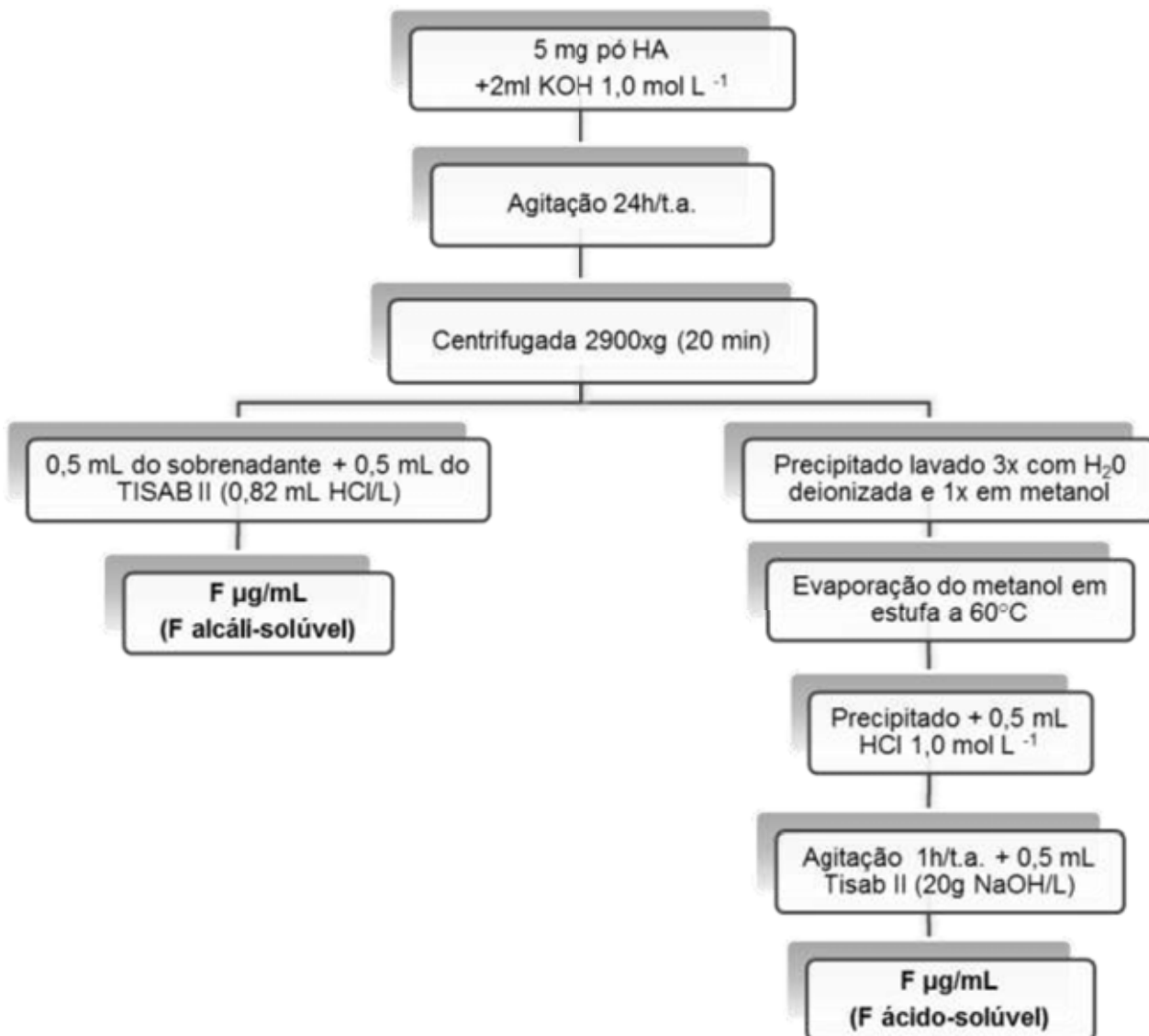
Após este processo, o pó foi filtrado e seco, e realizadas as análises bioquímicas e estruturais.

ANEXO D
ANÁLISE DE Ca E P NA HIDROXIAPATITA



ANEXO E

ANÁLISE DE F ÁLCALI- E ÁCIDO-SOLÚVEL NA HIDROXIAPATITA



ANEXO F

RESULTADOS DAS ANÁLISES BIOQUÍMICAS (CAPÍTULO 1)

Tabela 1 - Concentração média (\pm DP) em mg/g de cálcio (Ca), fósforo (P) e de fluoreto alcali-solúvel e ácido-solúvel na hidroxiapatita de acordo com as concentrações de TMP no grupo contendo 0 ppm F após o ciclo de pH

%TMP	Variáveis				Ca/P
	Ca	P	F alcali-solúvel	F ácido-solúvel	
0	323,6 (5,4)	168,7 (3,8)	0,0145 (0,002)	0,0183 (0,001)	1,49 (0,03)
0,1	312,1 (2,9)	164,9 (3,3)	0,0123 (0,001)	0,0164 (0,001)	1,47 (0,02)
0,2	303,3 (7,4)	159,7 (3,4)	0,0114 (0,000)	0,0149 (0,000)	1,47 (0,03)
0,4	296,6 (6,1)	156,7 (3,4)	0,0116 (0,000)	0,0151 (0,001)	1,47 (0,02)
0,6	289,8 (8,3)	153,8 (5,2)	0,0114 (0,000)	0,0165 (0,001)	1,46 (0,03)
0,8	289,7 (4,3)	153,3 (4,2)	0,0114 (0,001)	0,0156 (0,001)	1,46 (0,03)
1	289,5 (1,8)	152,9 (4,4)	0,0114 (0,001)	0,0138 (0,007)	1,47 (0,05)
2	297,5 (8,4)	156,6 (5,6)	0,0120 (0,001)	0,0143 (0,001)	1,47 (0,05)
4	288,0 (7,8)	149,0 (2,0)	0,0108 (0,001)	0,0135 (0,001)	1,50 (0,04)
6	289,4 (5,8)	148,4 (2,5)	0,0113 (0,004)	0,0151 (0,001)	1,51 (0,02)
8	282,7 (4,5)	145,4 (4,5)	0,0112 (0,003)	0,0138 (0,001)	1,51 (0,03)
10	281,7 (7,0)	146,6 (2,9)	0,0111 (0,001)	0,0141 (0,001)	1,49 (0,03)

Tabela 2 - Concentração média (\pm DP) em mg/g de cálcio (Ca), fósforo (P) e de fluoreto alcali-solúvel e ácido-solúvel na hidroxiapatita de acordo com as concentrações de TMP no grupo contendo 100 ppm F após o ciclo de pH

%TMP	Variáveis				Ca/P
	Ca	P	F alcali-solúvel	F ácido-solúvel	
0	318,1 (3,6)	164,1 (2,6)	0,24 (0,02)	3,11 (0,08)	1,50 (0,02)
0,1	319,6 (6,4)	165,1 (6,3)	0,14 (0,01)	2,99 (0,07)	1,50 (0,02)
0,2	319,0 (6,4)	158,9 (2,8)	0,13 (0,01)	2,82 (0,04)	1,56 (0,04)
0,4	325,5 (1,9)	159,7 (2,9)	0,16 (0,01)	3,27 (0,02)	1,58 (0,03)
0,6	317,3 (7,8)	158,9 (4,5)	0,17 (0,01)	3,16 (0,07)	1,55 (0,03)
0,8	313,0 (4,1)	156,6 (2,7)	0,17 (0,01)	2,96 (0,07)	1,55 (0,03)
1	310,7 (11,6)	155,6 (4,2)	0,18 (0,01)	3,05 (0,08)	1,55 (0,04)
2	306,4 (6,2)	155,2 (1,9)	0,18 (0,01)	2,80 (0,08)	1,53 (0,04)
4	312,5 (9,4)	159,5 (4,6)	0,26 (0,01)	2,56 (0,1)	1,52 (0,02)
6	306,5 (13,4)	158,0 (6,9)	0,30 (0,01)	2,54 (0,08)	1,50 (0,03)
8	305,7 (10,5)	157,8 (2,9)	0,24 (0,01)	2,22 (0,10)	1,50 (0,04)
10	299,8 (12,2)	154,7 (3,6)	0,23 (0,02)	1,99 (0,09)	1,50 (0,03)

Tabela 3 - Concentração média (\pm DP) em mg/g de cálcio (Ca), fósforo (P) e de fluoreto alcáli-solúvel e ácido-solúvel na hidroxiapatita de acordo com as concentrações de TMP no grupo contendo 250 ppm F após o ciclo de pH

%TMP	Variáveis				Ca/P
	Ca	P	F alcáli-solúvel	F ácido-solúvel	
0	316,3 (12,3)	160,6 (3,7)	1,19 (0,02)	3,02 (0,07)	1,53 (0,03)
0,1	317,6 (7,8)	161,4 (3,8)	1,11 (0,04)	3,00 (0,08)	1,53 (0,02)
0,2	319,6 (6,5)	154,6 (1,1)	0,97 (0,04)	2,94 (0,08)	1,60 (0,03)
0,4	330,6 (8,9)	155,9 (2,2)	0,86 (0,05)	2,68 (0,06)	1,64 (0,04)
0,6	327,6 (3,6)	156,1 (1,8)	0,75 (0,03)	2,48 (0,05)	1,63 (0,02)
0,8	332,7 (7,0)	159,3 (2,3)	0,83 (0,08)	2,48 (0,10)	1,62 (0,03)
1	327,2 (11,7)	157,0 (0,8)	1,28 (0,07)	1,78 (0,05)	1,61 (0,06)
2	328,0 (1,7)	157,3 (1,2)	1,17 (0,05)	1,56 (0,02)	1,62 (0,01)
4	319,6 (4,6)	155,2 (1,2)	1,11 (0,09)	1,12 (0,04)	1,60 (0,01)
6	311,2 (8,3)	153,1 (2,4)	1,06 (0,06)	1,04 (0,04)	1,58 (0,02)
8	312,0 (9,0)	154,1 (3,2)	1,15 (0,08)	1,09 (0,09)	1,57 (0,02)
10	307,4 (8,6)	152,2 (2,5)	1,11 (0,07)	1,14 (0,01)	1,57 (0,04)

Tabela 4 - Concentração média (\pm DP) em mg/g de cálcio (Ca), fósforo (P) e de fluoreto alcáli-solúvel e ácido-solúvel na hidroxiapatita de acordo com as concentrações de TMP no grupo contendo 500 ppm F após o ciclo de pH

%TMP	Variáveis				Ca/P
	Ca	P	F alcáli-solúvel	F ácido-solúvel	
0	368,1 (9,6)	181,3 (5,6)	0,26 (0,00)	4,62 (0,12)	1,57 (0,01)
0,1	360,1 (7,3)	174,5 (4,8)	0,24 (0,02)	4,88 (0,12)	1,60 (0,03)
0,2	358,6 (8,1)	169,8 (2,3)	0,23 (0,01)	4,75 (0,06)	1,64 (0,03)
0,4	362,4 (4,8)	171,6 (2,6)	0,20 (0,02)	4,29 (0,07)	1,64 (0,03)
0,6	371,4 (2,5)	173,7 (1,9)	0,22 (0,02)	3,55 (0,12)	1,66 (0,01)
0,8	355,6 (7,4)	166,4 (2,1)	0,29 (0,02)	3,61 (0,16)	1,66 (0,02)
1	349,3 (6,9)	162,4 (4,1)	0,35 (0,02)	3,46 (0,12)	1,67 (0,02)
2	353,8 (12,2)	164,3 (6,7)	0,48 (0,04)	3,31 (0,20)	1,67 (0,03)
4	337,7 (10,3)	160,9 (5,2)	0,46 (0,02)	2,78 (0,13)	1,63 (0,02)
6	338,8 (16,9)	169,2 (8,8)	0,46 (0,04)	2,82 (0,18)	1,55 (0,04)
8	324,2 (10,6)	164,4 (4,4)	0,54 (0,03)	2,54 (0,10)	1,53 (0,02)
10	319,8 (15,5)	161,4 (8,2)	0,65 (0,04)	2,40 (0,16)	1,54 (0,04)

ANEXO G

RESULTADOS DA ANÁLISE DE EDX (CAPÍTULO 1)

Tabela 1 - Valores da porcentagem (%) dos elementos atômicos cálcio (Ca), fósforo (P), oxigênio (O) e fluoreto (F) na hidroxiapatita de acordo com as concentrações de F e TMP avaliadas após o ciclo de pH

F (ppmF)	%TMP	Variáveis				Ca/P
		Ca	P	O	F	
0	0	20,25	13,43	66,32	-	1,51
	0,4	19,75	12,98	67,27	-	1,52
	1	20,04	13,56	66,40	-	1,48
	6	20,28	13,58	66,13	-	1,49
	10	20,28	13,51	66,21	-	1,50
100	0	20,25	12,60	67,01	0,73	1,56
	0,4	20,54	12,89	65,79	0,78	1,59
	1	20,32	13,19	65,76	0,73	1,54
	6	20,46	13,17	65,56	0,81	1,55
	10	20,26	12,74	66,15	0,73	1,59
250	0	20,76	12,40	65,50	1,34	1,67
	0,4	19,84	12,29	66,24	1,01	1,61
	1	19,78	11,59	67,75	0,88	1,71
	6	19,42	11,97	67,78	0,68	1,62
	10	19,85	11,89	67,78	0,68	1,67
500	0	19,74	11,43	67,54	1,28	1,73
	0,4	19,74	12,03	67,25	0,99	1,64
	1	20,35	12,20	66,73	0,90	1,67
	6	19,99	11,98	67,34	0,69	1,67
	10	20,01	11,97	67,28	0,74	1,67

* - indica que o elemento não foi observado.

ANEXO H

RESULTADOS DAS ANÁLISES BIOQUÍMICAS (CAPÍTULO 2)

Tabela 1 - Concentração média (\pm DP) em mg/g de cálcio (Ca), fósforo (P) e de fluoreto alcáli-solúvel e ácido-solúvel na hidroxiapatita de acordo com as concentrações de TMP no grupo contendo 0 ppm F após o ciclo de pH

%TMP	Variáveis				Ca/P
	Ca	P	F alcáli-solúvel	F ácido-solúvel	
0	323,6 (5,4)	168,7 (3,8)	0,0145 (0,002)	0,0183 (0,001)	1,49 (0,03)
0,1	312,1 (2,9)	164,9 (3,3)	0,0123 (0,001)	0,0164 (0,001)	1,47 (0,02)
0,2	303,3 (7,4)	159,7 (3,4)	0,0114 (0,000)	0,0149 (0,000)	1,47 (0,03)
0,4	296,6 (6,1)	156,7 (3,4)	0,0116 (0,000)	0,0151 (0,001)	1,47 (0,02)
0,6	289,8 (8,3)	153,8 (5,2)	0,0114 (0,000)	0,0165 (0,001)	1,46 (0,03)
0,8	289,7 (4,3)	153,3 (4,2)	0,0114 (0,001)	0,0156 (0,001)	1,46 (0,03)
1	289,5 (1,8)	152,9 (4,4)	0,0114 (0,001)	0,0138 (0,007)	1,47 (0,05)
2	297,5 (8,4)	156,6 (5,6)	0,0120 (0,001)	0,0143 (0,001)	1,47 (0,05)
4	288,0 (7,8)	149,0 (2,0)	0,0108 (0,001)	0,0135 (0,001)	1,50 (0,04)
6	289,4 (5,8)	148,4 (2,5)	0,0113 (0,004)	0,0151 (0,001)	1,51 (0,02)
8	282,7 (4,5)	145,4 (4,5)	0,0112 (0,003)	0,0138 (0,001)	1,51 (0,03)
10	281,7 (7,0)	146,6 (2,9)	0,0111 (0,001)	0,0141 (0,001)	1,49 (0,03)

Tabela 2 - Concentração média (\pm DP) em mg/g de cálcio (Ca), fósforo (P) e de fluoreto alcáli-solúvel e ácido-solúvel na hidroxiapatita de acordo com as concentrações de TMP no grupo contendo 1100 ppm F após o ciclo de pH

%TMP	Variáveis				Ca/P
	Ca	P	F alcáli-solúvel	F ácido-solúvel	
0	317,5 (7,0)	161,2 (3,2)	0,46 (0,01)	3,64 (0,12)	1,53 (0,03)
0,1	318,3 (3,6)	162,8 (2,4)	0,93 (0,04)	3,66 (0,23)	1,52 (0,02)
0,2	304,1 (10,8)	157,2 (4,4)	1,07 (0,12)	3,35 (0,17)	1,50 (0,02)
0,4	307,1 (5,6)	157,7 (2,6)	1,17 (0,13)	2,86 (0,11)	1,51 (0,03)
0,6	304,5 (6,8)	154,4 (4,3)	1,94 (0,09)	2,72 (0,13)	1,53 (0,03)
0,8	311,4 (6,6)	155,0 (2,4)	1,48 (0,12)	2,91 (0,12)	1,56 (0,03)
1	308,5 (5,3)	153,6 (4,1)	1,63 (0,06)	2,34 (0,09)	1,56 (0,03)
2	309,9 (8,6)	149,6 (6,1)	2,56 (0,15)	2,33 (0,07)	1,61 (0,02)
4	305,8 (1,9)	146,8 (1,3)	2,71 (0,14)	1,86 (0,09)	1,61 (0,01)
6	285,5 (7,6)	140,5 (2,8)	2,49 (0,11)	1,62 (0,19)	1,57 (0,03)
8	290,1 (7,7)	142,2 (3,7)	3,37 (0,20)	1,68 (0,14)	1,58 (0,01)
10	284,0 (7,4)	143,3 (4,0)	3,08 (0,18)	1,76 (0,11)	1,54 (0,01)

Tabela 3 - Concentração média (\pm DP) em mg/g de cálcio (Ca), fósforo (P) e de fluoreto alcáli-solúvel e ácido-solúvel na hidroxiapatita de acordo com as concentrações de TMP no grupo contendo 4500 ppm F após o ciclo de pH

%TMP	Variáveis				Ca/P
	Ca	P	F alcáli-solúvel	F ácido-solúvel	
0	361,6 (4,9)	179,5 (3,5)	0,36 (0,01)	6,71 (0,21)	1,56 (0,02)
0,1	364,3 (10,6)	181,6 (4,0)	0,41 (0,02)	6,95 (0,22)	1,55 (0,03)
0,2	367,6 (5,2)	183,6 (1,4)	0,41 (0,03)	6,50 (0,30)	1,55 (0,03)
0,4	378,4 (4,3)	183,1 (3,6)	0,45 (0,03)	6,18 (0,24)	1,60 (0,02)
0,6	381,2 (9,6)	185,6 (3,6)	0,54 (0,03)	4,75 (0,13)	1,59 (0,02)
0,8	372,4 (8,2)	179,6 (4,4)	0,51 (0,02)	4,49 (0,19)	1,61 (0,03)
1	369,6 (9,7)	179,4 (3,3)	0,56 (0,03)	4,43 (0,17)	1,60 (0,03)
2	373,6 (5,2)	177,7 (1,5)	0,66 (0,02)	4,16 (0,13)	1,63 (0,03)
4	368,6 (5,9)	173,2 (1,5)	0,78 (0,03)	3,98 (0,27)	1,65 (0,03)
6	353,2 (13,1)	165,0 (4,6)	0,70 (0,04)	3,51 (0,27)	1,66 (0,04)
8	350,1 (18,1)	164,1 (6,3)	0,70 (0,05)	3,62 (0,21)	1,65 (0,04)
10	320,5 (8,3)	156,5 (2,6)	0,77 (0,06)	3,79 (0,31)	1,59 (0,02)

Tabela 4 - Concentração média (\pm DP) em mg/g de cálcio (Ca), fósforo (P) e de fluoreto alcáli-solúvel e ácido-solúvel na hidroxiapatita de acordo com as concentrações de TMP no grupo contendo 9000 ppm F após o ciclo de pH

%TMP	Variáveis				Ca/P
	Ca	P	F alcáli-solúvel	F ácido-solúvel	
0	353,4 (9,3)	168,9 (1,9)	0,62 (0,03)	6,16 (0,17)	1,62 (0,03)
0,1	347,6 (8,9)	167,1 (3,0)	0,70 (0,03)	5,57 (0,25)	1,61 (0,03)
0,2	332,4 (11,6)	163,4 (5,8)	0,86 (0,03)	5,41 (0,28)	1,58 (0,02)
0,4	339,7 (4,9)	166,8 (4,0)	0,91 (0,03)	4,31 (0,19)	1,58 (0,03)
0,6	342,7 (2,6)	168,4 (3,3)	1,10 (0,05)	4,33 (0,19)	1,58 (0,04)
0,8	336,7 (6,8)	165,8 (2,9)	1,15 (0,09)	4,64 (0,21)	1,57 (0,03)
1	332,1 (5,7)	157,0 (2,0)	0,82 (0,03)	5,74 (0,29)	1,63 (0,03)
2	339,0 (10,2)	160,5 (4,0)	0,89 (0,08)	5,46 (0,25)	1,64 (0,03)
4	341,0 (10,3)	155,4 (3,2)	1,35 (0,09)	6,10 (0,18)	1,70 (0,03)
6	360,2 (7,3)	166,2 (1,5)	1,33 (0,09)	1,84 (0,14)	1,68 (0,02)
8	351,1 (4,8)	162,6 (2,1)	1,35 (0,08)	1,74 (0,17)	1,67 (0,03)
10	356,5 (5,2)	165,2 (2,8)	1,10 (0,08)	1,75 (0,07)	1,67 (0,03)

ANEXO I
RESULTADOS DA ANÁLISE DE EDX (CAPÍTULO 2)

Tabela 1 - Valores da porcentagem (%) dos elementos atômicos cálcio (Ca), fósforo (P), oxigênio (O) e fluoreto (F) na hidroxiapatita de acordo com as concentrações de F e TMP avaliadas após o ciclo de pH

F (ppmF)	%TMP	Variáveis				Ca/P
		Ca	P	O	F	
0	0	20,25	13,43	66,32	-	1,51
	1	20,04	13,56	66,40	-	1,48
	4	19,89	13,35	66,76	-	1,49
	10	20,28	13,51	66,21	-	1,50
1100	0	20,87	13,24	64,90	0,99	1,58
	1	19,99	12,34	66,49	1,19	1,62
	4	19,78	12,56	66,35	1,19	1,57
	10	19,58	12,33	66,93	1,17	1,59
4500	0	18,77	11,84	67,58	1,80	1,65
	1	20,70	12,34	66,02	0,94	1,68
	4	20,60	12,13	66,09	0,97	1,70
	10	20,02	12,52	65,94	1,31	1,60
9000	0	19,18	12,75	66,13	1,94	1,50
	1	20,77	12,51	65,23	1,49	1,66
	4	19,57	12,36	66,37	1,70	1,58
	0	20,18	12,50	65,89	1,44	1,61

* - indica que o elemento não foi observado.

ANEXO J

DETERMINAÇÃO DA TAXA DE DISSOLUÇÃO DA HIDROXIAPATITA



1. A determinação da taxa de dissolução inicial e final foi medida através do pH-stat.

2. Os discos de HA foram fixados, como mostrado na figura ao lado. Para cada medida da taxa de dissolução foram utilizados 30 mL de ácido cítrico 0,3 M. Quando a temperatura e pH alcançavam 37° C e 3.2, respectivamente, a reação era iniciada.

